This is to certify that the

dissertation entitled

MECHANISMS MEDIATING THE METHYLMERCURY-INDUCED ELEVATIONS IN THE INTRASYNAPTOSOMAL CONCENTRATIONS OF CALCIUM AND ZINC

presented by

Michael F. Denny

has been accepted towards fulfillment
of the requirements for

Ph.D. degree in Pharmacology and Toxicology

Gillian Atkinson
Major professor

Date 9/22/95

MECHANISMS MEDIATING THE METHYLMERCURY-INDUCED ELEVATIONS IN THE INTRASYNAPTOSOMAL CONCENTRATIONS OF CALCIUM AND ZINC

By

Michael F. Denny

A DISSERTATION

Submitted to Michigan State University in partial fulfillment of the requirements for the degree of

DOCTOR OF PHILOSOPHY

Department of Pharmacology and Toxicology
and
Institute for Environmental Toxicology

1995

ABSTRACT

MECHANISMS MEDIATING THE METHYLMERCURY-INDUCED ELEVATIONS IN THE INTRASYNAPTOSOMAL CONCENTRATIONS OF CALCIUM AND ZINC

By

Michael F. Denny

Methylmercury (MeHg) is an environmental neurotoxicant upon chronic and acute exposure. The mechanisms underlying cytotoxicity remain unknown, but may be due to disruption of divalent cation homeostasis because MeHg disrupts Ca^{2+}-dependent processes in several model systems. The effects of MeHg on divalent cation homeostasis were studied using isolated nerve terminals from the rat brain (synaptosomes) loaded with the Ca^{2+}-selective fluorescent indicator fura-2. MeHg (10-100 μM) caused an gradual increase in intrasynaptosomal Ca^{2+} concentration ($[Ca^{2+}]_i$) which was concentration-dependent with respect to both MeHg and extracellular Ca^{2+} (Ca^{2+}_e), and mediated by increased plasma membrane permeability. MeHg also caused an immediate elevation in the intrasynaptosomal concentration of an endogenous polyvalent cation other than Ca^{2+}, which was independent of Ca^{2+}_e and maximal at 25 μM MeHg. The endogenous metal could not be identified with complete certainty, however, it was postulated to be Zn^{2+}, based on its interactions with fura-2.

^{19}F-nuclear magnetic resonance (NMR) spectroscopy was performed on synaptosomes loaded with the polyvalent cation indicator 5F-BAPTA to identify the cation unequivocally. This technique allows for the identification and quantitation of several cations, simultaneously. MeHg caused a three-fold elevation in $[Zn^{2+}]_i$ which was independent of Ca^{2+}_e, but did not affect the concentration of cations other than Zn^{2+}.

Endogenous sources of Zn^{2+} in the nerve terminals include proteins, and synaptic vesicles. Pretreatment of fura-2 loaded synaptosomes with agents which mobilize synaptic vesicles did not attenuate the MeHg-induced elevations in $[Zn^{2+}]_i$, suggesting that synaptic vesicles do not contribute to the increases in $[Zn^{2+}]_i$. To determine if MeHg released Zn^{2+} from synaptosomal proteins, homogenates of synaptosomal suspensions were prepared, and fura-2 was added. Excitation scans were acquired before and after the addition of MeHg, and compared for effects consistent with release of Zn^{2+}. MeHg shifted fura-2 fluorescence in a manner consistent with release of Zn^{2+}, this activity was localized entirely to the soluble fraction. Anion exchange chromatography of this fraction resolved three peaks of MeHg-induced Zn^{2+} release, suggesting that more than one protein contributed to the elevation in $[Zn^{2+}]_i$.

DEDICATION

This dissertation is dedicated to the memory of my grandfather, Tony Crimarcki.

ACKNOWLEDGEMENTS

I would like to acknowledge the efforts of my guidance committee: Drs. Atchison, Bursian, Contreras, Galligan and Smith. I also would like to thank the many lab members who have been so helpful throughout my stay. In particular, the assistance of Michael, Jay, Yukun, Sue, Hong, Laura, Nana, Ravindra and Sandy is greatly appreciated.

I want to express my gratitude to Lynne for her constant support and patience during this whole process, anyone else would have given up on me a long time ago. I need to thank my family, to whom the details of my research project have been a never-ending source of amusement. The support and friendship of all the graduate students is also greatly appreciated, I truly feel we did more than keep the drinking establishments in the Lansing area in business. I also want to thank the departmental office staff for keeping track of the endless stream of appointment papers, order forms, travel vouchers, etc.

Lastly, I want to acknowledge my 12th grade English teacher, Ms. Hnankovich, who stood me up in front of the class one day and told me I would never amount to anything, which may be right, but at least I'm not a 12th grade English teacher.

TABLE OF CONTENTS

LIST OF FIGURES

LIST OF ABBREVIATIONS

A_{280}	optical absorbance at 280 nm
ACh	acetylcholine
AM	acetoxymethylester
AMPA	α-amino-3-hydroxy-5-methylisoxazolepropionic acid
ANOVA	analysis of variance
ATP	adenosine triphosphate
°C	degrees centigrade
$[Ca^{2+}]_i$	intracellular or intrasynaptosomal Ca^{2+} concentration
Ca^{2+}_e	extracellular Ca^{2+}
$[Ca^{2+}]_e$	extracellular Ca^{2+} concentration
CICR	Ca^{2+}-induced Ca^{2+} release
CNS	central nervous system
dia	diameter
DMSO	dimethyl sulfoxide
DTPA	diethylenetriaminepentaacetic acid
EDDA	ethylenediaminediacetic acid
EGTA	ethylene glycol bis-(ß-aminoethyl ether)-*N,N,N'N'*-tetraacetic acid
EPP	end-plate potential
ER	endoplasmic reticulum
5F-BAPTA	1,2-bis(2-amino-5-fluorophenoxy)ethane-*N,N,N'N'*-tetraacetic acid

HBS	Hepes buffered saline
g	gram
g	force of gravity
Hepes	*N*-(2-hydroxyethyl)piperazine-*N'*-(2-ethanesulfonic acid)
IP_3	inositol-1,4,5-tris-phosphate
K_d	dissociation constant
kDa	kilodalton
M	molar concentration
Mℏ	megaohm
MeHg	methylmercury
MEPP	miniature end-plate potential
MHz	megahertz
min	minute
ml	milliliter
MPP^+	1-methyl-4-phenylpyridinium
NG108-15	mouse neuroblastoma × rat glioma hybrid
NGF	nerve growth factor
nAChR	nicotinic acetylcholine receptor
nm	nanometer
NMDA	N-methyl-D-aspartate
NMR	nuclear magnetic resonance
P_{2b}	synaptosome enriched fraction
PC12	rat clonal pheochromocytoma cell

PKC	protein kinase C
PLA_2	phospholipase A_2
PLC	phospholipase C
ppm	parts per million
psi	pounds per square inch
R_{max}	340/380 nm ratio of fura-2 during Ca^{2+}-saturating conditions
R_{min}	340/380 nm ratio of fura-2 during Ca^{2+}-free conditions
SDS-PAGE	sodium dodecylsulfate-polyacrylamide gel electrophoresis
sec	second
S.E.M.	standard error of mean
S_{b2}	emission intensity of fura-2 at 380 nm during Ca^{2+}-saturating conditions
S_{f2}	emission intensity of fura-2 at 380 nm during Ca^{2+}-free conditions
TPEN	*N,N,N',N'*-tetrakis-(2-pyridylmethyl)ethylene-diamine
TTX	tetrodotoxin
v/v	volume per volume dilution
W	watt
YS035	*N,N*-bis-(3,4-dimethoxyphenethyl)-*N*-methylamine
$[Zn^{2+}]_i$	intracellular or intrasynaptosomal Zn^{2+} concentration

CHAPTER ONE

INTRODUCTION

A. General introduction.

Methylmercury (MeHg) is an environmental contaminant produced by industrial processes as well as through the biomethylation of inorganic, divalent Hg^{2+}. MeHg disrupts nervous system function, and is neurotoxic upon acute or chronic exposure (Takeuchi *et al.*, 1962; Bakir *et al.*, 1973). There exists a considerable body of information regarding the toxic actions of MeHg. Manifestations of MeHg intoxication include impairments of vision, hearing and speech, sensory disturbances and weakness in the extremities (Chang, 1980). These effects are believed to be mediated by disruption of the central nervous system (CNS), particular the cerebellum (Chang, 1977). Although the mechanisms of MeHg-induced neurotoxicity are not known, they have been the topic of intense investigation (Atchison and Hare, 1994). One area that has received much attention is the ability of MeHg to disrupt neuronal divalent cation regulation (Cooper *et al.*, 1984). The purpose of this dissertation was to study the biochemical basis of MeHg-induced alterations in neuronal divalent cation homeostasis as a mediator of neurotoxicity. Much of the previous information available regarding this topic had been acquired using indirect techniques or through inference. As such, a goal this study was to measure more directly the disruption in divalent cation homeostasis caused by MeHg.

B. Regulation of intracellular Ca^{2+} concentration ($[Ca^{2+}]_i$) in neurons.

Ca^{2+} homeostasis in neurons is dependent upon the precise coordination of processes which elevate $[Ca^{2+}]_i$, such as influx of extracellular Ca^{2+} (Ca^{2+}_e) or release of Ca^{2+} sequestered within organelles, and those which lower $[Ca^{2+}]_i$, either by extrusion or sequestration of intracellular Ca^{2+} (Blaustein, 1988). Under resting conditions, neurons

normally maintain an $[Ca^{2+}]_i$ of approximately 100 nM in the face of extracellular Ca^{2+} concentrations ($[Ca^{2+}]_e$) of the order of 1 to 2 mM. The maintenance of the large inward electrochemical gradient for Ca^{2+} is essential for proper neuronal function, and relies upon many factors which are interdependent in some instances (Miller, 1988; Choi, 1988).

In neurons, the primary route of influx of Ca^{2+}_e is through the activation of voltage-dependent or ligand-operated channels which are permeable to Ca^{2+} (Bertolino and Llinás, 1992). Activation of voltage-dependent Ca^{2+} channels, and the associated Ca^{2+} influx is required for the release of neurotransmitter from the presynaptic nerve terminal (Llinás *et al.*, 1992). The $[Ca^{2+}]_i$ may rise several-fold following the invasion of an action potential into the nerve terminal and subsequent Ca^{2+} influx. Activation of postsynaptic or presynaptic ligand-operated channels can also elicit an elevation in $[Ca^{2+}]_i$. Certain subtypes of neuronal nicotinic acetylcholine receptors (nAChR) (Vernino *et al.*, 1992) and subtypes of glutamate receptors sensitive to N-methyl-d-aspartate (NMDA) are permeable to Ca^{2+} following ligand binding (MacDermott *et al.*, 1986). Some receptors elicit an elevation in $[Ca^{2+}]_i$ by coupling to phospholipase C (PLC) *via* a membrane-associated guanine nucleotide-binding protein, or G-protein (Hokin, 1985). Ligand binding initiates a cascade of intracellular events in which the receptor-associated G-protein activates PLC. This stimulates the conversion of phoshotidylinositol into 1,4,5-inositol-*tris*-phosphate (IP_3) and diacylglycerol (Nahorski, 1988). IP_3 is a second messenger which binds an intracellular receptor located on the endoplasmic reticulum (ER) to cause release of Ca^{2+} which was sequestered previously (Henzi and MacDermott, 1992).

The plasma membrane is a permeability barrier which prevents direct influx of Ca^{2+}_e down its large electrochemical gradient. An intact plasma membrane is essential

for preventing unregulated elevations in $[Ca^{2+}]_i$ (Kinter and Pritchard, 1977). Loss of plasma membrane integrity could cause unregulated influx of Ca^{2+}_e, possibly leading to disruption of neuronal function or even cell death. Embedded within the plasma membrane are proteins which function to extrude intracellular Ca^{2+} (Nicotera *et al.*, 1992). The most prominent of these are the Ca^{2+}-ATPase and the Na^+/Ca^{2+} exchanger. The Ca^{2+}-ATPase uses the energy stored in ATP to pump Ca^{2+} against its electrochemical gradient (Michaelis *et al.*, 1987) while the Na^+/Ca^{2+} exchanger lowers $[Ca^{2+}]_i$ by facilitated diffusion (Sanchez-Armass and Blaustein, 1987). Here the energy associated with the influx of extracellular Na^+ down its electrochemical gradient is used to drive Ca^{2+} efflux. Because the inward Na^+ gradient is maintained by the Na^+/K^+-ATPase, both of these integral membrane proteins ultimately require ATP for their activity. Toxicants which alter neuronal plasma membrane integrity can cause elevations in $[Ca^{2+}]_i$ either directly by increasing the Ca^{2+} permeability of the membrane, or indirectly such as by membrane depolarization which results in the activation of Ca^{2+} channels, or by decreasing ATP content within the neuron thereby interfering with the ATP-dependent processes responsible for extruding Ca^{2+}.

Neurons also contain organelles which are capable of sequestering Ca^{2+} (Meldolesi *et al.*, 1988; Blaustein *et al.*, 1978). The most widely accepted are the ER and the mitochondria (Meldolesi *et al.*, 1992). These organelles differ in their mechanisms of Ca^{2+} uptake as well as their role in cellular Ca^{2+} regulation. The ER represents a high affinity, low capacity Ca^{2+} sequestration site believed to be responsible for buffering $[Ca^{2+}]_i$ in the physiological range. The ER membrane contains a Ca^{2+}-ATPase, distinct from that found in the plasma membrane, which transports Ca^{2+} from the cytosol to one

or more storage pools within the ER. This pool of sequestered Ca^{2+} in the ER can be mobilized by certain physiological or pharmacological stimuli, such as the production of IP_3 or the generation of so-called "trigger Ca^{2+}" necessary for Ca^{2+}-induced Ca^{2+} release, or CICR (McPherson and Campbell, 1993). The mitochondria, on the other hand, are a high capacity, low affinity site of Ca^{2+} sequestration (Rahamimoff *et al.*, 1975). The precise mechanism of Ca^{2+} uptake by the mitochondria is not clear, but may involve a ruthenium red-sensitive uniporter located on the inner mitochondrial membrane (Lehninger *et al.*, 1978). Because mitochondria have a K_m for Ca^{2+} uptake in the micromolar range, it is thought that their primary role in Ca^{2+} sequestration is to buffer abusive or pathological elevations in $[Ca^{2+}]_i$ (Åkerman and Nicholls, 1983). However, sequestration of Ca^{2+} by the mitochondria has been observed under physiological conditions (Rizzuto *et al.*, 1992; 1993).

A substantial amount of Ca^{2+} within a neuron is associated with various neuronal Ca^{2+} binding proteins (Habermann and Richardt, 1986). The activity of some of these proteins, such as protein kinase C (PKC) and calcineurin, is regulated by the binding of Ca^{2+} (Persechini *et al.*, 1989). Ca^{2+} also activates the important regulatory protein calmodulin. Neurons also contain other Ca^{2+}-binding proteins, such as calbindin and parvalbumin (Baimbridge *et al.*, 1992), which may act as a Ca^{2+} sink within the neuron. The localization of these proteins within the neuron may assist in buffering changes in $[Ca^{2+}]_i$ both temporally as well as spatially. Thus, Ca^{2+} binding proteins are important both for lowering $[Ca^{2+}]_i$ and maintaining neuronal function.

The regulation of $[Ca^{2+}]_i$ changes as a function of neuronal development and activity. Alterations in $[Ca^{2+}]_i$ homeostasis have been observed during a variety of

physiological processes. As stated above, activation of certain types of neurotransmitter receptors elevates $[Ca^{2+}]_i$ (Malinow *et al.*, 1994), and the process of vesicular release of neurotransmitters is dependent upon Ca^{2+} influx (Miledi, 1973). Maturation of amphibian spinal cord neurons in culture is promoted by elevations in $[Ca^{2+}]_i$ in the cytosol and nucleus (Holliday *et al.*, 1991). These increases in $[Ca^{2+}]_i$ are mediated by CICR and Ca^{2+} influx, and decline with neuronal maturation. Thus, the elevations in $[Ca^{2+}]_i$ which drive cellular development are, in turn, regulated by developmental state. $[Ca^{2+}]_i$ also regulates the outgrowth and morphology of the filopodia of neuronal growth cones (Rehder and Kater, 1992). Filopodia direct growth cones to their targets, and are essential for the development of the nervous system. In *Helisoma* neurons, experimentally-evoked elevations in $[Ca^{2+}]_i$ cause filopodial elongation, followed by retraction. The extent of these changes in filopodial morphology correlates closely with the peak elevation in $[Ca^{2+}]_i$, suggesting a possible role for regulation of $[Ca^{2+}]_i$ in the development of the nervous system. The regulation of $[Ca^{2+}]_i$ can be altered by the mitotic state of the cell (Preston *et al.*, 1991). In HeLa cells at interphase, Ca^{2+} influx is tightly coupled to release of Ca^{2+} from intracellular stores. However, during mitosis, this coupling of Ca^{2+} influx following depletion of Ca^{2+} stores ceases temporarily, demonstrating that regulation of $[Ca^{2+}]_i$ is itself a dynamic process.

Because $[Ca^{2+}]_i$ plays such an integral part in cellular physiology, unregulated or prolonged alterations $[Ca^{2+}]_i$ regulation could result in the disruption of many cellular processes (Rossi *et al.*, 1991; Nicotera *et al.*, 1992). For example, agents which cause undesired elevations in $[Ca^{2+}]_i$ would cause aberrant activation of Ca^{2+}-regulated proteins, possibly leading to cell death. Many toxic insults are believed to be mediated, at least

in part, by elevations in $[Ca^{2+}]_i$ (Tsokos-Kuhn, 1989; Kass, *et al.*, 1988). Hypoxia, induced by either KCN or reduction of O_2, causes elevations in $[Ca^{2+}]_i$ in neuronal tissue, possibly due to the loss of cellular ATP (Johnson *et al.*, 1994). Glutamate-induced excitotoxicity has also been suggested to be mediated by elevations in $[Ca^{2+}]_i$ resulting from abusive stimulation of postsynaptic NMDA receptors (Choi, 1987; Tymianski *et al.*, 1993; Badar-Goffer *et al.*, 1994). In some cell types, elevations in $[Ca^{2+}]_i$ may also be associated with the initiation of programmed cell death (McCabe *et al.*, 1992; Corcoran *et al.*, 1994).

C. Effects of MeHg on neuronal function as an index of disruption of cation regulation.

The focus of initial experiments to examine potential mechanisms of neurotoxicity of MeHg was to characterize the changes in neuronal excitability and synaptic transmission following primarily acute exposure. These studies utilized electrophysiological techniques and suggested that MeHg acts at multiple sites to disrupt neuronal cation homeostasis. Owing to the importance of cation homeostasis in neurons, it was proposed that the neurotoxicity of MeHg was mediated, at least in part, by disruption of neuronal cation homeostasis (Juang, 1976a,b).

Early studies focused on acute *in vitro* exposure to MeHg of frog sciatic nerve-sartorius muscle preparation (Juang, 1976a). Muscle contractions mediated by stimulation of the sciatic nerve were blocked at lower concentrations than those elicited by direct electrical stimulation of the muscle, suggesting that MeHg disrupted neuromuscular transmission by a preferential action on motor nerves. Possible explanations for the disturbances in neuronal function following MeHg application included block of axonal

conduction, reduced depolarization-dependent Ca^{2+} influx into the nerve terminal, impaired docking or fusion of synaptic vesicles with the presynaptic membrane, or inhibition of postsynaptic nAChR.

The possible neuronal sites of action of MeHg were explored initially using electrophysiological techniques (Juang, 1976b). These experiments yielded two key observations concerning the effects of MeHg on neuronal Ca^{2+} regulation. First, some of the effects of MeHg were consistent with a block of Ca^{2+} influx through voltage-dependent Ca^{2+} channels. Second, MeHg caused effects on neuronal function consistent with an alteration in Ca^{2+} homeostasis within the nerve terminal. The block of voltage-dependent Ca^{2+} channels and the increase in $[Ca^{2+}]_i$ were manifested as a decrease in end-plate potential (EPP) amplitude and an increase in the frequency of miniature end-plate potentials (MEPP), respectively (Atchison and Spitsbergen, 1994). MeHg blocked nerve-evoked EPPs at the isolated nerve-muscle synapse by a presynaptic action because it did not alter the response to iontophoretically-applied ACh (Atchison and Narahashi, 1982). The decrease in EPP amplitude, but not the time to complete block of EPPs, was antagonized partially by increasing $[Ca^{2+}]_e$ in the rat phrenic nerve-hemidiapharagm preparation (Atchison *et al.*, 1986; Traxinger and Atchison, 1987). This observation was consistent with a noncompetitive block of voltage-dependent Ca^{2+} channels in the nerve terminal resulting in decreased Ca^{2+} influx following nerve stimulation.

D. Alterations in Ca^{2+} channel function by MeHg.

Because of the indirect nature of investigations of Ca^{2+} channel function *via* examination of alterations in the electrophysiological properties of an isolated

neuromuscular junction, more direct methods of analysis were needed. The possibility that MeHg blocks depolarization-dependent influx of Ca^{2+} through voltage-dependent Ca^{2+} channels was investigated in several model systems, using a variety of techniques. In early studies, the effects of MeHg on Ca^{2+} influx were monitored by radiotracer flux analysis of depolarization-dependent uptake of $^{45}Ca^{2+}$ into synaptosomes isolated from rat cortex. Synaptosomes retain many of the structural and functional characteristics of an intact nerve terminal, and are a useful model system for studying presynaptic nerve terminal function (Gray and Whittaker, 1962).

MeHg inhibited $^{45}Ca^{2+}$ uptake elicited by K^+ depolarization, consistent with a block of voltage-dependent Ca^{2+} channels (Atchison *et al.*, 1986; Shafer and Atchison, 1989; Hewett and Atchison, 1992). The block of $^{45}Ca^{2+}$ uptake could not be reversed by increasing $[Ca^{2+}]_e$, and more detailed kinetic analysis revealed that MeHg acted by a noncompetitive mechanism (Hewett and Atchison, 1992). MeHg decreased the binding affinity of the dihydropyridine nitrendipine to synaptosomes, but effects of MeHg on total nitrendipine binding sites could not be established (Shafer and Atchison, 1989). In these studies, MeHg did not affect the synaptosomal [^{125}I]-conotoxin binding (Shafer *et al.*, 1990). Thus, MeHg appears to alter voltage-dependent Ca^{2+} channel function in synaptosomes, possibly as a noncompetitive inhibitor of dihydropyridine-sensitive Ca^{2+} channels.

Because the distribution of the different voltage-dependent Ca^{2+} channels in synaptosomes is not known, more detailed biochemical and electrophysiological analysis regarding the effects of MeHg on specific known Ca^{2+} channel subtypes were conducted using cells in culture as a model system. The advantage of using cells in culture is that

the effects of MeHg on specific Ca^{2+} channel subtypes could be studied directly using electrophysiological and biochemical techniques. These studies assessed the effects of MeHg on voltage-dependent Ca^{2+} channels expressed by a rat clonal pheochromocytoma cell line (PC12). PC12 cells grown in medium lacking nerve growth factor (NGF) morphologically resemble chromaffin cells of the adrenal medulla (Greene and Tischler, 1976). NGF causes these PC12 cells to differentiate into cells which resemble sympathetic neurons. Because differentiated PC12 cells possess fewer dihydropyridine-sensitive Ca^{2+} channels than undifferentiated cells, it is possible to alter the relative Ca^{2+}-channel distribution in these cells by including NGF in the incubation medium (Shafer and Atchison, 1991a).

MeHg blocked depolarization-dependent $^{45}Ca^{2+}$ uptake into both undifferentiated and NGF-differentiated PC12 cells (Shafer *et al.*, 1990). Electrophysiological analysis of Ba^{2+} currents in NGF-differentiated PC12 cells revealed inactivating and noninactivating components presumably mediated by N- and L-type Ca^{2+} channels, respectively (Shafer and Atchison, 1991b). In differentiated PC12 cells, MeHg decreased the peak Ba^{2+} current, and inhibited completely the rapidly inactivating component of Ba^{2+} current, consistent with a block of N-type Ca^{2+} channels. MeHg also reduced the non-inactivating current in these cells, which was interpreted as a block of L-type Ca^{2+} channels. Thus, MeHg reduces Ca^{2+} currents in differentiated PC12 cell by inhibiting both N- and L-type Ca^{2+} channels. The actions of MeHg Ca^{2+} channel function have also been studied in dorsal root ganglion cells in culture (Arakawa *et al.*, 1991). In this model system, MeHg inhibited total Ca^{2+} current and generated a slow inward current, possibly mediated by a nonspecific cation conductance.

E. Effects of MeHg on presynaptic Ca^{2+} regulation.

In addition to inhibiting EPP amplitude in isolated nerve-muscle preparations, presumably due to decreased ACh release mediated by block of presynaptic voltage-dependent Ca^{2+} channels, MeHg also altered spontaneous release of neurotransmitter measured as changes in the frequency of occurrence of MEPPs (Juang, 1976b; Atchison and Narahashi, 1982; Atchison, 1986). MEPPs are thought to result from the spontaneous fusion of a single synaptic vesicle, or quantum, with the presynaptic plasma membrane, resulting in the discharge of vesicular contents into the synaptic cleft. Agents can alter MEPP characteristics in two distinct ways, assuming there are no postsynaptic effects of a compound. First, the amplitude of individual MEPPs could be increased or decreased by altering the number of neurotransmitter molecules packaged within each vesicle. Changes in MEPP amplitude imply a disruption of neurotransmitter synthesis, storage, or metabolism within the presynaptic nerve terminal. Vesamicol, which impedes transport of ACh into vesicles (Anderson *et al.*, 1983), or hemicholinium-3, which impairs high affinity choline uptake from the synaptic cleft (Sacchi and Perri, 1973), both decrease MEPP amplitude. Another possible effect of toxicants is on the frequency of occurrence of MEPPs. Because the spontaneous fusion of a single vesicle with the presynaptic membrane is a probabilistic event, changes in the frequency of occurrence of MEPPs represent an alteration in the regulation of vesicular docking, fusion or release. Thus, it is possible to evaluate qualitatively the effects of toxicants on vesicular neurotransmitter content and release by monitoring changes in MEPP amplitude and frequency, respectively.

MeHg did not affect the amplitude of MEPPs, but MEPP frequency was first increased, then decreased (Juang and Yonemura, 1975; Juang, 1976b; Atchison and Narahashi, 1982), suggesting that MeHg did not alter ACh synthesis or metabolism within the nerve terminal, but did affect the process of transmitter release. These effects are consistent with an increase in resting Ca^{2+} concentration in the terminal (Miledi, 1973; Shalton and Wareham, 1979). The increases in MEPP frequency caused by MeHg were not affected by the voltage-dependent Na^+ channel blocker TTX or the voltage-dependent Ca^{2+} channel blocker Co^{2+}, either alone or in combination (Miyamoto, 1983). Therefore, the alterations in MEPP frequency could not be attributed to an unregulated increase in $[Ca^{2+}]_i$ mediated by activation of Na^+ or Ca^{2+} channels. This finding also suggested that MeHg does not need to enter the nerve terminal through these channels to elicit its effects. Thus, either the entry of MeHg is not essential, or MeHg is capable of entering the nerve terminal by a route other than the voltage-dependent Na^+ or Ca^{2+} channels, possibly by diffusing across the plasma membrane due to its enhanced lipophilicity.

Increasing the Ca^{2+} permeability at the nerve terminal hastened the time to onset of the MeHg-induced increase in MEPP frequency (Atchison, 1987). Pretreatment with solutions containing slightly elevated K^+ concentration, or the voltage-dependent Na^+ channel activator veratridine, shortened the interval necessary for increased MEPP frequency. This suggested that the increased Ca^{2+} permeability facilitated the entry of MeHg into the terminal, or exacerbated the MeHg-induced elevations in $[Ca^{2+}]_i$. The increase in spontaneous release of neurotransmitter could be attenuated, but not blocked, by removal of Ca^{2+}_e, suggesting a component of the MeHg-induced elevation in $[Ca^{2+}]_i$ was due to Ca^{2+} release from internal stores. Based on these studies it was proposed that

MeHg elevates resting $[Ca^{2+}]_i$ by at least two mechanisms. MeHg increases the plasma membrane permeability to Ca^{2+}_e, and releases Ca^{2+} from an intracellular site.

F. Mitochondrial Ca^{2+} regulation as a target of MeHg.

The observation that MeHg increased MEPP frequency in preparations bathed in Ca^{2+}-free solutions led to investigations to identify the intracellular target of MeHg. Initial studies focused on the possible role of the mitochondria as the intracellular source of Ca^{2+}. Microscopic examination of brain tissue from subjects exposed to MeHg revealed altered mitochondrial morphology (Chang, 1980). Histochemical staining of brain slices for heavy metals demonstrated that mercury was associated with the mitochondrial membrane. The effects of MeHg on mitochondrial function have also been studied. MeHg depolarized the mitochondrial membrane (Hare and Atchison, 1992), inhibited ATP generation (Kauppinen *et al.*, 1989) and disrupted mitochondrial respiration (Levesque and Atchison, 1991). As such, the mitochondria were investigated as the intracellular source of Ca^{2+}.

The effects of MeHg on spontaneous transmitter release were mimicked by several inhibitors of mitochondrial function such as dicoumarol, dinitrophenol, valinomycin and ruthenium red (Levesque and Atchison, 1987). Although these agents interfere with mitochondrial function through different mechanisms, they all increased MEPP frequency. Dicoumarol and dinitrophenol uncouple oxidative phosphorylation, valinomycin is a K^+ ionophore and ruthenium red is a putative inhibitor of the mitochondrial Ca^{2+} uniporter. Ruthenium red was unique in that application of MeHg to nerve-muscle preparations pretreated with ruthenium red did not elicit an increase in MEPP frequency, suggesting

that both agents acted on a common Ca^{2+} pool, possibly the mitochondria. This effect could not be attributed to a ruthenium red-induced depletion of vesicular stores or block of postsynaptic nAChR since La^{3+} increased MEPP frequency in ruthenium red-treated preparations. Another inhibitor of mitochondrial Ca^{2+} regulation, *N,N*-bis(3,4-dimethoxyphenethyl)-*N*-methylamine (YS035), also blocked the effects of MeHg, but not La^{3+}, on MEPP frequency (Levesque and Atchison, 1988). These results suggested that release of Ca^{2+} previously sequestered in the mitochondria contributed to the MeHg-induced elevations in $[Ca^{2+}]_i$.

The effects of MeHg on mitochondrial Ca^{2+} regulation were studied directly using intact mitochondria isolated from rat brain (Levesque and Atchison, 1991). Ca^{2+} uptake by isolated mitochondria occurs by two mechanisms which differ in magnitude and ATP requirement. $^{45}Ca^{2+}$ uptake *via* the ATP-dependent mechanism is approximately an order of magnitude greater than the ATP-independent component. MeHg inhibited both components of mitochondrial Ca^{2+} uptake. The ability of MeHg to release Ca^{2+} sequestered within the mitochondria was studied by loading the mitochondria with $^{45}Ca^{2+}$, in the absence or presence of ATP, prior to MeHg exposure. MeHg reduced mitochondrial $^{45}Ca^{2+}$ content which had previously been loaded into the mitochondria, regardless of ATP. The reduction in mitochondrial $^{45}Ca^{2+}$ content could be due to stimulation of Ca^{2+} efflux, or block of Ca^{2+} uptake necessary for Ca^{2+} cycling. Ruthenium red also reduced the loading of $^{45}Ca^{2+}$ into the mitochondria, in the absence or presence of ATP. Ruthenium red prevented the MeHg-induced reduction in mitochondrial $^{45}Ca^{2+}$ content, but did not block the binding of Me[^{203}]Hg to the mitochondria (Levesque and Atchison, 1991). Taken together, this evidence suggested that MeHg-induced disruption

mitochondria Ca^{2+} regulation contributed to the elevations in $[Ca^{2+}]_i$ in the nerve terminal, and that ruthenium red acted on a similar Ca^{2+} pool of mitochondrial Ca^{2+} as MeHg.

While it was apparent that MeHg was capable of disrupting mitochondrial Ca^{2+} regulation, the relationship of this effect to the elevations in $[Ca^{2+}]_i$ and spontaneous release of neurotransmitter was unknown. The magnitude of MeHg-induced release of transmitter was quantified using synaptosomes preloaded with various radiolabelled neurotransmitters. MeHg caused release of dopamine, γ-aminobutyric acid and ACh from nondepolarized synaptosomes prepared from striatum, cortex and hippocampus (Minnema *et al.*, 1989). MeHg did not affect the release of these neurotransmitters elicited by depolarization with solutions containing elevated concentrations of K^+. This suggested that, in synaptosomes, the block of voltage-dependent Ca^{2+} channel by MeHg was not sufficient to impede transmitter release. MeHg also released $^{45}Ca^{2+}$ preloaded into isolated mitochondria, but did not release preloaded $^{45}Ca^{2+}$ from intact synaptosomes. It was concluded that MeHg released of Ca^{2+} from the mitochondria, and that this Ca^{2+} remained within the cytosol of the intact synaptosomes to cause an elevation in $[Ca^{2+}]_i$. The amount of Ca^{2+} released from the mitochondria was sufficient to support spontaneous release of neurotransmitter from synaptosomes. However, the experimental design for loading the synaptosomes with $^{45}Ca^{2+}$ may have allowed for exchange of the radiolabelled $^{45}Ca^{2+}$ within the synaptosomes for nonradioactive Ca^{2+} in the extrasynaptosomal buffer. This could have caused depletion of $^{45}Ca^{2+}$ from the radiolabelled intracellular pool prior to the addition of MeHg. If remaining pools of $^{45}Ca^{2+}$ within the synaptosomes are not mobilized by MeHg, then these experiments would conclude incorrectly that MeHg did not affect $[Ca^{2+}]_i$.

Ruthenium red also increased spontaneous release of ACh from synaptosomes, although the amount of released ACh was not as great as that elicited by MeHg (Levesque *et al.*, 1992). Pretreatment of synaptosomes with ruthenium red caused a concentration-dependent reduction in MeHg-induced ACh release in the presence or absence of added Ca^{2+}_e. While this evidence suggested disruption of mitochondrial Ca^{2+} regulation following MeHg exposure was sufficient to elicit spontaneous release of ACh, it was by no means conclusive. Moreover, MeHg-induced depolarization of the mitochondrial membrane was not inhibited by ruthenium red, suggesting that either the effects of ruthenium red or MeHg were not mediated by depolarization of the mitochondria.

G. Techniques for measuring $[Ca^{2+}]_i$.

The limitation of previous experiments studying the effects of MeHg on $[Ca^{2+}]_i$ in the nerve terminal is that they relied upon indirect measurements, or inference, in most instances. The synthesis of indicators based on polyvalent cation chelators (Smith *et al.*, 1983; Tsien *et al.*, 1982; Grynkiewicz *et al.*, 1985; Minta *et al.*, 1989) allowed for the measurement of $[Ca^{2+}]_i$ in isolated neuronal preparations (Komulainen and Bondy, 1987a). These compounds had several significant advantages over their predecessors. Unlike the photoprotein aequorin and the fluorochrome arsenazo III, these new indicators were not structurally inactivated upon binding of Ca^{2+}. They also interacted with Ca^{2+} in a reversible manner, with dissociation constants for Ca^{2+} in the physiological range, allowing changes in $[Ca^{2+}]_i$ to be monitored more consistently over time. The new indicators could also be loaded into cells, and calibrated, relatively easily. Some

disadvantages of Ca^{2+} detection remained, however. The new compounds were not entirely Ca^{2+} specific (Grynkiewicz *et al.*, 1985), and certain cells could actively transport the dyes from the cytosol (DiVirgilio *et al.*, 1988). Even these problems could be circumvented by the use of cell-permeant heavy metal chelators (Arslan *et al.*, 1985), and inhibitors of the organic anion transporter.

The most commonly utilized structural design of these Ca^{2+}-sensitive indicators is to position a fluorescent group near the Ca^{2+}-binding region of the chelator (Fig. 1.1). The binding of Ca^{2+} distorts the electronic configuration of the nearby fluorescent group, resulting in a shift in the fluorescent properties of the dye in the Ca^{2+}-free and Ca^{2+}-bound form. The relatively high sensitivity of fluorometry permits excellent temporal and spatial resolution of $[Ca^{2+}]_i$. Some Ca^{2+}-sensitive fluorescent indicators have been designed for specific purposes or techniques. For example, fura-2 is used extensively in epifluorescence microscopy, indo-1 is used primarily in continuous and stopped-flow cytometry, and fluo-3 is used primarily in fluorescence-activated cell sorting and confocal microscopy. In this way, a Ca^{2+}-sensitive fluorescent dye exists for virtually every detection system. There are limitations to the use of fluorescent dyes, though. A major drawback lies in their affinity for cations other than Ca^{2+} (Grynkiewicz *et al.*, 1985; Tomsig and Suszkiw, 1990; Hechtenberg and Beyersmann, 1993; Hinkle *et al.*, 1992). The interaction of these indicators with cations other than Ca^{2+} confounds accurate determination of $[Ca^{2+}]_i$ (Arslan *et al.*, 1985; Mason and Grinstein, 1990). Another problem is the intrinsic fluorescence of certain cells, such as red blood cells, makes fluorescence analysis difficult, if not impossible (Murphy *et al.*, 1986).

FIG. 1.1. The chemical structure of the fluorescent cation indicator fura-2. The four carboxylic acid groups form the cation binding pocket, while the polycyclic ring system is fluorescent group. Binding of cations alters the electronic configuration of the fluorescent moiety, causing a shift in the fluorescence properties of the molecule.

Fig. 1.1.

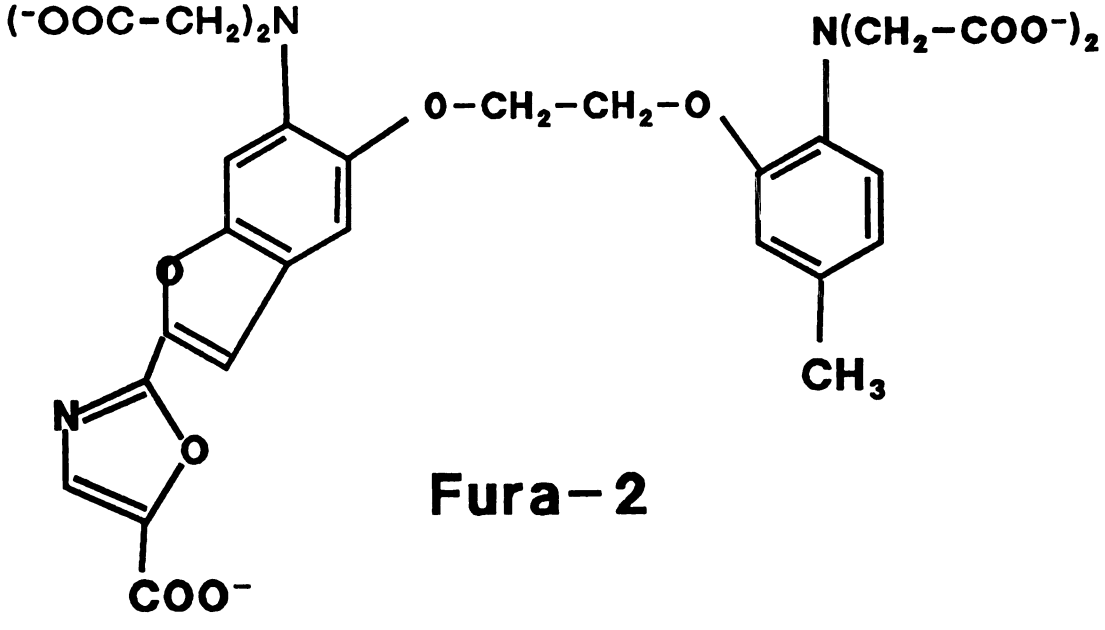

Fura-2

Indicators resembling the fluorescent dyes have also been constructed for use with ^{19}F-nuclear magnetic resonance (NMR) spectroscopy (Smith *et al.*, 1983). The structure of these indicators contains equivalent fluorine nuclei instead of the fluorescent groups (Fig 1.2). When a cation binds to the indicator, it withdraws the electrons surrounding the fluorine nuclei, deshielding it from the applied magnetic field. This alters the resonance properties of the fluorine nuclei, and generates a resonance peak in the ^{19}F spectrum. Since each cation deshields the fluorine nuclei to a different extent, their corresponding resonance peaks are distinct. ^{19}F-NMR spectroscopy has several advantages over fluorescence-based systems (Bachelard and Badar-Goffer, 1993). First, nonspecificity is not a problem since the identity of the cation binding to the fluorinated indicator is readily apparent. Second, the changes in the intracellular concentrations of several cations can be monitored simultaneously. For example, using ^{19}F-NMR spectroscopy of NG108-15 cells loaded with the fluorinated chelator 5F-BAPTA, changes in the intracellular concentrations of Ca^{2+}, Pb^{2+} and Zn^{2+} can be measured concurrently following Pb^{2+} exposure (Schanne *et al.*, 1989). Third, in a single preparation, the changes in the cellular concentrations of polyvalent cations and high energy phosphates can be monitored by using ^{19}F- and ^{31}P-NMR spectroscopy in tandem (Badar-Goffer *et al.*, 1994). Fourth, because no endogenous fluorine is present in cell, there are no difficulties associated with intrinsic fluorine resonance. The main disadvantage of ^{19}F-NMR spectroscopy is that its low sensitivity necessitates lengthy spectral acquisition intervals, reducing temporal resolution to tens of minutes, as opposed to the tenths of seconds resolution obtained with fluorescent indicators. Another drawback of this technique is its inability to generate useful spatial information at the cellular level.

FIG 1.2. The chemical structure of the fluorinated cation indicator 5F-BAPTA. The four carboxylic acid groups form the cation binding pocket, while the resonance of the fluorine nuclei is observable using NMR spectroscopy. Binding of cations withdraws the electrons which surround the fluorine nuclei, altering its resonance properties.

Fig. 1.2.

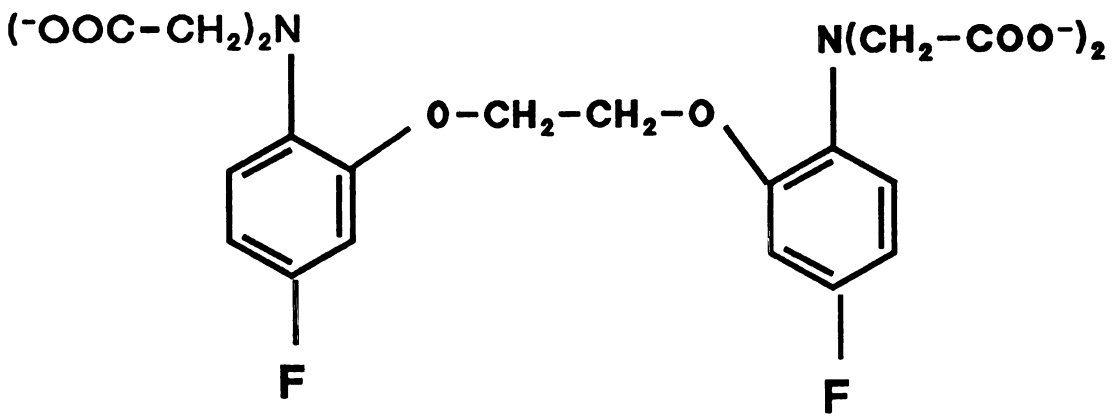

5F-BAPTA

H. Effects of MeHg on neuronal divalent cation homeostasis.

Acute exposure of synaptosomes loaded with the fluorescent chelator fura-2 to MeHg caused a time- and concentration-dependent increase in $[Ca^{2+}]_i$ (Komulainen and Bondy, 1987b). The elevations in $[Ca^{2+}]_i$ were also dependent on $[Ca^{2+}]_e$, and were not reduced by the voltage-dependent Ca^{2+} channel blocker verapamil. This suggested MeHg did not cause Ca^{2+} influx through these channels, consistent with results gathered using radiotracer flux analysis and electrophysiological techniques. The MeHg-induced elevations in $[Ca^{2+}]_i$ were potentiated by ouabain or depletion of cellular ATP. Depolarization of the mitochondrial membrane with rotenone and oligomycin decreased these elevations in $[Ca^{2+}]_i$ providing additional suggestive evidence for MeHg-induced disruption of mitochondrial Ca^{2+} regulation.

The concentration-dependence of the possible contributions of extracellular and mitochondrial Ca^{2+} sources to the MeHg-induced elevations in $[Ca^{2+}]_i$ was investigated in greater detail using fura-2 loaded synaptosomes (Kauppinen *et al.*, 1989). MeHg concentrations below 30 μM increased $[Ca^{2+}]_i$, but did not increase fura-2 leak from the synaptosomes, suggesting that MeHg acted at an intracellular target without significantly disrupting the plasma membrane. These concentrations of MeHg also altered mitochondrial function without affecting the plasma membrane potential. Higher concentrations of MeHg caused pronounced elevations in $[Ca^{2+}]_i$, and increased Mn^{2+} quenching of fura-2, which coincided with depolarization of the plasma membrane. This suggested that lower concentrations of MeHg increased $[Ca^{2+}]_i$ by an action at an intracellular Ca^{2+} store, possibly the mitochondria, while higher concentrations increased the plasma membrane permeability to $Ca^{2+}{}_e$.

Additional analysis of the effects of MeHg on neuronal divalent cation homeostasis revealed that in addition to elevating the $[Ca^{2+}]_i$, MeHg also increased the intrasynaptosomal concentration Zn^{2+} ($[Zn^{2+}]_i$) (Denny *et al.*, 1993; Denny and Atchison, 1994). The mechanisms mediating the elevations in $[Ca^{2+}]_i$ and $[Zn^{2+}]_i$ are distinct both temporally and mechanistically. The elevations in $[Zn^{2+}]_i$ are immediate and precede the gradual increase in $[Ca^{2+}]_i$. The increases in $[Zn^{2+}]_i$ are mediated by release of Zn^{2+} from several soluble synaptosomal proteins, while the elevations in $[Ca^{2+}]_i$ are due to increased plasma membrane permeability to Ca^{2+} leading to a Ca^{2+}_e-dependent elevation in $[Ca^{2+}]_i$ (Denny *et al.*, 1993, Denny and Atchison, 1995). The elevations in $[Ca^{2+}]_i$ are believed to be responsible for alterations in spontaneous transmitter release observed following MeHg treatment.

Similar findings have been obtained in other neuronal model systems. MeHg also elevates the intracellular concentrations of Ca^{2+} and another endogenous polyvalent cation, presumed to be Zn^{2+}, in neuroblastoma × glioma (NG108-15) hybrid cells (Hare *et al.*, 1993) and isolated cerebellar granule cells in culture (Marty *et al.*, 1995). In NG108-15 cells, a component of the elevations in $[Ca^{2+}]_i$ is mediated by release of Ca^{2+} which was sequestered previously in the IP_3-sensitive Ca^{2+} pool of the ER (Hare and Atchison, 1995). However, MeHg mobilizes this Ca^{2+} pool without generating IP_3. In NG108-15 cells treated with MeHg these elevations in $[Ca^{2+}]_i$ can be delayed by nifedipine or TTX (Hare and Atchison, 1996). This suggests voltage-dependent Ca^{2+} or Na^+ channels are involved in the MeHg-induced increases in plasma membrane permeability to Ca^{2+}, possibly by augmenting MeHg entry into the cells.

CHAPTER TWO

METHYLMERCURY ALTERS INTRASYNAPTOSOMAL CONCENTRATIONS OF ENDOGENOUS POLYVALENT CATIONS

ABSTRACT

The effects of MeHg on intrasynaptosomal polyvalent cation concentrations were examined using fura-2. In the presence of Ca^{2+}_e, MeHg caused a concentration-dependent, biphasic elevation in the ratio of fluorescence intensity at the emission wavelength of 505 nm following excitation at 340 and 380 nm (340/380 nm ratio). The first phase was independent of Ca^{2+}_e and complete within five sec. The second phase was dependent upon Ca^{2+}_e and not complete within six min. MeHg increased the synaptosomal membrane permeability to Mn^{2+} suggesting that the second phase was due to influx of Ca^{2+}_e. Ruthenium red (20 μM), mitochondrial depolarization (10 mM NaN_3 plus 4 μg/ml oligomycin), thapsigargin (1 μM), or caffeine (40 mM) did not elevate $[Ca^{2+}]_i$ or alter the response of the synaptosomes to MeHg. Upon closer inspection, we noticed that MeHg simultaneously increased the fluorescence intensity at the excitation wavelengths of 340 and 380 nm, and at the Ca^{2+}-insensitive excitation wavelength of 360 nm. Pretreatment of synaptosomes with the cell-permeant heavy metal chelator *N,N,N',N'*-tetrakis-(2-pyridylmethyl)ethylene-diamine (TPEN, 50 μM) blocked the MeHg-induced elevations in 360 nm intensity and 340/380 nm ratio. TPEN given after MeHg, reversed the elevations in 360 nm intensity. The cell-impermeant heavy metal chelator diethylenetriaminepentaacetic acid (DTPA, 150 μM) had no effect. We conclude that MeHg disrupts polyvalent cation homeostasis by at least two mechanisms. The first involves release of endogenous non-Ca^{2+} polyvalent cations while the second is due to increased Ca^{2+} permeability of the plasma membrane.

INTRODUCTION

Fluctuations in $[Ca^{2+}]_i$ regulate many cellular processes, including neurotransmitter release, cell differentiation, growth cone elongation and excitation-contraction coupling (Bertolino and Llinàs, 1992). Sustained or unregulated excessive elevations in $[Ca^{2+}]_i$ are toxic (Nicotera *et al.*, 1992). CCl_4-induced hepatotoxicity (Tsokos-Kuhn *et al.*, 1986; Tsokos-Kuhn, 1989) and 1-methyl-4-phenylpyridinium (MPP^+) toxicity in the *substantia nigra* (Kass *et al.*, 1988) are both believed to be related to loss of Ca^{2+}-regulating ability. Excitatory amino acid neurotoxicity is also thought to be associated with pathological elevations of $[Ca^{2+}]_i$ *via* activation of NMDA receptors (Choi, 1987).

Neurons are sensitive to sustained elevations in $[Ca^{2+}]_i$. Nerve terminals are particularly affected by impaired $[Ca^{2+}]_i$ homeostasis, because of their large surface area to volume ratio, and the importance of tightly controlled spatial and temporal changes in $[Ca^{2+}]_i$ necessary for secretion (Blaustein, 1988). Changes in $[Ca^{2+}]_i$ at the nerve terminal alter many processes, including synaptic transmission.

MeHg, a known neurotoxicant, causes alterations in synaptic transmission which are characteristic of impairments in normal entry of Ca^{2+} during depolarization and sustained, unregulated elevations of $[Ca^{2+}]_i$ within the nerve terminal. Acute application of MeHg to isolated nerve terminals elevates $[Ca^{2+}]_i$ (Komulainen and Bondy, 1987a; 1987b; Kauppinen *et al.*, 1989). Effects of MeHg on Ca^{2+} homeostasis are believed to be mediated in part by increased plasma membrane permeability to Ca^{2+} since reducing the $[Ca^{2+}]_e$ decreases the functional effects of MeHg at intact synapses (Atchison, 1986) and synaptosomes (Levesque *et al.*, 1992). Removal of Ca^{2+}_e decreases, but does not block the MeHg-induced elevations in $[Ca^{2+}]_i$ in synaptosomes (Komulainen and Bondy,

1987b). Disruption of intracellular Ca^{2+} regulation is believed to mediate the effects of MeHg on $[Ca^{2+}]_i$ and nerve terminal function following removal of Ca^{2+}_e.

Because normal secretory function requires tight spatial and temporal regulation of $[Ca^{2+}]_i$, Ca^{2+} homeostasis within the nerve terminal is maintained by the concerted buffering action of Ca^{2+} binding proteins, endoplasmic reticulum (ER) and mitochondria (Blaustein *et al.*, 1980; Åkerman and Nicholls, 1983). The respective contributions of these storage pools varies according to the extent and duration of the Ca^{2+} load. Disruption of Ca^{2+} regulating abilities results in responses typically associated with elevations in $[Ca^{2+}]_i$. Several lines of evidence implicate disruption of intracellular Ca^{2+} regulation in the toxic actions of at least acute, *in vitro* application of MeHg. In isolated mitochondria, MeHg prevents uptake of $^{45}Ca^{2+}$ and induces its release following preloading (Levesque and Atchison, 1991). Inhibition of Ca^{2+} release by YS035 (Deana *et al.*, 1984) and ruthenium red (Moore, 1971), a putative inhibitor of the mitochondrial Ca^{2+}-uniporter, blocks the spontaneous release of transmitter induced by MeHg at intact peripheral synapses (Levesque and Atchison, 1987; 1988) and isolated central nerve terminals (Levesque *et al.*, 1992). Ruthenium red also blocks MeHg-induced release of $^{45}Ca^{2+}$ from preloaded mitochondria (Levesque and Atchison, 1991). Additionally, MeHg disrupts mitochondrial functions (Verity *et al.*, 1975; Levesque and Atchison, 1991). Finally, inhibitors of oxidative phosphorylation such as dinitrophenol and dicoumarol cause effects similar to those of MeHg at intact synapses (Levesque and Atchison, 1987).

The present study was initiated to determine the respective contributions of intracellular Ca^{2+} stores to the MeHg-induced elevations in $[Ca^{2+}]_i$. We focused initially on the mechanism of block by ruthenium red of MeHg-induced effects on mitochondrial

Ca^{2+} buffering and its potential relationship to the putative changes in $[Ca^{2+}]_i$. We hypothesized that ruthenium red would prevent MeHg-induced elevations in $[Ca^{2+}]_i$ by preventing release of mitochondrial Ca^{2+} stores. Paradoxically, mitochondria did not contribute to changes in fura-2 fluorescence in synaptosomes. During the course of these experiments, we observed changes in the fura-2 fluorescence signals induced by MeHg which were inconsistent with changes in $[Ca^{2+}]_i$. As such, we examined these changes in some detail with respect to their implications for the action of MeHg on nerve terminal cation homeostasis.

MATERIALS AND METHODS

Chemicals and Solutions: Methylmercuric chloride (MeHg) was obtained from K and K Labs, Plainview, N.Y. Fura-2 pentapotassium salt, the acetoxymethyl ester derivative of fura-2 (fura-2AM) and TPEN were purchased from Molecular Probes, Eugene, OR. Thapsigargin was purchased from LC Services, Woburn, MA. Sodium azide was supplied by Aldrich, Milwaukee, WI. Caffeine, DTPA, oligomycin, ethyleneglycol-bis(β-aminoethyl ether)-*N,N,N',N'*-tetraacetic acid (EGTA), Na^+-Hepes, ruthenium red, Trizma base, and Trizma HCl were obtained from Sigma, St. Louis, MO. Dimethyl sulfoxide (DMSO) was obtained from J.T. Baker, Phillipsburg, NJ. All other chemicals were reagent grade.

Hepes buffer (HBS) contained (mM): NaCl, 135; KCl, 5; $MgCl_2$, 1; d-glucose, 10; and *N*-(2-hydroxyethyl)piperazine-*N'*-(2-ethanesulfonic acid) (Na^+-Hepes), 10. The pH at room temperature was adjusted to 7.4 with Trizma HCl. HBS contained 6 μM Ca^{2+} as measured by inductively coupled plasma spectroscopy (Atchison, 1986), and is hereafter referred to as 6 μM Ca^{2+}-HBS. During loading of synaptosomes with fura-2AM, 200 μM $CaCl_2$ was present in the HBS (200 μM Ca^{2+}-HBS). A 1 mM stock solution of fura-2AM was prepared twice a week in anhydrous DMSO. MeHg was prepared weekly as a 10 mM stock solution in appropriate HBS. Ruthenium red was prepared in 200 μM Ca^{2+}-HBS and diluted six-fold upon addition to synaptosomes. NaN_3 was prepared daily in deionized water as a 1 M stock solution. Oligomycin stock solutions (4 mg/ml) were dissolved in absolute ethanol. TPEN (2 mM) was dissolved in a solution of 50% (v/v) ethanol/deionized water which yielded a final ethanol concentration of 1.25% after addition to the synaptosomal suspension. EGTA (1 M) for R_{min} determination was

dissolved in deionized water and the pH at room temperature adjusted with Trizma base to greater than 8. DTPA was prepared as a 15 mM stock solution in deionized water and dissolved by addition of NaOH. Caffeine was prepared as a 1.33 M stock solution and gently heated until dissolved. Thapsigargin was prepared as a 100 µM stock solution in 0.5% (v/v) DMSO. Control solutions contained appropriate concentrations of the solvents used.

Preparation of Synaptosomes: Synaptosomes were prepared by discontinuous sucrose gradient centrifugation as described in detail by Shafer and Atchison (1989) with slight modifications. The sucrose buffers were prepared in 3 mM Na_2HPO_4 buffer adjusted to pH 7.4 with HCl. The P_{2b} fraction (Gray and Whittaker, 1964) was resuspended in 6 µM Ca^{2+}-HBS, centrifuged at 10,000 x *g* for 10 min and resuspended in 10 ml 200 µM Ca^{2+}-HBS. The synaptosomal preparation was then split into two 5 ml fractions; fura-2AM was added to one fraction (5 µM final concentration) while the other received DMSO alone. The final concentration of DMSO in both fractions was 0.5% (v/v). Both fractions were incubated at 30°C for 30 min to allow for uptake and hydrolysis of the fura-2AM. The fractions were then diluted six-fold by addition of 25 ml of 200 µM Ca^{2+}-HBS and incubated for an additional 15 min at 30°C to promote diffusion of partially hydrolyzed fura-2AM from the synaptosomes. After centrifugation at 10,000 x *g* for 5 min, the pellets were resuspended in 10 ml 200 µM Ca^{2+}-HBS, and kept on ice until needed, but no longer than three hr.

Determination of 340/380 nm ratio and $[Ca^{2+}]_i$: Although concentrations of MeHg up to 1 mM did not affect the fluorescence of 0.5 μM fura-2 pentapotassium salt when tested in a cuvette (Fig. 2.1), the addition of MeHg to fura-2 loaded synaptosomes changed fura-2 fluorescence in ways inconsistent with elevations in $[Ca^{2+}]_i$ (see below). This effect was inhibited by a cell-permeant heavy metal chelator. Some concentrations of MeHg also caused leakage of fura-2 from the synaptosomes. For these reasons, the conversion of ratios to $[Ca^{2+}]_i$ was precluded in most instances. Instead, the results are usually reported as changes in the ratio of 340 nm to 380 nm excitation intensity monitored at 505 nm (340/380 nm ratio). In certain instances, when low concentrations of MeHg were used and the increase in intracellular heavy metal concentration was prevented by a cell-permeant chelator, $[Ca^{2+}]_i$ determination could be made.

Fura-2 loaded synaptosomes were centrifuged at 12,500 x *g* for 30 sec. The resulting pellet was resuspended in two ml of either 6 μM Ca^{2+}-HBS (for studies involving $[Ca^{2+}]_e$ of 6 μM or 0.1 μM) or 200 μM Ca^{2+}-HBS (for studies involving 200 μM $[Ca^{2+}]_e$), transferred to a test tube, and incubated for 10 min at 37°C. The suspension was transferred to a polystyrene cuvette containing a magnetic stir bar and placed into a spectrofluorometer (SPEX Industries, Edison, NJ) equipped with a thermally jacketed cuvette holder at 37°C. The emission intensity was monitored at 505 nm (bandpass of 3.77 nm) following excitation (450 W xenon lamp) of the synaptosomal suspension at 340 and 380 nm, or 360 and 380 nm. Alternating excitation wavelengths were obtained using a beam chopper. Ratios and $[Ca^{2+}]_i$ were corrected for intrinsic fluorescence using synaptosomes treated with 0.5% DMSO only. The intensity recordings of fura-2 loaded synaptosomes were also corrected for leakage of fura-2 from synaptosomes not exposed

FIG. 2.1. The effect of MeHg on the fluorescence properties of fura-2. Excitation scans of fura-2 in 6 μM Ca^{2+}-HBS were acquired before (*solid line*) and after (*dashed line*) the addition of 50 μM MeHg. Fluorescence intensity was monitored at the emission wavelength following excitation at integer wavelength values between 320 and 400 nm. Concentrations of MeHg up to 1 mM did not affect the fluorescence properties of fura-2.

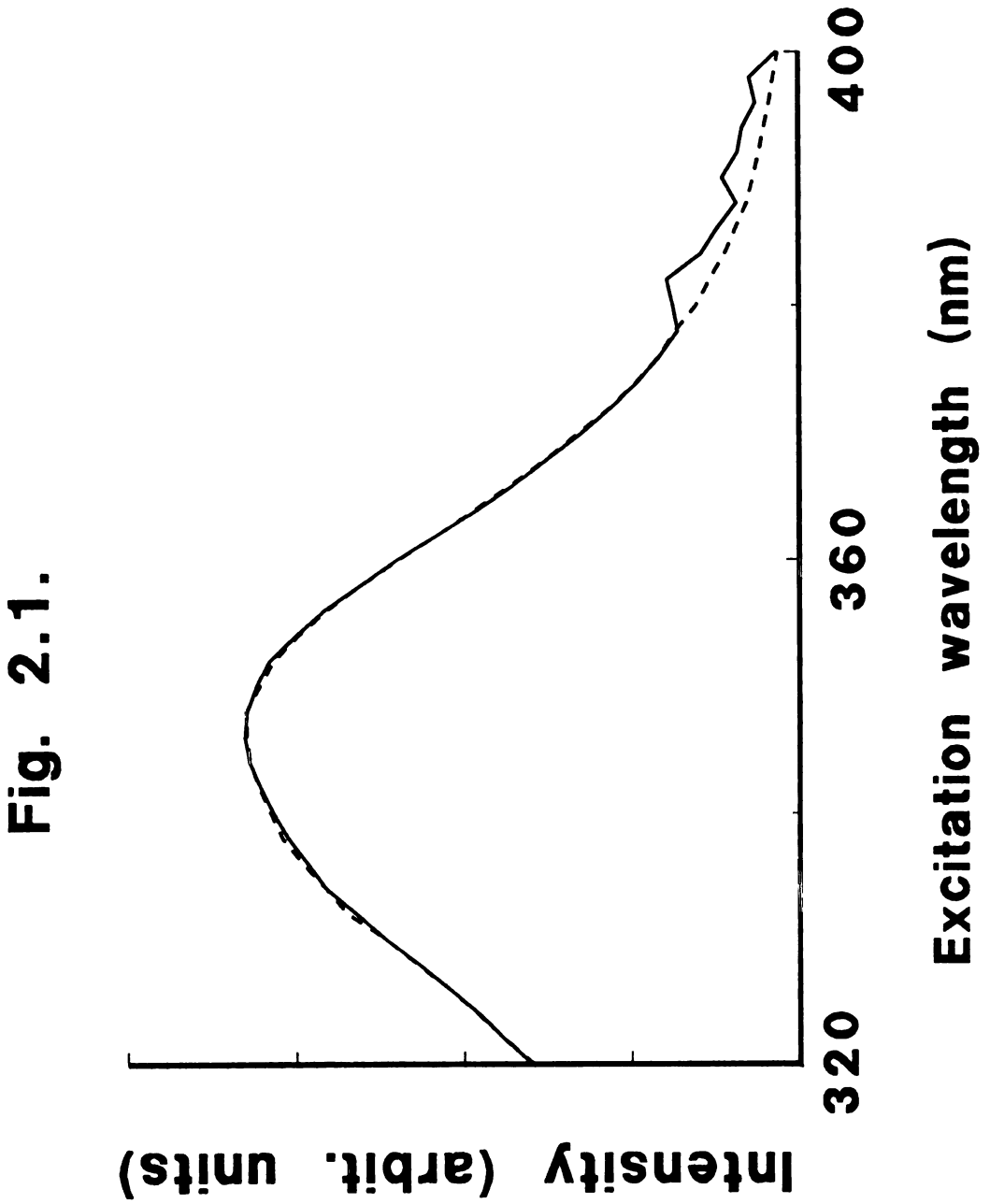
Intensity (arbit. units)
320
360
400
Excitation wavelength (nm)

Fig. 2.1.

to MeHg. Mn^{2+} (final concentration 40 μM) was added to a fura-2 loaded synaptosomal suspension and the fluorescence intensity remaining two sec after addition was subtracted from the intensity prior to Mn^{2+} addition. This difference was due to extracellular fura-2 and was subtracted from all intensity recordings from that preparation. The sample used for determination of extracellular fura-2 was not used for any other experiments. Ratios were determined by dividing the corrected intensity recording from excitation at 340 nm by that of 380 nm excitation. When appropriate, $[Ca^{2+}]_i$ was calculated from the equation of Grynkiewicz, *et al.* (1985): $[Ca^{2+}]_i=K_d[(R-R_{min})/(R_{max}-R)]x(S_{f2}/S_{b2})$: where R_{max} is the 340/380 nm ratio during Ca^{2+} saturation, and R_{min} is the 340/380 nm ratio during Ca^{2+}-free conditions. S_{f2} and S_{b2} are the emission intensities at 380 nm excitation during Ca^{2+}-free and Ca^{2+}-saturating conditions, respectively. R_{max} was determined by lysing the synaptosomes with 0.1% (v/v) TritonX-100 in 2 mM Ca^{2+}. R_{min} was determined on the same sample by adding 50 mM EGTA (pH remained at 7.4). Synaptosomal preparations yielding R_{max} values less than 3.00 were rejected due to inadequate fura-2AM hydrolysis.

Assessment of synaptosomal permeability to divalent cations after MeHg treatment: Quenching of the fura-2 signal by Mn^{2+} was used to assess the permeability of the synaptosomal plasma membrane to divalent cations. Synaptosomal preparations were incubated with MeHg (0 - 100 μM) for six min. The fluorescence intensity at the Ca^{2+}-insensitive wavelength of 360 nm was monitored every 0.2 sec. After establishing a ten sec baseline, Mn^{2+} (40 μM final concentration) was added directly into the cuvette from an overhead injection port without interrupting data acquisition. The ability of the Mn^{2+} to quench total fura-2 fluorescence was monitored for four min.

To assess the immediate effects of MeHg on divalent cation permeability, Mn^{2+} was added prior to MeHg. Leak of fura-2 from the synaptosomes was determined by the subsequent addition of 150 μM DTPA to the synaptosomal suspension after a three min exposure to MeHg. If MeHg elevated extracellular fura-2 concentrations during the three min exposure, the immediate reversal in quenching produced by DTPA should exceed the initial quench produced by Mn^{2+} addition.

Evaluation of non-Ca^{2+} polyvalent cation contributions to fluorescence: Many cations interact with fura-2 (Grynkiewicz *et al.*, 1985). Thus since some of the alterations in fura-2 fluorescence were inconsistent with changes in $[Ca^{2+}]_i$, MeHg might alter the intracellular concentrations of cation(s) other than Ca^{2+}. To test this possibility, the effects of either the cell-permeant heavy metal chelator TPEN or the cell-impermeant heavy metal chelator DTPA on MeHg-induced elevations in 340/380 nm ratio and 360 nm excitation intensity were monitored.

Statistical analysis: Elevations in 340/380 nm ratio were analyzed by a one-way block analysis of variance. *Post-hoc* analysis was performed using Tukey's test ($p<0.05$) (Steel and Torrie, 1980).

RESULTS

In 200 µM Ca^{2+}-HBS, MeHg caused a biphasic increase in the 340/380 nm ratio that was concentration- and time-dependent (Fig. 2.2). The first phase increase was rapid and complete within five sec after MeHg addition. The magnitude of this phase was determined by subtracting the average ratio value ten sec prior to MeHg addition (50-60 sec) from that obtained ten sec following MeHg addition (62-72 sec) (inset, Fig. 2.2). Addition of 200 µM Ca^{2+}-HBS caused a change in the resting 340/380 nm ratio of 0.06 ± 0.01 (mean ± standard error of the mean, S.E.M.) during this initial phase. MeHg concentrations of 10, 25, 50 and 100 µM caused 340/380 nm ratio changes of 0.18 ± 0.04, 0.25 ± 0.06, 0.25 ± 0.07 and 0.25 ± 0.08, respectively. These changes were not statistically different from control (n=3, $p>0.05$), but suggest that the initial phase was concentration-dependent up to 25 µM MeHg.

The rate of increase in 340/380 nm ratio during the second phase was gradual with no plateau occurring during the six min exposure period. Unlike the first phase, the second phase was not maximal at 25 µM MeHg. With the exception of 10 µM MeHg, the second phase elevations were several-fold greater than the initial elevations. The second phase was concentration-dependent with respect to both MeHg and Ca^{2+}_e. Lowering $[Ca^{2+}]_e$ to 6 µM reduced the second phase elevations relative to those at 200 µM $[Ca^{2+}]_e$ for all MeHg concentrations tested (not shown).

To determine the extent of Ca^{2+}_e dependence of the two phases, EGTA was added to the synaptosomal suspension to reduce $[Ca^{2+}]_e$ further. Since $[Ca^{2+}]_i$ in nerve terminals ranges between 100 to 300 nM (Nachshen, 1985; Komulainen and Bondy, 1987a,b; Kauppinen *et al.*, 1989), and the Ca^{2+} content of synaptosomes can be readily depleted

FIG. 2.2. The effect of MeHg on the 340/380 nm ratio in 200 μM Ca^{2+}-HBS. MeHg (0-100 μM) was added at 1 min to fura-2 loaded synaptosomes in 200 μM Ca^{2+}-HBS. Changes in the ratio emission intensity at 505 nm following excitation at 340 and 380 nm were monitored. Each trace represents the mean of three experiments. *Inset*: The immediate elevations in 340/380 nm ratio caused by the various concentrations of MeHg were determined by subtracting the average ratio value 10 sec prior to MeHg addition from that 10 sec following addition and presented as the mean ± S.E.M. for three experiments. These MeHg-induced changes in 340/380 nm ratio were then compared by a one-way block analysis of variance (ANOVA). None of the elevations differed statistically ($p>0.05$, $n=3$).

Fig. 2.2.

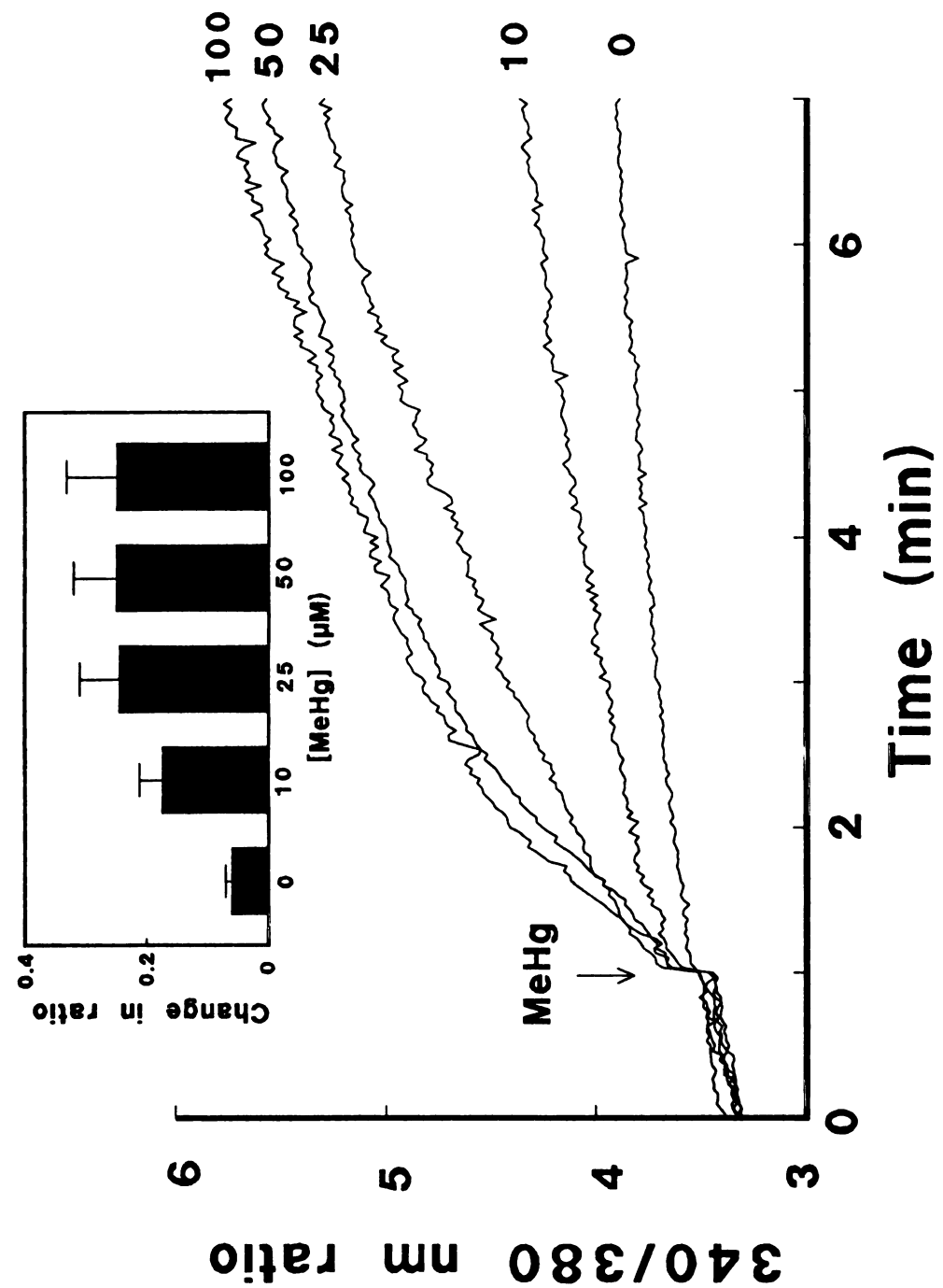
340/380 nm ratio
Time (min)
MeHg
100
50
25
10
0
[MeHg] (μM)
Change in ratio

by incubation with low Ca^{2+} solutions (Scott *et al.*, 1980; Komulainen and Bondy, 1987a; Xaing *et al.*, 1990) the $[Ca^{2+}]_e$ was lowered to approximately 0.1 μM by addition of 20 μM EGTA (Bartfai, 1979). At this $[Ca^{2+}]_e$ (confirmed using fura-2 pentapotassium salt) membrane depolarization did not elevate $[Ca^{2+}]_i$. EGTA caused a reduction in 340/380 nm ratio which stabilized within four min (Fig. 2.3). Subsequent addition of MeHg caused concentration-dependent elevations in 340/380 nm ratio. MeHg concentrations of 25 μM or greater differed statistically from control while 10 μM was less effective (inset, Fig 2.3). After correcting for changes in baseline, the magnitude of MeHg-induced first phase elevations observed in 200 μM Ca^{2+}-HBS were not different from those in 0.1 μM Ca^{2+}-HBS ($p>0.05$). Therefore the apparent reduction in $[Ca^{2+}]_i$ caused by 20 μM EGTA did not alter the MeHg-induced immediate elevation in the 340/380 nm ratio. The second phase elevations observed in 6 or 200 μM Ca^{2+}-HBS were reduced or abolished in 0.1 μM Ca^{2+}-HBS, suggesting the second phase was primarily Ca^{2+}_e-dependent (compare Fig. 2.3 to Fig. 2.2). No significant difference between the first phase elevations were observed when MeHg was added one or four min following EGTA (not shown), thus depletion of Ca^{2+} from intracellular stores was unlikely.

The Ca^{2+}_e-dependent second phase elevation in 340/380 nm ratio could be due to influx of extracellular Ca^{2+} and/or release of sequestered intracellular Ca^{2+}. To identify the source, we monitored the ability of Mn^{2+} to quench total fura-2 fluorescence of synaptosomes following MeHg treatment. Mn^{2+} has similar paths of entry in synaptosomes as does Ca^{2+} (Drapeau and Nachshen, 1984; Nelson, 1986), but unlike Ca^{2+}, Mn^{2+} quenches fura-2 fluorescence (Grynkiewicz *et al.*, 1985). Mn^{2+} is commonly used in conjunction with fura-2 to assess the permeability of the plasma membrane to divalent

FIG. 2.3. The effect of MeHg on the 340/380 nm ratio in 0.1 μM Ca^{2+}-HBS. Fura-2 loaded synaptosomes in 6 μM Ca^{2+}-HBS were treated with 20 μM EGTA to reduce $[Ca^{2+}]_e$ to approximately 0.1 μM. The 340/380 nm ratio stabilized four min following addition of EGTA. Various concentrations of MeHg were then added to the synaptosomal suspensions as indicated at right. Each trace represents the mean of three experiments. *Inset*: The immediate elevations in 340/380 nm ratio caused by MeHg were determined as described for **Figure 1**. The elevations were analyzed by one-way block ANOVA. Each bar is the mean ± S.E.M. for three experiments. *Post hoc* analysis was performed by Tukey's test. *Asterisk* indicates statistical difference from control ($p<0.05$, $n=3$).

Fig. 2.3.

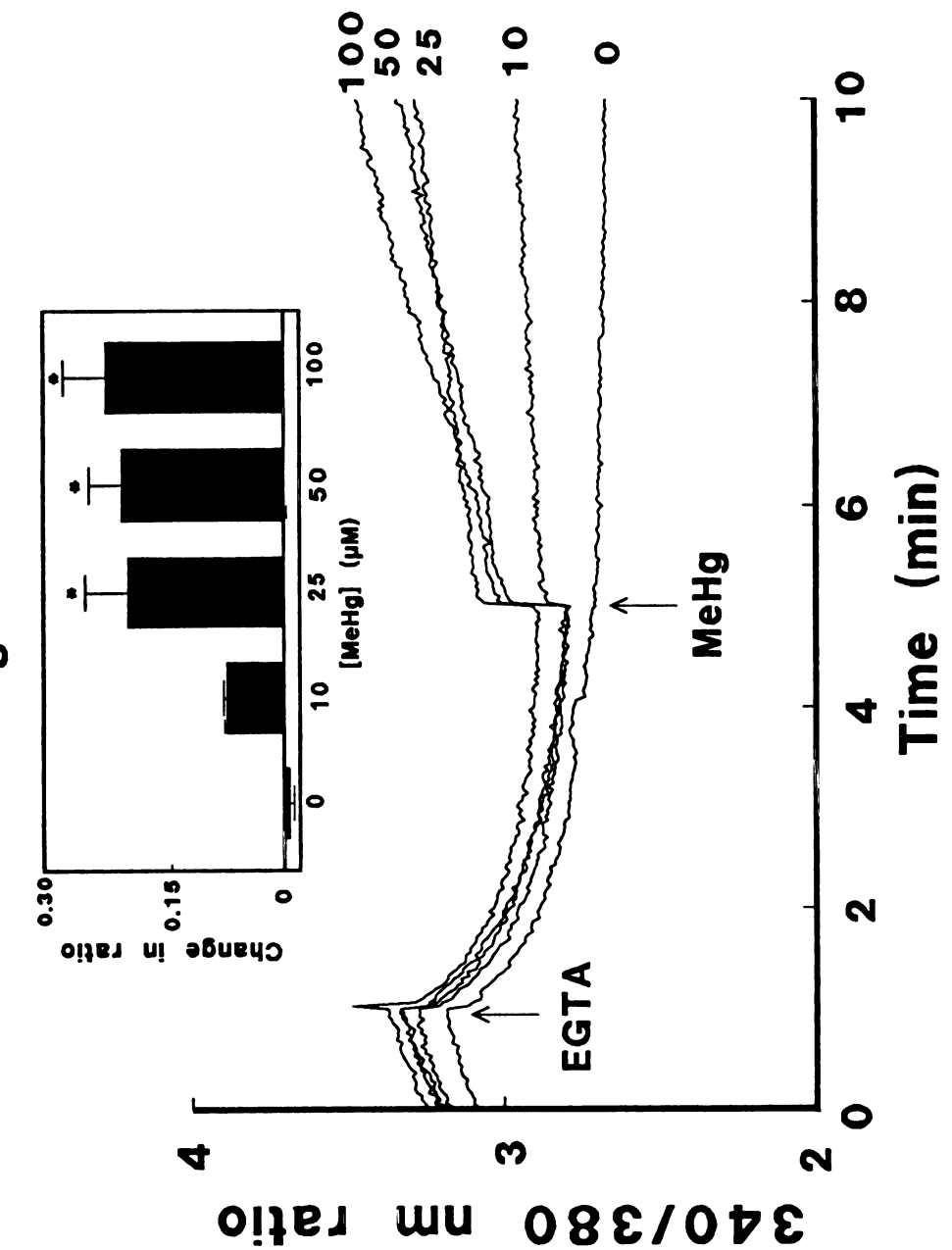
340/380 nm ratio
4
3
2
0
2
4
6
8
10
Time (min)
EGTA
MeHg
100
50
25
10
0
Change in ratio
0.30
0.15
0
0
10
25
50
100
[MeHg] (μM)
*
*
*

cations (Merritt *et al.*, 1989; Kass *et al.*, 1990; Clementi *et al.*, 1992). Because the concentration of Mn^{2+} within synaptosomes is minimal, decreases in fluorescence intensity result only from entry of extracellular Mn^{2+}. This provides a more critical evaluation of plasma membrane permeability than simply monitoring changes in 340/380 nm ratio.

Mn^{2+} quenching of fura-2 fluorescence intensity occurs in two distinct phases. First, extracellular fura-2 is quenched immediately following Mn^{2+} addition. Second, intracellular fura-2 is quenched upon Mn^{2+} entry into the synaptosome. Mn^{2+} quenching of fura-2 was monitored at the Ca^{2+}-insensitive excitation wavelength of 360 nm. To determine the time-course of Mn^{2+} quenching of extracellular fura-2, 40 μM Mn^{2+} was added to a cuvette containing 0.5 μM fura-2 pentapotassium salt without synaptosomes. The 360 nm intensity decreased by 85% within 0.8 sec (Fig. 2.4, dashed line). If MeHg caused release of fura-2 from the synaptosomes during the six min incubation, the immediate quenching of the fluorescence intensity by Mn^{2+} would be enhanced. The second component of Mn^{2+} quenching would be expected to occur gradually as Mn^{2+} quenched intracellular fura-2. Increased Mn^{2+} permeability would result in a greater rate of quenching during this phase.

As expected, Mn^{2+} (40 μM) quenched the fura-2 signal in two distinct phases (Fig. 2.4). Immediately following addition of Mn^{2+} to fura-2 loaded synaptosomes, there was a rapid decrease in fluorescence intensity, similar to that observed in a cell-free system. The immediate quenching was quantitated as the percent difference between the average fluorescence intensity ten sec prior to the addition of Mn^{2+} (0 to 10 sec) and average fluorescence intensity over the two sec which followed the first full sec after Mn^{2+} addition (11 to 13 sec). The immediate quench in synaptosomes treated with up to 25 μM

FIG. 2.4. Quench of fluorescence intensity in MeHg-treated, fura-2 loaded synaptosomal suspensions. Synaptosomal suspensions were incubated with MeHg (0 - 100 μM) for six min, and the quenching of fura-2 fluorescence by 40 μM Mn^{2+} was monitored at the Ca^{2+}-insensitive excitation wavelength of 360 nm (*solid lines*). The quenching of 0.5 μM fura-2 pentapotassium salt in 200 μM Ca^{2+}-HBS without synaptosomes (*dashed line*) was complete (85% decline in intensity) within 0.8 sec following Mn^{2+} addition. Incubation of synaptosomal suspensions with 50 or 100 μM MeHg increased the amount of quenching observed during this 0.8 sec interval. First phase quenching was quantitated as the percent decrease in average fluorescence intensity from ten sec prior to Mn^{2+} addition (0 to 10 sec) over the two sec which followed the first full sec after Mn^{2+} addition (11 to 13 sec). The continual decline in fluorescence intensity was most likely due to quenching of intracellular fura-2. Each solid line represents the average of three experiments; intensity recordings were taken every 0.2 sec in real time. The values of the fluorescence intensity traces were adjusted slightly to facilitate presentation.

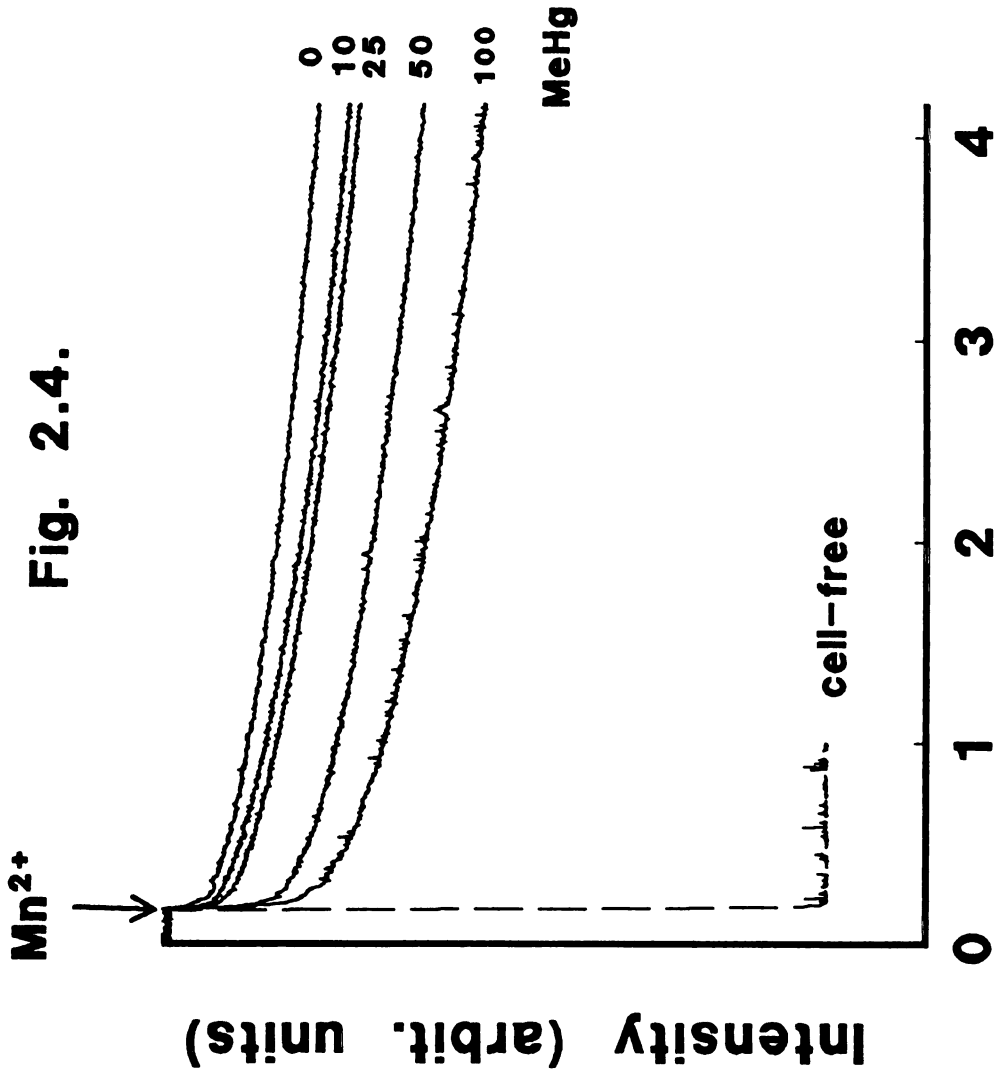
Mn2+
0
10
25
50
100
MeHg
cell-free
0
1
2
3
4
Time (min)
Intensity (arbit. units)

Fig. 2.4.

MeHg was not different from control, but at higher concentrations (50 and 100 μM) there was a significant ($p<0.05$) increase in quench. This effect could be due either to increased fura-2 leakage from synaptosomes, lysis of a select population of synaptosomes or facilitation of quenching of intracellular fura-2. All concentrations of MeHg tested increased the quenching of intracellular fura-2 relative to controls (Fig. 2.4). Alternatively, the gradual decrease in fura-2 signal could reflect quenching of fura-2 leaking from damaged synaptosomes. In either case, however, MeHg altered the plasma membrane permeability which supports the notion that the second phase elevations in 340/380 nm ratio observed in Ca^{2+}-HBS were due to increased Ca^{2+} flux across the plasma membrane, and not CICR.

A few other conclusions can be made based on the Mn^{2+} study. First, quenching of extracellular fura-2 by Mn^{2+} in cell suspensions is essentially complete within one sec. Fura-2 which is quenched after one sec is most likely intracellular. Thus, the difference in intensity just prior to and immediately following Mn^{2+} addition yields a correction factor for extracellular fura-2 without significant quenching of intracellular fura-2. Second, because Mn^{2+} gradually enters the cytoplasm and quenches intracellular fura-2 fluorescence at 340 and 380 nm excitation unequally (Goldman and Blaustein, 1990), extended incubation with Mn^{2+} precludes estimation of $[Ca^{2+}]_i$.

Since the initial elevation in 340/380 nm ratio was independent of $[Ca^{2+}]_e$, experiments were undertaken to determine the intracellular source of this elevation. Previous studies at the neuromuscular junction have shown that some uncouplers of oxidative phosphorylation produce effects similar to those of MeHg (Levesque and Atchison, 1987; 1988). MeHg has a number of effects on mitochondrial function (Verity

et al., 1975; Cheung and Verity, 1981; Kauppenin *et. al.*, 1989; Hare and Atchison, 1992), all of which have been shown to elevate $[Ca^{2+}]_i$ (Scott *et al.*, 1980; Heinonen ***et al.***, 1984). Therefore, we sought to determine if the mitochondria were responsible for the immediate elevation in 340/380 nm ratio. In 0.1 µM Ca^{2+}-HBS, depolarization of the mitochondrial membrane with 10 mM sodium azide plus 4 µg/ml oligomycin did not change the 340/380 nm ratio (Fig. 2.5). Subsequent addition of MeHg (0 - 100 µM) caused concentration-dependent increases in 340/380 nm ratio similar to those in the absence of mitochondrial inhibitors. Depolarization of synaptosomal mitochondria in 200 µM Ca^{2+}-HBS also failed to elevate the 340/380 nm ratio, and did not alter the response to MeHg (not shown). Thus, depolarization of mitochondria *per se* was not sufficient to elevate $[Ca^{2+}]_i$ in synaptosomes. Moreover, the intracellular actions of MeHg on fura-2 fluorescence did not involve alterations in mitochondrial Ca^{2+} buffering.

Ruthenium red, a putative inhibitor of the mitochondrial Ca^{2+} uniporter (Moore, 1971), attenuates the spontaneous release of neurotransmitter induced by MeHg (Levesque and Atchison, 1987; Levesque *et al.*, 1992). Ruthenium red also blocks MeHg-induced efflux of Ca^{2+} from preloaded isolated mitochondria (Levesque and Atchison, 1991). Since depolarization of the synaptosomal mitochondrial membrane did not alter the 340/380 nm ratio, experiments were performed to determine if the protective effects of ruthenium red on transmitter release or Ca^{2+} release were due to an action at another site. Ruthenium red shifted the 340/380 nm ratio to higher values due to preferential quenching of the 380 nm excitation intensity over 340 nm intensity (not shown). In 0.1 µM Ca^{2+}-HBS, pretreatment of synaptosomes with 10 or 20 µM ruthenium red for at least 30 min did not block the initial phase elevation in 340/380 nm ratio caused by MeHg (Fig. 2.6).

FIG. 2.5. The effect of mitochondrial depolarization on the MeHg-induced elevations in 340/380 nm ratio in 0.1 μM Ca^{2+}-HBS. The synaptosomal mitochondrial membrane was depolarized *in situ* using 4 μg/ml oligomycin and 10 mM NaN_3 prior to addition of MeHg. EGTA (20 μM) was added to lower $[Ca^{2+}]_e$ to approximately 0.1 μM. Each trace represents the mean of three experiments. *Inset*: The immediate elevation in 340/380 nm ratio caused by MeHg was determined as described in **Figure 1** (mean ± S.E.M.). *Asterisk* indicates statistically different from control ($p<0.05$, $n=3$).

Fig. 2.5.

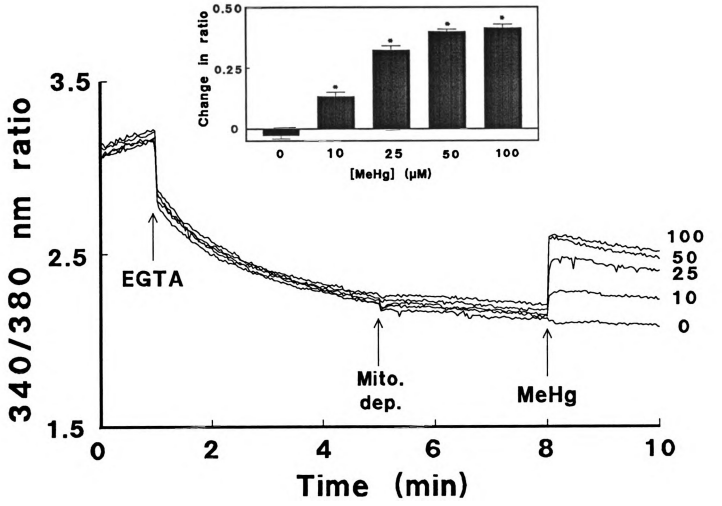
Change in ratio
0.50
0.25
0
0
10
25
50
100
[MeHg] (μM)
340/380 nm ratio
3.5
2.5
1.5
EGTA
Mito.
dep.
MeHg
100
50
25
10
0
0
2
4
6
8
10
Time (min)

FIG. 2.6. The effect of ruthenium red on the MeHg-induced elevations in 340/380 nm ratio in 0.1 μM Ca^{2+}-HBS. Synaptosomal suspensions were incubated with 20 μM ruthenium red in 200 μM Ca^{2+}-HBS red for at least 30 min. EGTA was added prior to MeHg to lower $[Ca^{2+}]_e$ to 0.1 μM. Each trace represent the mean of three experiments. *Inset*: The immediate elevation in 340/380 nm ratio as determined in **Figure 1** (mean ± S.E.M.). Those values statistically different from control ($p<0.05$, $n=3$) are indicated by the *asterisk*.

Fig. 2.6.

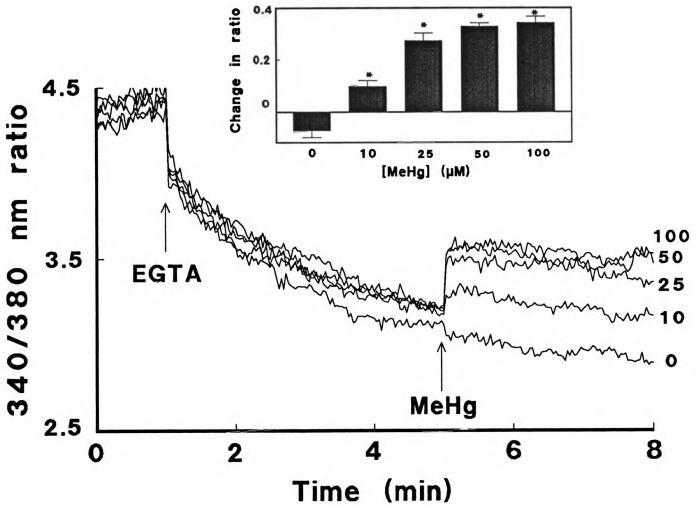
Change in ratio
0.4
0.2
0
*
*
*
*
0
10
25
50
100
[MeHg] (μM)
340/380 nm ratio
4.5
3.5
2.5
EGTA
MeHg
100
50
25
10
0
0
2
4
6
8
Time (min)

In 200 μM Ca^{2+}-HBS, ruthenium red pretreatment did not affect the second phase elevations in 340/380 nm ratio, but did block the elevation in ratio elicited by K^+ depolarization (not shown). It is possible that the shift in ratio caused by ruthenium red makes direct quantitative comparisons of 340/380 nm ratio values inappropriate.

Since neither the depolarization of mitochondria nor ruthenium red affected the MeHg-induced immediate elevations in 340/380 nm ratio, other potential intracellular sources for these increases were examined. The ER is thought to buffer Ca^{2+} in synaptosomes (McGraw *et al.*, 1980; Rasgado-Flores and Blaustein, 1987). ER Ca^{2+} can be mobilized by agents such as caffeine, 1,4,5-inositol-tris-phosphate, thapsigargin, or Ca^{2+} (Miller, 1988). In 0.1 μM Ca^{2+}-HBS, caffeine (at concentrations up to 40 mM) was ineffective at increasing $[Ca^{2+}]_i$, or preventing the MeHg-induced elevations of 340/380 nm ratio (Fig 2.7). Likewise, thapsigargin, an inhibitor of the ER Ca^{2+}-ATPase, did not elevate $[Ca^{2+}]_i$ or block the effects of MeHg in 0.1 μM Ca^{2+}-HBS (Fig 2.8). Apparently, the initial phase increase in 340/380 nm ratio was not due to Ca^{2+} release from the ER.

In experiments originally designed to evaluate the temporal aspects of MeHg-induced increases in plasma membrane permeability, 40 μM Mn^{2+} was added prior to MeHg. We anticipated that the higher concentrations of MeHg (50 and 100 μM) might cause an enhanced rate of fura-2 signal quenching due to increased disruption of the plasma membrane. These experiments were conducted at the Ca^{2+}-insensitive excitation wavelength of 360 nm (Grynkiewicz *et al.*, 1985). Mn^{2+} caused in a biphasic decrease in fluorescence intensity (Fig. 2.9). Addition of MeHg two min after Mn^{2+} caused an immediate elevation in 360 nm fluorescence intensity which was maximal at 25 μM

FIG. 2.7. The effect of caffeine on the MeHg-induced elevations in 340/380 nm ratio in 0.1 μM Ca^{2+}-HBS. Synaptosomal suspensions were treated with 40 mM caffeine in 0.1 μM Ca^{2+}-HBS for two min. Each trace represent the mean of three experiments. *Inset*: The immediate elevation in 340/380 nm ratio as determined in **Figure 1** (mean ± S.E.M.). Those values statistically different from control ($p<0.05$, $n=3$) are indicated by the *asterisk*.

Fig. 2.7.

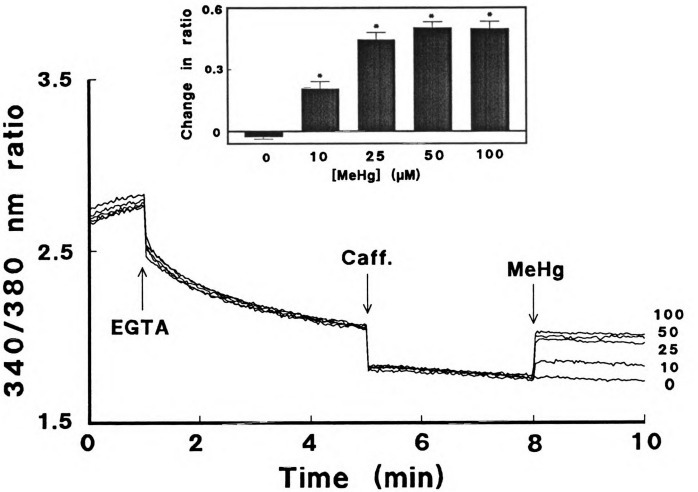
Change in ratio
0.6
0.3
0
0
10
25
50
100
[MeHg] (μM)
340/380 nm ratio
3.5
2.5
1.5
EGTA
Caff.
MeHg
100
50
25
10
0
0
2
4
6
8
10
Time (min)

FIG. 2.8. The effect of thapsigargin on the MeHg-induced elevations in 340/380 nm ratio in 0.1 μM Ca^{2+}-HBS. Synaptosomal suspensions were treated with 1 μM thapsigargin in 0.1 μM Ca^{2+}-HBS for three min. Each trace represent the mean of three experiments. *Inset*: The immediate elevation in 340/380 nm ratio as determined in **Figure 1** (mean ± S.E.M.). Those values statistically different from control ($p<0.05$, $n=3$) are indicated by the *asterisk*.

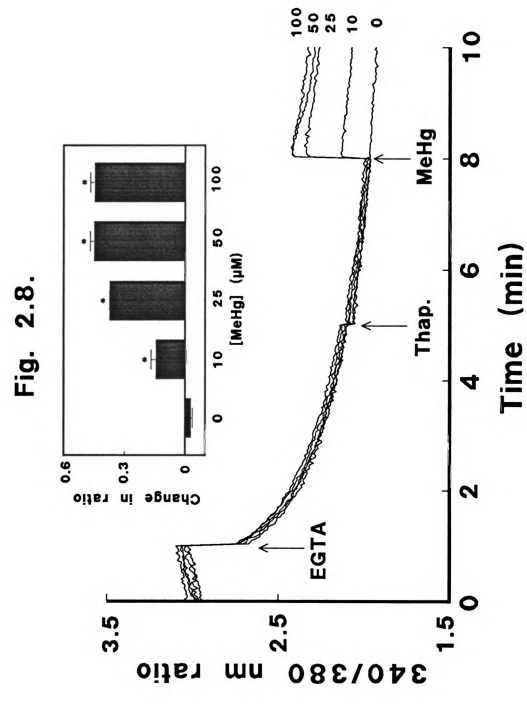
Fig. 2.8.
340/380 nm ratio
3.5
2.5
1.5
0
2
4
6
8
10
Time (min)
EGTA
Thap.
MeHg
100
50
25
10
0
Change in ratio
0.6
0.3
0
0
10
25
50
100
[MeHg] (μM)

FIG. 2.9. MeHg-induced alterations in Ca^{2+}-insensitive fluorescence intensity and Mn^{2+} permeability of synaptosomes. Mn^{2+} (40 μM) was added to fura-2 loaded synaptosomes prior to MeHg addition and the fluorescence intensity monitored at the Ca^{2+}-insensitive excitation wavelength of 360 nm. MeHg was added at two min followed three min later by addition of the cell-impermeant heavy metal chelator DTPA (150 μM). Each line represents the average of three experiments. Position of intensity values on the Y-axis were adjusted to aid in presentation.

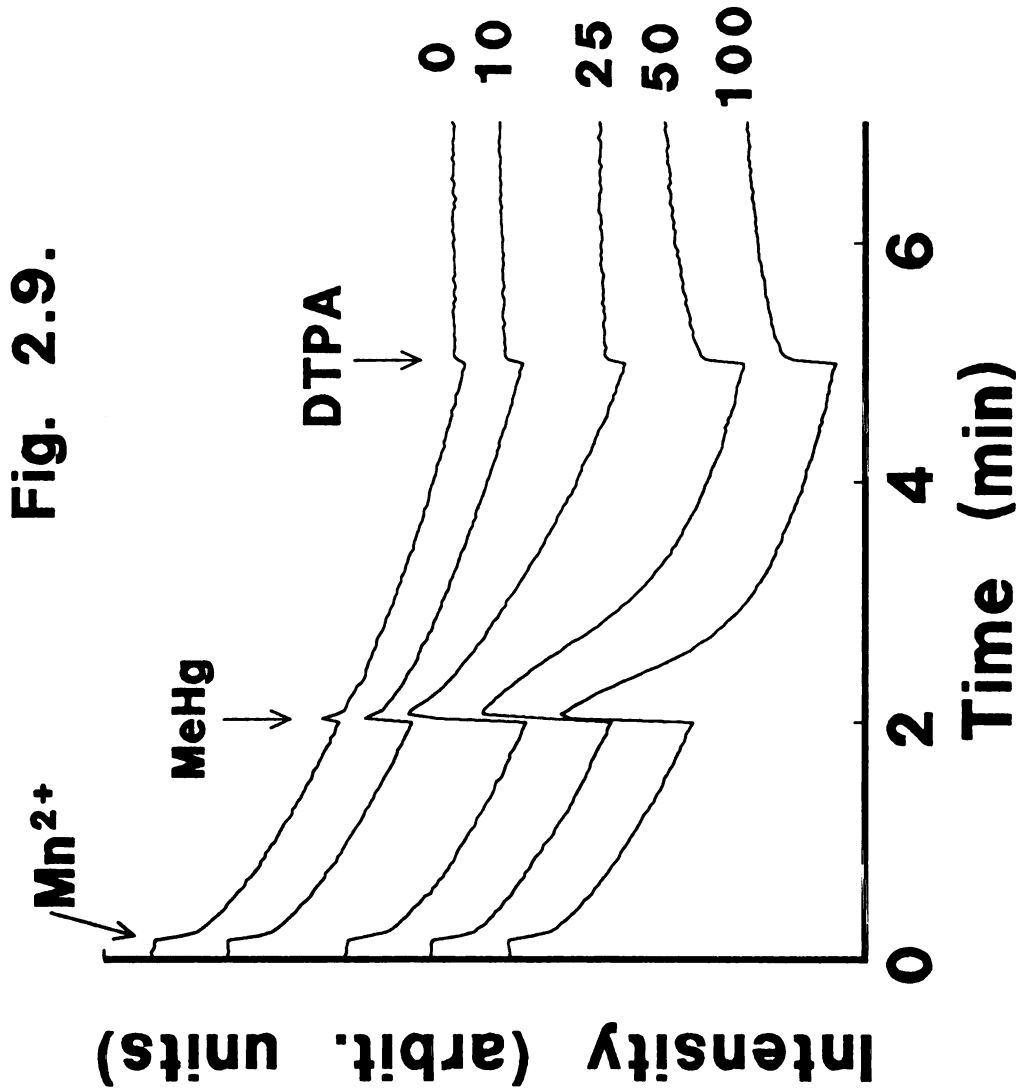
Intensity (arbit. units)
Time (min)
0
2
4
6
0
10
25
50
100
DTPA
MeHg
Mn2+

Fig. 2.9.

MeHg. Following this increase in fluorescence intensity, the subsequent rate of Mn^{2+} quench was enhanced in a concentration-dependent fashion consistent with increased plasma membrane permeability. To determine if MeHg caused fura-2 leak, the cell-impermeant, heavy metal chelator DTPA was used. DTPA (150 μM) caused an immediate increase in fluorescence intensity presumably due to chelation of Mn^{2+} previously bound to extracellular fura-2 (Fig. 2.9). In the case of 50 and 100 μM MeHg, the increase in intensity following DTPA addition was larger than the initial quench produced by Mn^{2+}, suggesting that extracellular fura-2 concentrations had increased. In fact, at these MeHg concentrations, there was a gradual increase in fluorescence following DTPA addition. This may represent chelation of Mn^{2+} previously complexed to fura-2 which had leaked from MeHg-damaged synaptosomes.

The MeHg-induced increases in fura-2 fluorescence intensity at the Ca^{2+}-insensitive excitation wavelength of 360 nm could be due to several factors. First, fura-2 interacts with other cations, some of which alter the fluorescence pattern similar to Ca^{2+} (Grynkiewicz *et al.*, 1985). Although MeHg does not interact with fura-2 (Fig. 2.1) it could elevate the intracellular concentrations of other cations which increase the fluorescence intensity at the excitation wavelength of 360 nm. Second, MeHg could release fura-2 from an intracellular store which was previously intractable to fluorescence. Third, MeHg could have some effect which results in the unquenching of fura-2 in the cytoplasm. Fourth, MeHg could alter the physical properties of the intracellular milieu (ie. viscosity, pH, polarity, etc.) resulting in a shift to the right of the fluorescence pattern of fura-2.

If non-Ca^{2+} polyvalent cation homeostasis was disrupted by MeHg, the cell-permeant heavy metal chelator TPEN should prevent or reverse the effects of MeHg on fura-2 fluorescence. TPEN was tested for its ability to bind MeHg by adding 100 µM MeHg to a solution of TPEN and Mn^{2+} adjusted to half-maximally quench the fluorescence of 0.5 µM fura-2 pentapotassium salt. If MeHg interacted with TPEN it would have to displace Mn^{2+}. The Mn^{2+} would then bind to the fura-2 and quench the fura-2 fluorescence. No changes in fluorescence intensity were observed upon addition of MeHg (not shown).

TPEN was then tested in fura-2 loaded synaptosomes treated with MeHg. Concentrations of MeHg greater than 25 µM were not tested because the elevation in 360 nm excitation intensity was maximal at 25 µM, and higher concentrations caused leak of fura-2. Addition of 20 µM EGTA to fura-2 loaded synaptosomes produced minimal changes in 360 nm excitation intensity confirming the Ca^{2+}-insensitivity of this wavelength (Fig. 2.10). Subsequent addition of 50 µM TPEN decreased the 360 nm fluorescence intensity, suggesting an interaction of fura-2 with some non-Ca^{2+} cation(s) in the cytoplasm. Addition of MeHg had no effect on fura-2 fluorescence intensity. Addition of 10 or 25 µM MeHg prior to 50 µM TPEN caused a concentration-dependent elevation in fluorescence intensity which was rapidly reversed by the TPEN. Thus the MeHg-induced increases in intensity at 360 nm were due to an elevation in the intracellular concentration of non-Ca^{2+} cation(s).

The origin of these cations was uncertain because TPEN chelates both intra- and extracellular heavy metals. However, if the source was extracellular, the cell-impermeant chelator DTPA (150 µM) should block the effects of MeHg. Pretreatment of

FIG. 2.10. Effect of the cell-permeant heavy metal chelator TPEN on MeHg-induced alterations in Ca^{2+}-insensitive fura-2 fluorescence. The fluorescence intensity was monitored at 505 nm following excitation at 360 nm. All lines are the mean of three experiments. ***Top,*** EGTA (20 μM) was added to fura-2 loaded synaptosomes at 1 min to reduced $[Ca^{2+}]_e$ to 0.1 μM. At five min, 50 μM TPEN was added followed by MeHg (0 - 25 μM) at six min. ***Bottom,*** MeHg was added to fura-2 loaded synaptosomes in 0.1 μM Ca^{2+}-HBS at five min, followed by 50 μM TPEN addition one min later.

Fig. 2.10.

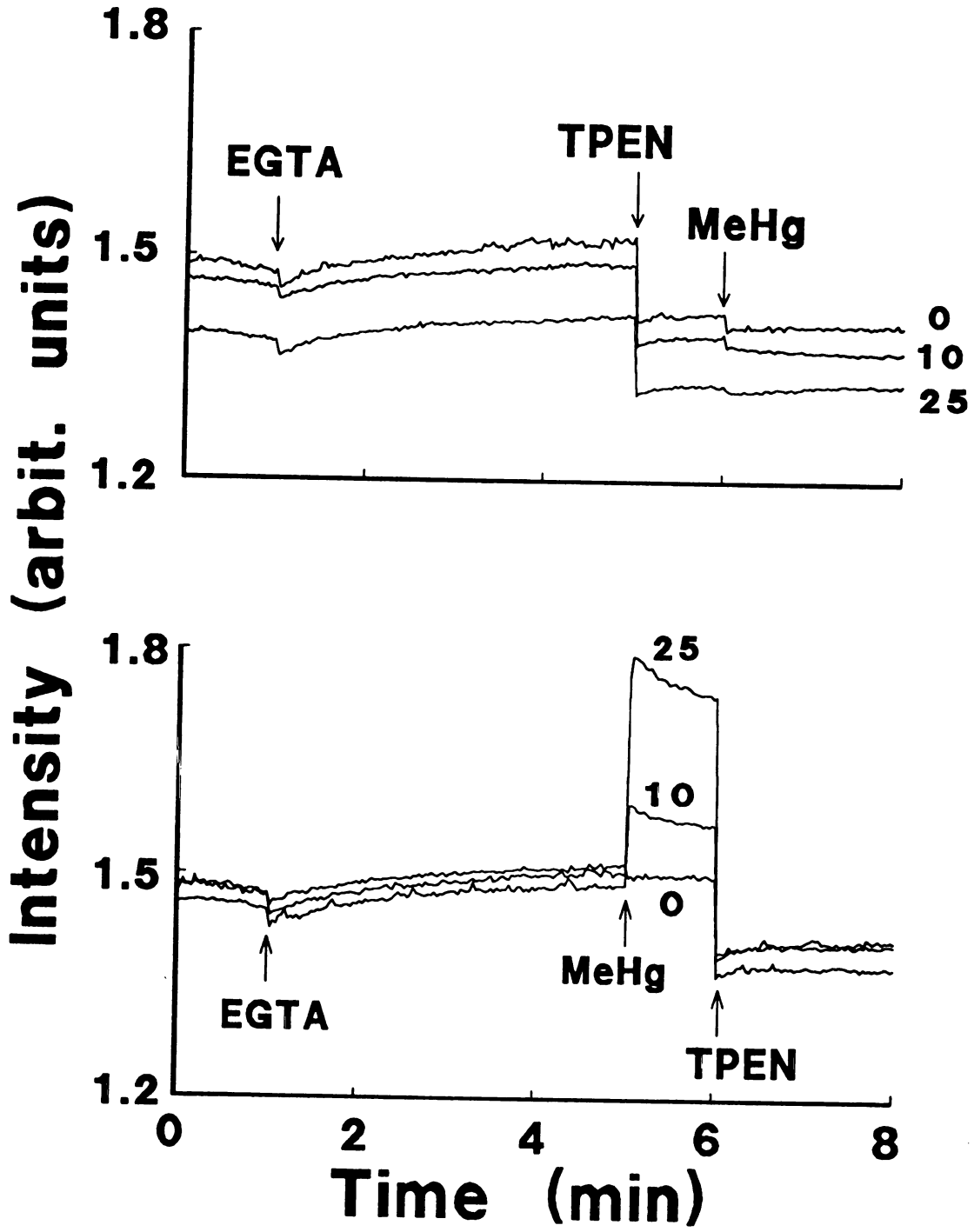
1.8
1.5
1.2
EGTA
TPEN
MeHg
0
10
25
Intensity (arbit. units)
1.8
1.5
1.2
25
10
0
EGTA
MeHg
TPEN
0
2
4
6
8
Time (min)

synaptosomes with DTPA did not alter elevation in 360 nm excitation intensity caused by 25 µM MeHg (Fig. 2.11). Subsequent addition of TPEN reversed the elevation in fluorescence intensity. Thus, MeHg increased the free intrasynaptosomal concentration of an endogenous cation(s) other than Ca^{2+}.

Experiments in Figures 2.2 and 2.3 were repeated in the presence of 50 µM TPEN since the non-Ca^{2+} cations could interfere with accurate measurement of $[Ca^{2+}]_i$. TPEN had minimal influence on the baseline 340/380 nm ratio despite the interaction of fura-2 with non-Ca^{2+} cations in the cytoplasm during resting conditions (Fig. 2.12). No MeHg-induced initial elevation in 340/380 nm ratio was observed in synaptosomes pretreated with 50 µM TPEN in 200 µM Ca^{2+}-HBS. The second phase elevation in 340/380 nm ratio was not blocked and, in fact, was enhanced relative to TPEN-free conditions. In 0.1 µM Ca^{2+}-HBS, MeHg did not elevate 340/380 nm ratio in TPEN-treated synaptosomes. Thus, under resting conditions interference from non-Ca^{2+} polyvalent cations on $[Ca^{2+}]_i$ determination is minimal. However, increases in the concentrations of these cations by MeHg hinders accurate determination of $[Ca^{2+}]_i$.

FIG. 2.11. Effect of the cell-impermeant heavy metal chelator DTPA on MeHg-induced alterations in Ca^{2+}-insensitive fluorescence. The cell-impermeant heavy metal chelator DTPA (150 μM) was added to fura-2 loaded synaptosomes in 0.1 μM Ca^{2+}-HBS at five min. Addition of 25 μM MeHg at six min elevated the fluorescence intensity at 505 nm following excitation at 360 nm. Subsequent addition of 50 μM TPEN reversed the increase in fluorescence intensity. Each line is the average of three experiments.

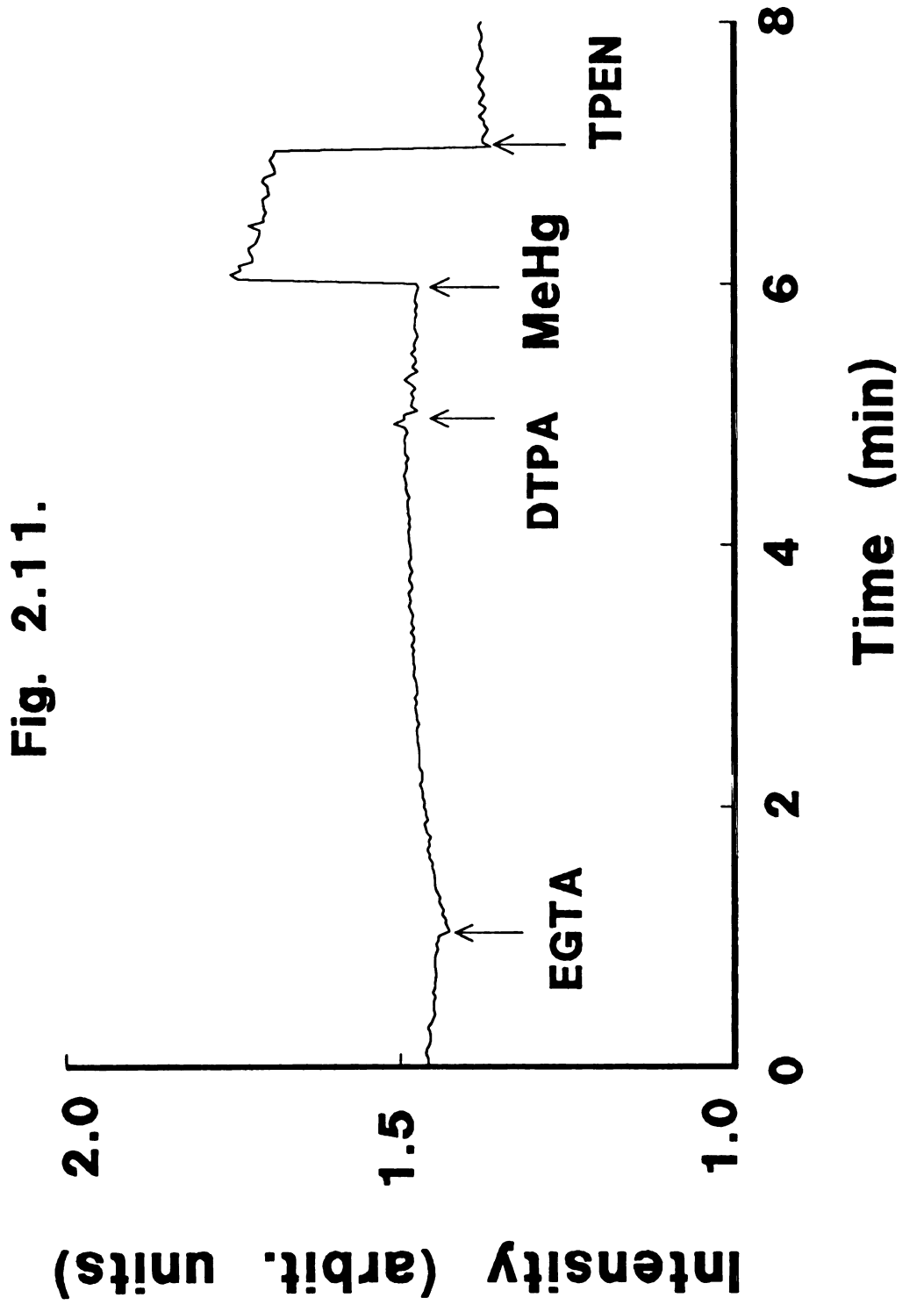
Intensity (arbit. units)
2.0
1.5
1.0
0
2
4
6
8
Time (min)
EGTA
DTPA
MeHg
TPEN

Fig. 2.11.

FIG. 2.12. Effect of MeHg (0 - 25 μM) on the 340/380 nm ratio. Each trace is the mean of three experiments. $[Ca^{2+}]_i$ is indicated on the right. ***Top,*** In 200 μM Ca^{2+}-HBS, synaptosomes were exposed to 50 μM TPEN at 1 min followed by MeHg at 2 min. ***Bottom,*** In 0.1 μM Ca^{2+}-HBS, synaptosomes were exposed to 50 μM TPEN at 1 min followed by 20 μM EGTA at 2 min. MeHg (0 - 25 μM) was then added at six min.

Fig. 2.12.

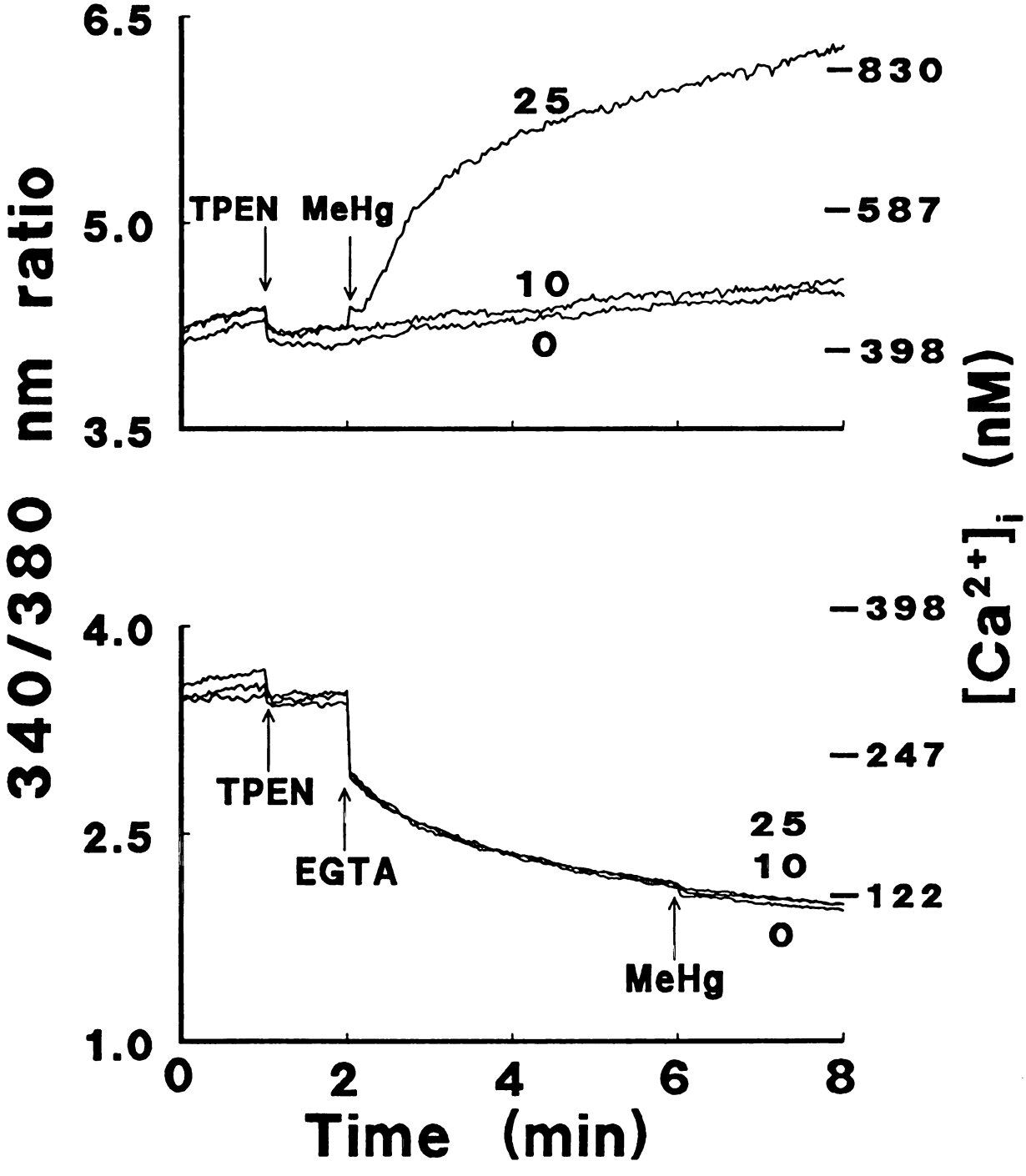
6.5
5.0
3.5
4.0
2.5
1.0
340/380 nm ratio
TPEN
MeHg
25
10
0
TPEN
EGTA
MeHg
25
10
0
-830
-587
-398
-398
-247
-122
[Ca2+]i (nM)
0
2
4
6
8
Time (min)

DISCUSSION

Results of the present study confirm several earlier observations of MeHg-induced elevations in $[Ca^{2+}]_i$, (Komulainen and Bondy, 1987b; Kauppinen *et al.*, 1989), but more importantly, have extended them in the following ways. First, MeHg appears to elevate the concentration of non-Ca^{2+} endogenous cations within the terminal. Second, ruthenium red did not prevent the intracellularly-mediated changes in fura-2 fluorescence induced by MeHg. Third, unlike mitochondria isolated from whole brain, intrasynaptosomal mitochondria did not appear to release appreciable Ca^{2+} in response to MeHg. Moreover, under the conditions of our experiments, intrasynaptosomal mitochondria did not release measurable amounts of Ca^{2+}. Fourth, the temporal effects of MeHg on fura-2 fluorescence are complex and involve at least two phases: an immediate effect due to elevation of intra-synaptosomal non-Ca^{2+} polyvalent cation concentrations, and a gradual effect due to influx of Ca^{2+}_e. Fifth, MeHg causes an immediate increase in plasma membrane permeability to divalent cations. This increased permeability mediates the second phase, extracellular Ca^{2+}-dependent increases in fura-2 fluorescence.

This paper is the first to report the disruption by MeHg of homeostasis of endogenous polyvalent cations other than Ca^{2+}. Though this was not an original aim of the study, the observation was felt to be of sufficient importance to warrant attention. Though fura-2 is relatively selective for Ca^{2+}, several studies have reported interactions of non-Ca^{2+} polyvalent cations with fura-2 (Smith *et al.*, 1989; Tomsig and Suszkiw, 1990) as well as other fluorescent Ca^{2+} indicators (Komulainen and Bondy, 1987a; Arslan *et al.*, 1985; Mason and Grinstein, 1990). Whereas MeHg itself did not interact with fura-2, it nevertheless altered the synaptosomal fura-2 fluorescence in ways inconsistent

with elevations in $[Ca^{2+}]_i$. The cell-permeant heavy metal chelator TPEN blocked the MeHg-induced immediate elevations in both 340/380 nm ratio and 360 nm fluorescence intensity. The cell-impermeant heavy metal chelator DTPA had no effect. This strongly suggests that the first phase elevations in 340/380 nm ratio arise from endogenous intrasynaptosomal cations.

The cation(s) responsible must be present in synaptosomes in sufficient quantities and possess adequate affinity for fura-2. The endogenous cations which best fit these criteria are Fe^{2+}, Zn^{2+} and Cu^{2+}. Aside from Ca^{2+} and Mg^{2+}, these are the most abundant polyvalent cations typically found in neurons. The affinity of fura-2 for Fe^{2+} and Zn^{2+} is 3-10x and 100x greater, respectively, than its affinity for Ca^{2+} (Grynkiewicz *et al.*, 1985). Similarly, Cu^{2+} has an extremely high affinity for EGTA (Bartfai, 1979), the parent compound of fura-2. It is unlikely that the cation(s) was introduced during the synaptosomal preparation since the concentrations of iron, zinc and copper in our buffers were 229, 158 and 108 nM, respectively, as measured by inductively coupled plasma spectroscopy (unpublished results). The MeHg-induced changes were characterized by increased fluorescence intensity. Therefore, the cation is not likely to be Fe^{2+} or Cu^{2+} because these ions quench fura-2 fluorescence (Grynkiewicz *et al.*, 1985; unpublished results). However, Zn^{2+} possess a fura-2 spectrum similar to Ca^{2+} (Grynkiewicz *et al.*, 1985), and is present in most nerve terminals in high concentrations, particularly in the forebrain (Frederickson *et al.*, 1987). Within the mossy fibers of the hippocampus, Zn^{2+} is believed to be associated with the synaptic vesicles, and is mobilized upon electrophysiological stimulation possibly due to release of vesicular contents (Assaf and Chung, 1984). Given the effects of MeHg on the plasma and mitochondrial membranes

of nerve terminals (Kauppinen *et al.*, 1989; Hare and Atchison, 1992), it is conceivable that MeHg is also capable of disrupting the vesicular membrane causing release of endogenous Zn^{2+} into the synaptosomal cytosol.

The cation is not likely to be Hg^{2+} for several reasons. First, Hg^{2+} quenches fura-2 fluorescence (Vignes *et al.*, 1993). Second, DTPA would prevent Hg^{2+} effects on fura-2 fluorescence if the Hg^{2+} was added exogenously as a contaminant of MeHg. Third, demethylation of MeHg does not occur in brain tissue on the timescale of our measurements.

A major impetus for the present study was to clarify the role of the mitochondria in MeHg-induced elevations of $[Ca^{2+}]_i$ in the nerve terminal. The role of mitochondria in regulation of $[Ca^{2+}]_i$ is unsettled (Rahamimoff *et al.*, 1975; Scott *et al.*, 1980; Heinonen *et al.*, 1984; Nachshen, 1985; Rasgado-Flores and Blaustein, 1987). There are conflicting reports of the relative importance of intraterminal mitochondria in buffering elevations in $[Ca^{2+}]_i$, as well as the treatments required for causing Ca^{2+} release from mitochondria (Heinonen *et al.*, 1984; Nachshen, 1985). Since MeHg releases Ca^{2+} preloaded into isolated mitochondria (Levesque and Atchison, 1991) we sought to determine whether intrasynaptosomal mitochondria release measurable amounts of Ca^{2+}, and to evaluate the importance of mitochondrial Ca^{2+} stores with respect to elevations of $[Ca^{2+}]_i$ by MeHg. In the absence of MeHg, depolarization of mitochondria caused no detectable changes in the 340/380 nm ratio. Either depolarization of the mitochondria alone is insufficient to elevate $[Ca^{2+}]_i$, or in our experimental paradigm the mitochondria do not sequester substantial amounts of Ca^{2+} at rest. Depolarization of the mitochondria did not affect the response of the synaptosomes to subsequent addition of MeHg.

We hypothesized originally that ruthenium red would prevent the elevation in $[Ca^{2+}]_i$ induced by MeHg in the absence of Ca^{2+}_e. Ruthenium red blocks the actions of MeHg at both intact synapses and synaptosomes (Levesque and Atchison, 1987; 1991; Levesque *et al.*, 1992), possibly by preventing Ca^{2+} efflux from mitochondria by blocking the mitochondrial Ca^{2+} uniporter (Moore, 1971). Since the mitochondria could not be induced to release Ca^{2+} it is unlikely that effects of ruthenium red on synaptosomes are related to its actions on the mitochondrial Ca^{2+} uniporter. Since neurotransmitter release is dependent upon Ca^{2+}, ruthenium red could act at another Ca^{2+}-dependent site. Ruthenium red reduces the intrinsic fluorescence of the smooth muscle plasma membrane Ca^{2+} pump (Moutin *et al.*, 1992) and blocks voltage-operated Ca^{2+} channels in synaptosomes (Goddard and Robinson, 1976; Tapia *et al.*, 1985). MeHg entry into the terminal is not blocked since ruthenium red does not block the MeHg-induced depolarization of intraterminal mitochondria (Levesque *et al.*, 1992). Ruthenium red did not alter either phase of MeHg-induced elevations in 340/380 nm ratio. However, because ruthenium red shifted the 340/380 nm ratio to higher values such comparisons between ratio values in the presence and absence of ruthenium red may not be valid.

The disruption of non-Ca^{2+} cation buffering was the only intracellular effect of MeHg observed in the present study. Pretreatment with caffeine or thapsigargin did not elevate the 340/380 nm ratio, nor affect the immediate elevation in 340/380 nm ratio caused by MeHg. Either Ca^{2+} is not sequestered in the ER of the synaptosomes to a significant extent, or this pool was insensitive to agents which cause release of Ca^{2+} in other systems. The regulation of the endogenous non-Ca^{2+} cation(s) is independent of

intracellular Ca^{2+} regulation since disruption of putative intracellular Ca^{2+} regulatory systems had no effect.

Previous studies of the effect of MeHg on $[Ca^{2+}]_i$ have relied on static measurements -i.e. before and after treatment with MeHg (Komulainen and Bondy, 1987b; Kauppinen *et al.*, 1989). Therefore we undertook a more thorough temporal characterization of the actions of MeHg. Due to this enhanced temporal sensitivity we observed a biphasic elevation in 340/380 nm ratio whose components were distinguishable by their temporal separation and ionic composition. The first phase was immediate and complete within five sec; its magnitude was concentration-dependent and maximal at 25 μM MeHg. This phase was due to elevations in the intracellular concentrations of non-Ca^{2+} cation(s). The second phase developed gradually; the rate of elevation of 340/380 nm ratio was concentration-dependent with respect to MeHg as well as Ca^{2+}_e. The second phase was not apparent at MeHg concentrations less than 25 μM. TPEN enhanced the second phase possibly due to chelation of the interfering cytoplasmic non-Ca^{2+} cations.

Because both $[Ca^{2+}]_i$ and total cell Ca^{2+} are altered by manipulations of $[Ca^{2+}]_e$ (Scott *et al.*, 1980; Nachshen, 1985; Xiang *et al.*, 1990), we could not establish unequivocally that the second phase was due to Ca^{2+} influx. For this reason, we used Mn^{2+} to test the hypothesis that the second phase is mediated by an influx of Ca^{2+}_e (Merritt *et al.*, 1989; Kass *et al.*, 1990; Clementi *et al.* 1992). All concentrations of MeHg increased the rate of Mn^{2+} quench of intracellular fura-2. Higher concentrations (50, 100 μM) of MeHg also increased Mn^{2+} quench of extracellular fura-2. These observations confirm those of Kauppinen *et al.* (1989). MeHg increased immediately the

plasma membrane permeability to Mn^{2+}, suggesting the onset of the second phase was also immediate.

The route of entry of Ca^{2+}_e following MeHg treatment was not identified; possibilities include: direct compromise of the plasma membrane, entry through non-specific cation channels, receptor-operated ion channels or voltage-dependent Ca^{2+} channels. Since voltage-gated Ca^{2+} channels in synaptosomes and PC12 cells are blocked by the concentrations of MeHg used in the present study (Atchison *et al.*, 1986; Shafer and Atchison, 1989; 1991; Shafer *et al.*, 1990; Hewett and Atchison, 1992) it is unlikely these channels mediate the second phase elevations in 340/380 nm ratio. A non-specific cation conductance could not be distinguished in the present study, but has been demonstrated for high concentrations of MeHg in isolated dorsal root ganglion cells (Arakawa *et al.*, 1991). Similarly, receptor-activated entry of Ca^{2+} cannot be excluded. Direct compromise of the membrane seems likely at high MeHg concentrations since fura-2 efflux is observed. However, lysis of synaptosomes is unlikely since concentrations of MeHg up to 50 μM do not cause lactate dehydrogenase release (Cheung and Verity, 1981).

In conclusion, *in vitro* exposure of isolated nerve terminals to MeHg disrupts cation homeostasis. The effects are an intracellular release of an as-yet unidentified endogenous polyvalent cation and a plasma membrane action which increases Ca^{2+} entry. These effects may cause disturbances in signalling processes within the terminal. For instance, prolonged elevations in $[Ca^{2+}]_i$ produce deficits in transmitter release such as decreased synchronous quantal release and increased asynchronous quantal release (Alnaes and Rahamimoff, 1975; Shalton and Wareham, 1979). Such changes are also observed

initially upon acute application of MeHg to an intact synapse. The elevations in non-Ca^{2+} polyvalent cations might represent actions of MeHg upon synaptic vesicles, potentially producing alterations in neurotransmission distinct from those due to elevations in $[Ca^{2+}]_i$. It is possible the gradual reduction in asynchronous quantal release may be due to destruction of vesicles in the nerve terminal. These cations may only be markers of other intracellular effects, or they could possess additional toxicity.

CHAPTER THREE

METHYLMERCURY-INDUCED ELEVATIONS IN INTRASYNAPTOSOMAL ZINC CONCENTRATIONS: AN ^{19}F-NMR STUDY

ABSTRACT

MeHg increases the $[Ca^{2+}]_i$ and another endogenous polyvalent cation in both synaptosomes (Denny *et al.*, 1993) and NG108-15 cells (Hare *et al.*, 1993). In synaptosomes, the elevation in $[Ca^{2+}]_i$ was strictly dependent upon Ca^{2+}_e; similarly, in NG108-15 cells, a component of the elevations in $[Ca^{2+}]_i$ was Ca^{2+}_e-dependent. The MeHg-induced elevations in endogenous polyvalent cation concentration were independent of Ca^{2+}_e in synaptosomes and NG108-15 cells. The alterations in fura-2 fluorescence suggested the endogenous polyvalent cation may be Zn^{2+}. Using ^{19}F-nuclear magnetic resonance (^{19}F-NMR) spectroscopy of rat cortical synaptosomes loaded with the fluorinated chelator 1,2-*bis*(2-amino-5-fluorophenoxy)ethane-*N,N,N',N'*-tetraacetic acid (5F-BAPTA) we have determined unambiguously that MeHg increases the free intrasynaptosomal Zn^{2+} concentration ($[Zn^{2+}]_i$). In buffer containing 200 µM EGTA to prevent the Ca^{2+}_e-elevations in $[Ca^{2+}]_i$, the $[Zn^{2+}]_i$ was 1.37 ± 0.20 nM; following a 40 min exposure to MeHg-free buffer $[Zn^{2+}]_i$ was 1.88 ± 0.53 nM. Treatment of synaptosomes for 40 min with 125 µM MeHg yielded $[Zn^{2+}]_i$ of 2.69 ± 0.55 nM, while 250 µM MeHg significantly elevated $[Zn^{2+}]_i$ to 3.99 ± 0.68 nM. No Zn^{2+} peak was observed in synaptosomes treated with the cell-permeant heavy metal chelator TPEN (100 µM) following 250 µM MeHg exposure. $[Ca^{2+}]_i$ in buffer containing 200 µM EGTA was 338 ± 26 nM, and 370 ± 64 nM following an additional 40 min exposure to MeHg-free buffer. $[Ca^{2+}]_i$ was 498 ± 28 nM or 492 ± 53 nM during a 40 min exposure to 125 or 250 µM MeHg, respectively. None of the values of $[Ca^{2+}]_i$ differed significantly from either pretreatment levels or buffer-treated controls.

INTRODUCTION

MeHg disrupts Ca^{2+} homeostasis within isolated central nerve terminals (Komulainen and Bondy, 1987; Kauppinen *et al.*, 1989; Denny *et al.*, 1993) as well as neuronal × glioma hybrid (NG108-15) cells in culture (Hare *et al.*, 1993). Recently, we described effects of MeHg on the fluorescence properties of the Ca^{2+}-selective fluorescent indicator fura-2 which were inconsistent with an elevation in intracellular Ca^{2+} concentration ($[Ca^{2+}]_i$) alone (Denny *et al.*, 1993; Hare *et al.*, 1993). These effects include increases in the fluorescence intensity at the Ca^{2+}-insensitive excitation wavelength of 360 nm (Grynkiewicz *et al.*, 1985), and could not be attributed to a direct interaction of MeHg with fura-2. This elevation in fluorescence intensity was inhibited or reversed by the cell-permeant heavy metal chelator TPEN, but not by the cell-impermeant chelator DTPA. This suggested that MeHg also elevates the intracellular concentration of an endogenous polyvalent cation other than Ca^{2+}. Unlike the increases in $[Ca^{2+}]_i$, which were gradual and dependent upon Ca^{2+}_e, the elevations in endogenous heavy metal content were rapid and independent of Ca^{2+}_e. Although the identity of the cation could not be established, we postulated it may be Zn^{2+} due to its presence within certain mammalian central nerve terminals (Frederickson *et al.*, 1987) and its characteristic effects on fura-2 fluorescence (Grynkiewicz *et al.*, 1985; Hechtenberg and Beyersmann, 1993).

To identify and quantify intracellular polyvalent cation concentrations in synaptosomes exposed to MeHg, we performed ^{19}F-NMR spectroscopy on synaptosomes loaded with the fluorinated chelator 5F-BAPTA (Smith *et al.*, 1983; Bachelard and Badar-Goffer, 1993). ^{19}F-NMR spectroscopy of fluorine-labeled chelators has been used in many systems to monitor changes in $[Ca^{2+}]_i$ (Murphy *et al.*, 1986; Levy *et al.*, 1987;

Badar-Goffer *et al.*, 1990; Dowd and Gupta, 1993). A major advantage of ^{19}F-NMR spectroscopy over fluorescence analysis is that the identity of the cations bound to the indicator is apparent. ^{19}F-NMR has been particular useful in the simultaneous measurement of $[Ca^{2+}]_i$ and intracellular Pb^{2+} concentration following acute exposure of Pb^{2+} to isolated osteoblasts, NG108-15 cells or platelets (Schanne *et al.*, 1989a,b; Dowd and Gupta, 1991).

We monitored changes in the cytosolic concentrations of endogenous polyvalent cations by ^{19}F-NMR spectroscopy of 5F-BAPTA loaded synaptosomes exposed to MeHg. A peak corresponding to Zn^{2+} was observed in 5F-BAPTA loaded synaptosomes prior to MeHg exposure which increased following MeHg exposure. Thus, MeHg increased the free ionized intrasynaptosomal Zn^{2+} concentration ($[Zn^{2+}]_i$). This is the first report of an effect of MeHg on $[Zn^{2+}]_i$.

MATERIALS AND METHODS

Chemicals and Solutions: 5F-BAPTA tetrapotassium salt was obtained from Teflabs (Austin, Tx). 5F-BAPTA acetoxymethyl ester (5F-BAPTA/AM) and TPEN were obtained from Molecular Probes (Eugene, OR). Methylmercuric chloride was obtained from K+K Labs (Plainview, NY). Pyrithione, ionomycin, 6-fluorotryptophan, EGTA, and Hepes were obtained from Sigma (St. Louis, MO). $ZnCl_2$ was obtained from Aldrich (Milwaukee, WI). Deuterium oxide (D_2O) was obtained from Isotec (Miamisburg, OH). All other chemicals were reagent grade or better. Deionized water (18 MΩ) was used in all buffers. Sucrose buffers contained 3 mM Na_2HPO_4 (pH 7.4). Hepes-buffered saline (HBS) contained (mM): 145 NaCl, 5 KCl, 1 $MgCl_2$, 10 d-glucose, 10 Hepes (pH 7.4 with Trizma base). For ^{19}F-NMR analysis of 5F-BAPTA loaded synaptosomes, 200 µM EGTA was added to the HBS to reduce contaminating Ca^{2+} concentrations. NMR tubes (8" length, 5 mm dia) were obtained from Wilmad (Buena, NJ).

^{19}F-NMR Spectroscopy of 5F-BAPTA loaded Synaptosomes: Synaptosomes were prepared by discontinuous sucrose density gradient ultracentrifugation from the forebrains of male Sprague-Dawley rats (Harlan, 175-199 g) as described previously (Denny *et al.*, 1993). The P_{2b} fraction (Gray and Whittaker, 1962) was resuspended in three volumes of HBS and centrifuged for 10 min at 10,000 × *g*. The synaptosomal pellet was resuspended by homogenization in 10 ml of HBS containing 31.3 µM 5F-BAPTA/AM and incubated for 30 min at 37°C. The synaptosomal suspensions were diluted by addition of 30 ml HBS, incubated for five min at 37°C, centrifuged at 10,000 × *g* for five min,

and resuspended in 1.5 ml HBS containing 10% (v/v) D_2O and 200 µM EGTA. Aliquots (0.6 ml) were transferred to NMR tubes and kept on ice.

A Varian VXR-500 MHz NMR spectrometer equipped with a 5 mm $^1H/^{19}F$-NMR probe tuned to 470.3 MHz was used. Sample temperature was maintained at 30°C and samples were spun at 20 Hz throughout the experiment. The resonance peaks of 5F-BAPTA loaded synaptosomes were compared to those of aqueous solutions of 5F-BAPTA free acid and saturating concentrations of various metals relative to the reference standard 6-fluorotryptophan. The 5F-BAPTA loaded synaptosomal samples were locked to internal deuterium. The ^{19}F-NMR parameters used were: 23 µsec 45° pulse width, 0.25 sec acquisition period followed by a 0.3 sec delay, and 32 kHz spectral width. Increasing the interpulse interval to 0.9 s did not alter the spectral characteristics. A filter bandwidth of 7.7 kHz was used to reduce high frequency noise. Spectra consisted of 4,000 transients accumulated over 40 min. Data acquisition was paused after 2,000 transients, and the suspensions were mixed by inversion. Spectra of synaptosomal metal content before and after acute MeHg exposure resulted from a Fourier transformation of the transients using a line broadening factor of 40 Hz.

$[Ca^{2+}]_i$ and $[Zn^{2+}]_i$ were calculated by the equation: $[M^{n+}]_i = K_{d,M} \times [M^{n+}:5F\text{-}BAPTA]/[5F\text{-}BAPTA]$, where $[M^{n+}:5F\text{-}BAPTA]/[5F\text{-}BAPTA]$ is the ratio of the peak areas of the metal-bound peak to the free 5F-BAPTA peak (Smith *et al.*, 1983). K_d values of 5F-BAPTA for Ca^{2+} and Zn^{2+} were 500 nM and 7.9 nM, respectively (Schanne *et al.*, 1989b; 1990). Peak areas were determined using Varian NMR software.

Protein Assays: Protein content was determined by the method of Lowry *et al.* (1951) using bovine serum albumin as a standard.

Statistical Analysis: Comparisons of $[Zn^{2+}]_i$ or $[Ca^{2+}]_i$ before and after MeHg treatment were made using a one-way ANOVA ($p \leq 0.05$), and *post-hoc* analysis using the Bonferroni multiple comparison test.

RESULTS AND DISCUSSION

5F-BAPTA in aqueous solution produced a single resonance peak approximately 1.0 ppm downfield of the reference standard 6-fluorotryptophan (Fig. 3.1). A single resonance peak at 1.0 ppm was also observed in solutions containing equimolar concentrations of 5F-BAPTA and MeHg. The Zn^{2+}, Cd^{2+} and Ca^{2+} complexes of 5F-BAPTA were observed 4.6, 6.0 and 6.8 ppm downfield, respectively (Fig. 3.1). 5F-BAPTA loaded synaptosomes treated with 250 μM Zn^{2+} and the Zn^{2+} ionophore pyrithione (50 μM) had a single peak at 4.5 ppm, consistent with an elevation in $[Zn^{2+}]_i$ (Fig. 1). Similarly, 250 μM Ca^{2+} and the Ca^{2+} ionophore ionomycin (5 μM) produced a single peak at 6.7 ppm (Fig. 3.1). Several resonance peaks were observed in 5F-BAPTA loaded synaptosomes in HBS which contained 200 μM EGTA (Fig. 3.2). Broad peaks corresponding to unbound and Ca^{2+}-bound 5F-BAPTA were observed at 1.2 and 6.7 ppm, respectively, as well as a peak of lower magnitude at 4.5 ppm corresponding to Zn^{2+}. $[Zn^{2+}]_i$ was 1.37 ± 0.20 nM (mean ± S.E.M., n=23) prior to MeHg exposure. Thus, the cytoplasm of synaptosomes contained detectable amounts of ionized Zn^{2+} under resting conditions. Treatment of the same 5F-BAPTA loaded synaptosomal suspensions with MeHg-free buffer, 125 μM, or 250 μM MeHg for an additional 40 min yielded $[Zn^{2+}]_i$ of 1.88 ± 0.53 nM (n=11), 2.69 ± 0.55 nM (n=4), or 3.99 ± 0.68 nM (n=8), respectively (Fig 3.3A). $[Zn^{2+}]_i$ following exposure to 250 μM MeHg differed significantly from both the pretreatment and HBS-treated control value. No Zn^{2+} peak was observed in synaptosomes treated with 100 μM TPEN after exposure to 250 μM MeHg (n=4, not shown). $[Ca^{2+}]_i$ prior to MeHg exposure was 338 ± 26 nM (n=23), and 370 ± 64 nM (n=11) in HBS-treated controls (Fig. 3.2). $[Ca^{2+}]_i$ in synaptosomes exposed to 125 μM or 250 μM MeHg

FIG. 3.1. ***A:*** Resonance positions of free 5F-BAPTA and various metal chelates in aqueous solution relative to the reference standard 6-fluorotryptophan (1.25 mM). The position of 2.5 mM 5F-BAPTA tetrapotassium salt was determined in metal-free buffer containing 150 mM KCl and 50 mM Hepes free acid (pH 7.1), and in solutions containing saturating concentrations of Zn^{2+}, Cd^{2+}, or Ca^{2+}. The spectrum of 5F-BAPTA with 2.5 mM MeHg was indistinguishable from that of 5F-BAPTA alone. ***B:*** Resonance positions of 5F-BAPTA loaded synaptosomes during a 40 min exposure to 250 μM Zn^{2+} and 50 μM pyrithione (*top*), or 250 μM Ca^{2+} and 5 μM ionomycin (*bottom*).

A

Fig. 3.1.

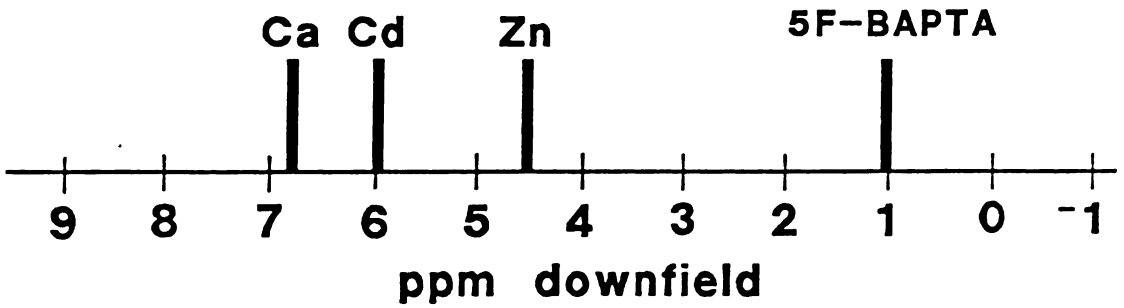
Ca
Cd
Zn
5F-BAPTA
9
8
7
6
5
4
3
2
1
0
-1
ppm downfield

B

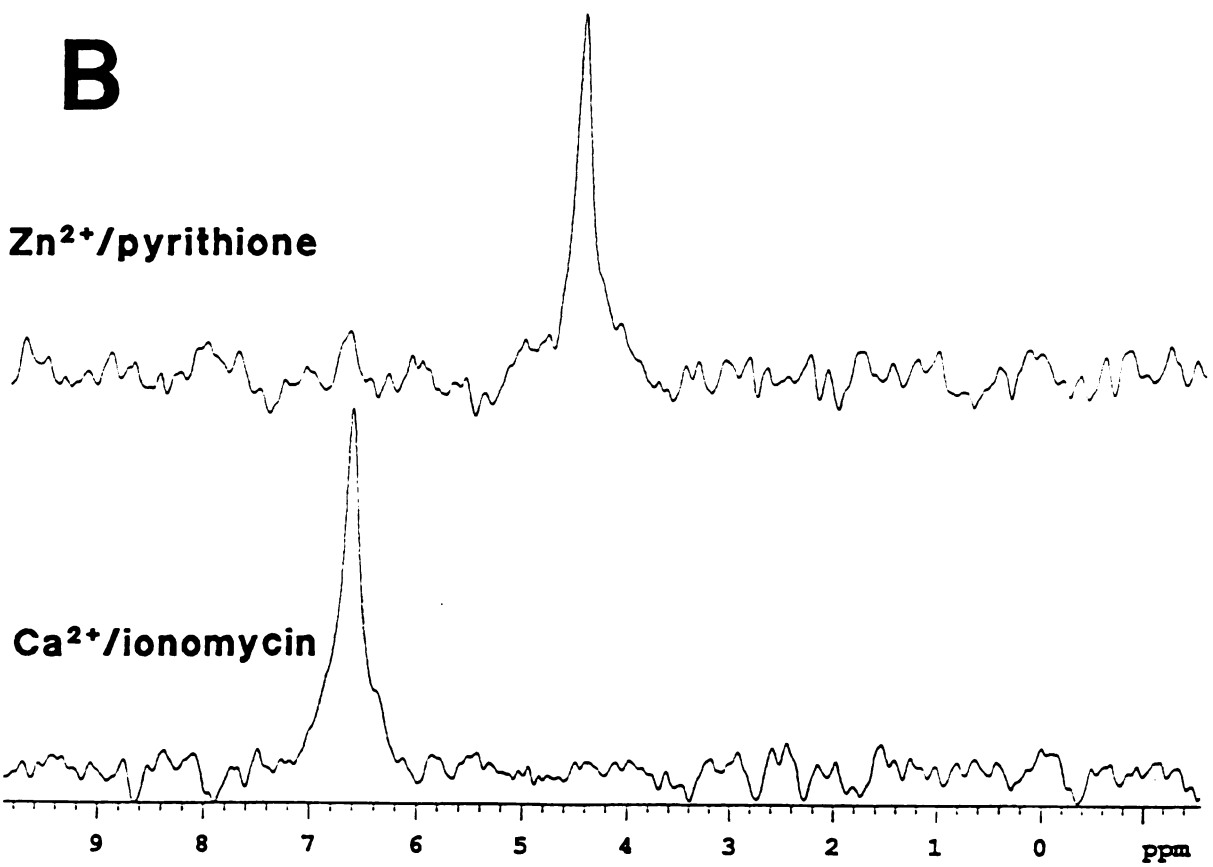
Zn2+/pyrithione
Ca2+/ionomycin
9
8
7
6
5
4
3
2
1
0
ppm

FIG. 3.2. Spectra of 5F-BAPTA loaded synaptosomes in HBS containing 200 μM EGTA before and after MeHg treatment. Spectra were generated by Fourier transformation of the sum of independently acquired transients of 5F-BAPTA loaded synaptosomal preparations. An initial spectrum (*top*, n=23) was acquired for 40 min prior to exposure of the same synaptosomal suspension to MeHg-free buffer (*middle*, n=11), or 250 μM MeHg (*bottom*, n=8) during another 40 min acquisition interval.

Fig. 3.2.

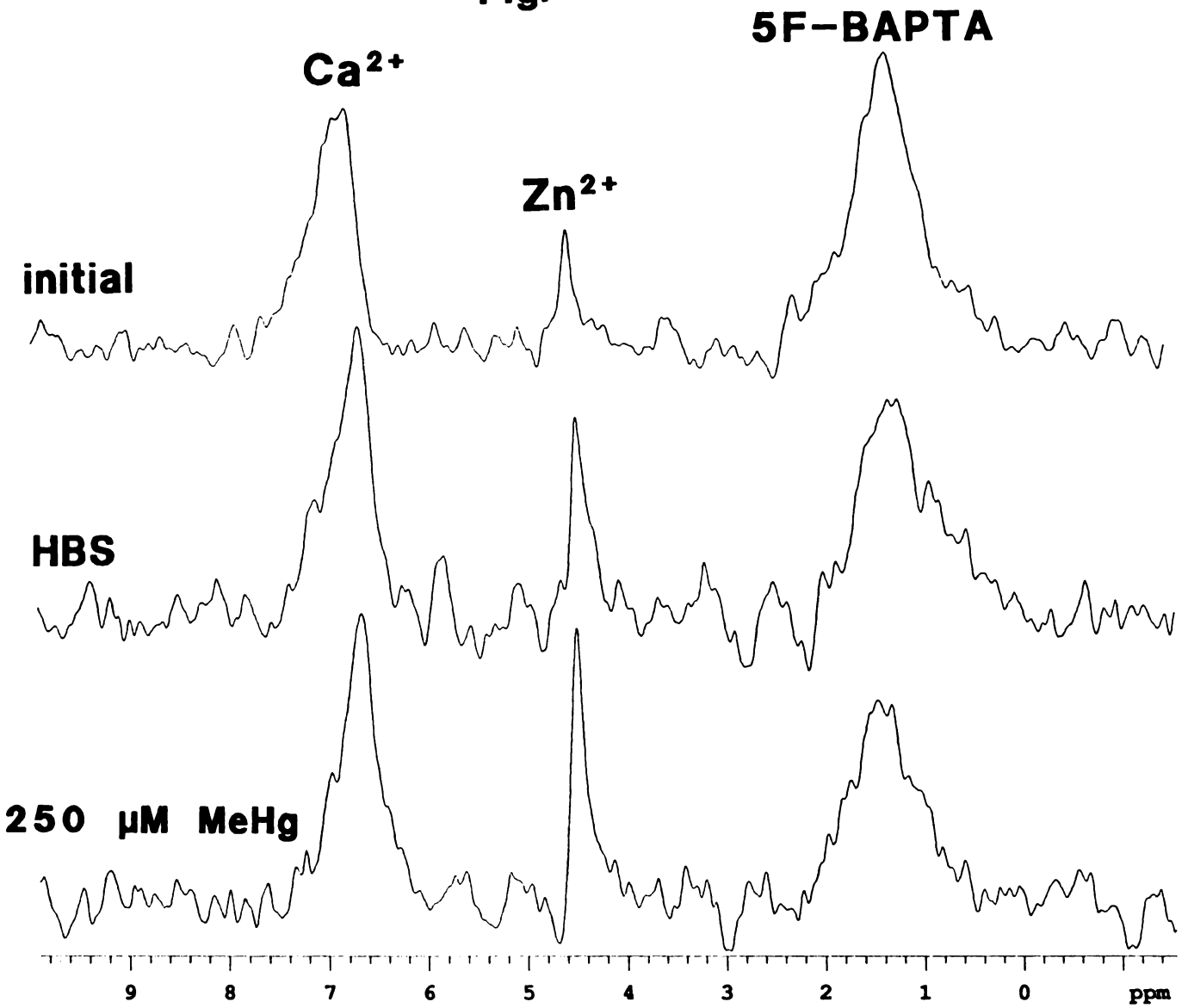

FIG. 3.3. $[Zn^{2+}]_i$ and $[Ca^{2+}]_i$ in 5F-BAPTA loaded synaptosomes before and after acute exposure to MeHg. $[Zn^{2+}]_i$ (***A***) and $[Ca^{2+}]_i$ (***B***) were calculated in a synaptosomal suspension over a 40 min acquisition interval prior to MeHg exposure (n=23), and after the same suspension was exposed to MeHg-free buffer (n=11), 125 (n=4) or 250 µM MeHg (n=8) during another consecutive 40 min acquisition period. The asterisk (*) indicates a value which differs significantly from the initial value; the pound sign (#) indicates a value which differs significantly from the HBS-treated control.

Fig. 3.3.

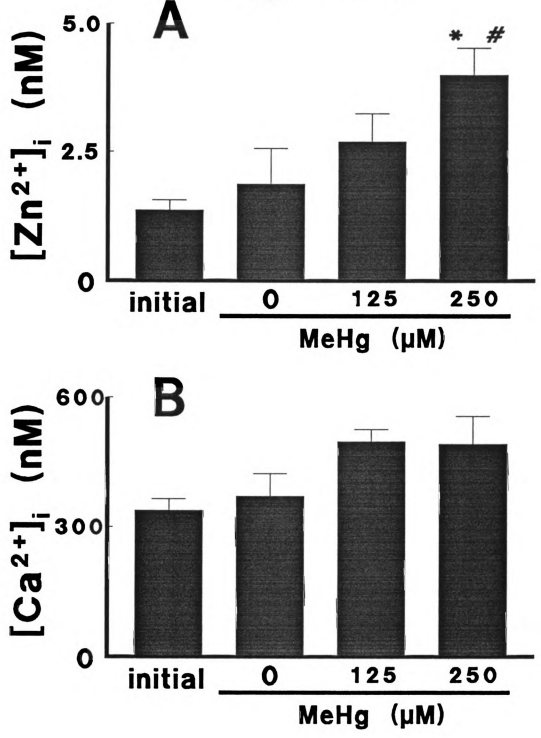
A
5.0
2.5
0
$[Zn^{2+}]_i$ (nM)
* #
initial
0
125
250
MeHg (μM)
B
600
300
0
$[Ca^{2+}]_i$ (nM)
initial
0
125
250
MeHg (μM)

was 498 ± 28 nM (n=4) or 492 ± 53 nM (n=8), respectively. None of these values of $[Ca^{2+}]_i$ differed significantly (Fig. 3.3B). These findings are consistent with the previous report in synaptosomes that the elevations in endogenous polyvalent cation concentration are independent of Ca^{2+}_e while the elevations in $[Ca^{2+}]_i$ are strictly dependent upon Ca^{2+}_e (Denny *et al.*, 1993).

The present study demonstrates clearly that MeHg increases $[Zn^{2+}]_i$ in rat cortical synaptosomes. Although, it was not possible to study the temporal characteristics of these elevations using ^{19}F-NMR, fluorescence analysis of fura-2 loaded synaptosomes demonstrated that the increase in the free endogenous heavy metal content occurred rapidly upon MeHg exposure (Denny *et al.*, 1993; Hare *et al.*, 1993). The elevations in endogenous heavy metal concentrations in synaptosomes were complete immediately following addition of MeHg, and were independent of Ca^{2+}_e. Taken together, the previous studies using fluorometric analysis and the present study utilizing ^{19}F-NMR spectroscopy establish that MeHg causes an immediate elevation in $[Zn^{2+}]_i$ in rat cortical synaptosomes, and possibly in NG108-15 cells. The elevations in $[Zn^{2+}]_i$ are independent of Ca^{2+}_e.

The concentrations of MeHg used in this study were approximately ten-fold greater than those used previously for fluorescence analysis (Denny *et al.*, 1993) because of the ten-fold greater synaptosomal protein content. The increase in protein content was necessary due to the low signal sensitivity of ^{19}F-NMR spectroscopy relative to fluorometric analysis. As a result of the increase in protein content it was necessary to adjust MeHg concentrations accordingly to account for nonspecific binding of MeHg to synaptosomal proteins. Thus, the maximal MeHg exposure was 16 µmol MeHg per mg

protein in this study as well as the previous study using fluorometric analysis of fura-2 loaded synaptosomes (Denny *et al.*, 1993).

While the source of the Zn^{2+} within the synaptosomes is unknown, Zn^{2+} is associated with numerous proteins (Coleman, 1992; Vallee and Falchuk, 1993). Protein-associated Zn^{2+} can be bound by negatively-charged amino acids and/or the sulfhydryl group of cysteine (Vallee and Auld, 1990). Since mercurials have a high affinity for sulfhydryl groups of proteins, it is possible that MeHg displaces the endogenous Zn^{2+} bound to protein(s) within the synaptosomes causing an increase in $[Zn^{2+}]_i$. Inorganic Hg^{2+} and Zn^{2+} both bind to isolated metallothionein (Hamer, 1986). Similarly, organomercurial reagents displace Zn^{2+} bound to the regulatory subunit of bacterial aspartate carbamyltransferase (Hunt *et al.*, 1984). Therefore, displacement of endogenous Zn^{2+} from an intrasynaptosomal protein by MeHg administered exogenously is quite conceivable. Since Zn^{2+} is distributed heterogeneously within the brain and synaptosomes are also a heterogenous population, it is possible that the MeHg-induced increases in $[Zn^{2+}]_i$ occur from only subpopulation of synaptosomes in the suspension. However, this possibility could not be addressed using ^{19}F-NMR spectroscopy. The nature of the elevations in $[Zn^{2+}]_i$ will be the focus of future experiments as well as identifying the source of the endogenous Zn^{2+}.

CHAPTER FOUR

METHYLMERCURY CAUSES RELEASE OF ZINC FROM SOLUBLE SYNAPTOSOMAL PROTEINS

ABSTRACT

MeHg increases $[Ca^{2+}]_i$ and $[Zn^{2+}]_i$. The elevations in $[Ca^{2+}]_i$ are dependent upon Ca^{2+}_e while the Zn^{2+} is endogenous in origin. This study explores the possible sources of endogenous Zn^{2+} which contribute to MeHg-induced elevations in $[Zn^{2+}]_i$. Specifically, the role of the Zn^{2+} associated with synaptic vesicles, as well as Zn^{2+} associated with synaptosomal proteins was investigated. Alterations in fura-2 excitation spectra were used to discern changes in Zn^{2+} concentration from those of Ca^{2+}. If vesicular Zn^{2+} contributed to the MeHg-induced elevations in $[Zn^{2+}]_i$, then mobilization of synaptic vesicles should attenuate the increase in $[Zn^{2+}]_i$ caused by MeHg. Treatment of fura-2 loaded synaptosomes with pharmacological agents known to cause vesicle release (45 mM K^+, 6 nM α-latrotoxin, or 0.1 mM veratridine) for five min did not affect the elevations in $[Zn^{2+}]_i$ upon subsequent addition of 25 μM MeHg. Thus, vesicular Zn^{2+} does not appear to contribute appreciably to the MeHg-induced elevations in $[Zn^{2+}]_i$. The possible role of synaptosomal proteins was investigated using fura-2 spectrofluorometry of synaptosomal homogenates. Synaptosomes were homogenized in 50 mM Hepes (pH 8.0), and separated into soluble and particulate fractions. Samples of each fraction were analyzed for MeHg-induced Zn^{2+} release. Fura-2 excitation spectra were compared before and after MeHg (50 μM) addition for changes consistent with an increase in Zn^{2+}. The soluble fraction contained measurable Zn^{2+} release, but none was observed in the particulate fraction. Thus, soluble synaptosomal proteins contributed to the MeHg-induced elevations in $[Zn^{2+}]_i$. Separation of these proteins by anion exchange chromatography revealed three distinct peaks of activity. Peak 1 eluted with the flow through, Peak 2 eluted from the column at pH 8.6 to 9.4, and Peak 3 eluted near pH 12.0.

Cation exchange and gel filtration chromatography of Peak 2 yielded a single peak of activity in the molecular weight range of 50 to 55 kDa. SDS-PAGE analysis revealed this fraction contains more than one protein band. Additional chromatography is required to purify the protein to homogeneity. Once purified, the protein can then be identified by sequence analysis and/or immunoblotting. The results obtained will hopefully assist in the purification and identification of the proteins present in the other anion exchange chromatography peaks. In conclusion, synaptic vesicles and particulate synaptosomal proteins do not contribute to MeHg-induced elevations in $[Zn^{2+}]_i$, whereas more than one soluble synaptosomal protein does release endogenous Zn^{2+} upon MeHg exposure.

INTRODUCTION

Methylmercury (MeHg) is a well known neurotoxicant (Chang, 1980). The pathology and clinical features of MeHg intoxication have been characterized for both acute (Bakir *et al.*, 1973) and chronic exposure (Takeuchi *et al.*, 1959), but the mechanisms of MeHg-induced toxicity remain unknown. MeHg is more toxic to the fetus and infants than adults suggesting an ability to disrupt neuronal development (Reuhl and Chang, 1979). In the human CNS, the granule cells of the cerebellum and the neurons of the calcarine cortex are the most sensitive to MeHg (Hunter and Russell, 1954). The molecular basis for this sensitivity is not known, but may involve disruption of intracellular signalling (Atchison and Hare, 1994).

Studies using the fluorescent chelator fura-2 revealed a pronounced increase in $[Ca^{2+}]_i$ following acute exposure of MeHg to synaptosomes (Komulainen and Bondy, 1987; Kauppinen *et al.*, 1989; Denny *et al.*, 1993) or NG108-15 cells (Hare *et al.*, 1993; Hare and Atchison, 1995). The elevations in $[Ca^{2+}]_i$ in synaptosomes were strictly dependent upon Ca^{2+}_e and are most likely due to Ca^{2+}_e influx (Denny *et al.*, 1993), while in NG108-15 cells, both intracellular and extracellular Ca^{2+} components contribute to this effect (Hare *et al.*, 1993; Hare and Atchison, 1995). These studies, designed originally to monitor $[Ca^{2+}]_i$, also revealed that the intracellular concentration of another polyvalent cation was increased by MeHg. In synaptosomes, the increase was immediate and independent of Ca^{2+}_e, and could be blocked or reversed by the cell-permeant chelator TPEN (Arslan *et al.*, 1985), but not the cell-impermeant chelator DTPA. Thus, the cation was likely to be an endogenous heavy metal, although it could not be identified unambiguously due to the limitations of spectrofluorometry. The heavy metal was

identified as Zn^{2+} using ^{19}F-nuclear magnetic resonance spectroscopy of synaptosomes loaded with the fluorinated chelator 5F-BAPTA (Denny and Atchison, 1994). In this study, the elevation in $[Zn^{2+}]_i$ was also independent of Ca^{2+}_e, and could be reversed by the cell permeant chelator TPEN.

Zn^{2+} is an essential trace metal which is required for the activity of many proteins and enzymes (Vallee and Falchuk, 1993). Proteins which require Zn^{2+} exist in each of the six classes of enzymes. Zn^{2+} bound to proteins can serve several purposes (Coleman, 1992). Zn^{2+} can be used in the active site of enzymes for catalysis, or as a structural component to maintain protein conformation or stabilize quaternary structure. Multiple Zn^{2+} ions bind to metallothionein, which is believed to be the major protein responsible for maintaining intracellular Zn^{2+} homeostasis (Vallee and Falchuk, 1993). The Zn^{2+}-finger motifs of many DNA binding proteins are essential for interacting with DNA.

Protein-associated Zn^{2+} is usually coordinated with side chain groups of the amino acids histidine and aspartate or glutamate, or with the sulfhydryl side chains of several cysteines (Vallee and Auld, 1990). Mercurials, such as MeHg, also have a high affinity for sulfhydryls, as well as modest affinity for histidine (Clarkson, 1986). It is possible that MeHg could interact with the Zn^{2+}-binding domain of certain neuronal proteins thereby displacing the associated Zn^{2+}. Organomercurial reagents have been reported to interact with the Zn^{2+}-binding domains of proteins in isolation. The structural Zn^{2+} ions responsible for maintaining the quaternary structure of aspartate carbamyltransferase are rapidly displaced by the organomercurial *p*-hydroxymercuriphenylsulfonate resulting in subunit dissociation (Hunt *et al.*, 1984). Both Zn^{2+} and Hg^{2+} bind to metallothionein through sulfhydryl bridges although exchange of Zn^{2+} for Hg^{2+} has not been studied

(Hamer, 1986). Mercurials can also activate certain metalloendoproteases by binding to a cysteine in a regulatory region of the zymogen causing a conformational change and switching the Zn^{2+} binding motif from a structural to a catalytic form (Springman *et al.*, 1990).

The goals of this study were to determine if the Zn^{2+} associated with synaptic vesicles contributed to the MeHg-induced increases in $[Zn^{2+}]_i$, and to identify the proteins responsible for these elevations. Although the study is not complete, several key observations have been made. Synaptic vesicles and membrane-associated proteins do not appear to contribute to the MeHg-induced elevations in $[Zn^{2+}]_i$. Rather, the source of the Zn^{2+} appears to be several soluble synaptosomal proteins. The isolation and characterization of these proteins is ongoing at this time.

MATERIALS AND METHODS

Chemicals and Solutions: MeHg chloride was obtained from K and K Labs (Plainview, NY). Fura-2 pentapotassium salt, fura-2 acetoxymethyl ester (fura-2/AM) and TPEN were purchased from Molecular Probes (Eugene, OR). Ultrapure $ZnCl_2$ was obtained from Aldrich (Milwaukee, WI). α-Latrotoxin (α-LTX) was obtained from Almone Labs, Inc. (Jerusalem, Israel). Veratridine free base, Hepes free acid, Trizma base, ethylenediaminediacetic acid (EDDA), EGTA, and DTPA were obtained from Sigma Chemical Co. (St. Louis, MO). Macro-Prep High Q anion exchange chromatography support and Bio-Gel P-100 were obtained from BioRad, Inc. (Piscataway, NJ). Molecular weight standards for SDS-PAGE were obtained from New England BioLabs (Beverly, MA). Deionized water (18 MΩ) was used in all buffers. All other chemicals were reagent or electrophoresis grade.

HBS contained (mM): NaCl, 135; KCl, 5; $MgCl_2$, 1; d-glucose, 10; and Hepes free acid, 10. The pH at room temperature was adjusted to 7.4 with Trizma base. HBS typically has a contaminating Ca^{2+} concentration of 6 μM as determined by inductively coupled plasma spectroscopy (Denny *et al.*, 1993). The sucrose buffers (1.2, 0.8 and 0.32 M) were prepared in 3 mM Na_2HPO_4 buffer adjusted to pH 7.4 with HCl.

Fura-2 excitation profiles of Ca^{2+} or Zn^{2+}: Fura-2 (0.5 μM) fluorescence intensity was monitored at the emission wavelength of 505 nm. The fluorescence intensity was determined between the excitation wavelengths of 320 to 400 nm. The Ca^{2+} or Zn^{2+} concentration was varied by mixing buffers which contained a metal chelator only and

one with equimolar concentrations of chelator and Ca^{2+} or Zn^{2+}. EGTA was used to vary Ca^{2+} concentration while EDDA was used to buffer Zn^{2+}.

Preparation of Synaptosomes: Synaptosomes were prepared from the forebrains of male Sprague-Dawley rats (Harlan, 175-199 g) by discontinuous sucrose density gradient centrifugation as described in detail by Shafer and Atchison (1989) with slight modifications (Denny *et al.*, 1993). The synaptosome-enriched fraction (P_{2b}) was collected from the 1.2/0.8 M sucrose interface, resuspended in three volumes of HBS and centrifuged for 10 min at 10,000 × *g*. The pellet was resuspended in 10 ml HBS then loaded with fura-2.

Spectrofluorometry of Fura-2 Loaded Synaptosomes: Five ml of the P_{2b} fraction were incubated with 4 µM fura-2/AM while the remaining five ml were incubated with 0.4% DMSO for 40 min at 30°C. The synaptosomal suspensions were diluted seven-fold by addition of 30 ml HBS and incubated for an additional 20 min at 30°C to promote diffusion of incompletely hydrolyzed fura-2/AM from the synaptosomes. The suspensions were centrifuged at 10,000 × *g* for five min and resuspended in 20 ml fresh HBS.

One ml aliquots of fluorescent indicator-loaded synaptosomes were centrifuged for 30 sec at 12,500 × *g* in a tabletop centrifuge, the pellet was resuspended in two ml of fresh HBS, transferred to a test tube and incubated for 10 min at 37°C. The suspension was transferred to a polystyrene cuvette containing a magnetic stir bar, placed into a spectrofluorometer equipped with a thermally jacketed cuvette holder and magnetic stir

plate (SPEX Industries, Edison, NJ). Excitation scans of fura-2 loaded synaptosomes were acquired and corrected for intrinsic synaptosomal fluorescence.

Protein purification: Synaptosomes were prepared from six rats, the individual washed P_{2b} pellets were resuspended in 5 ml of ice cold 50 mM Hepes (pH 8.0) each and homogenized together at 750 rpm for three strokes. The synaptosomal homogenates were centrifuged at 12,500 x *g* for 10 min, and the supernatant was transferred to a clean centrifuge tube. The pellet was rehomogenized in 30 ml of 50 mM Hepes, and centrifuged at 25,000 x *g* for 20 min along with the previous supernatants. The supernatants were pooled and the soluble fraction was concentrated on an Amicon ultrafiltration concentrator equipped with a PM10 membrane at 40 psi to a final volume of approximately 20 ml. The soluble protein fraction was filtered through a 0.22 µm disposable filter, and applied to a Macro-Prep High Q anion exchange column (20 cm long x 1.5 cm dia). The column was washed with 50 mM Hepes (pH 8.0) at a flow rate of 2.0 ml/min until the absorbance at 280 nm (A_{280}) returned to baseline. Fractions were collected throughout the isolation every three min using a fraction collector operating in fixed interval mode. A continuous pH gradient was used to elute proteins from the column. The starting buffer contained 250 ml of 50 mM Hepes (pH 8.0) and the final buffer contained 250 ml of starting buffer with an additional 1 M NaOH (pH > 14.0). Upon completion of the pH gradient the column was washed with an additional 100 ml of final buffer, regenerated with 250 ml 50 mM Hepes (pH 8.0) containing 1 M NaCl and equilibrated with at least 300 ml of 50 mM Hepes (pH 8.0). MeHg-induced Zn^{2+} release from soluble synaptosomal proteins was monitored qualitatively by fura-2

spectrofluorometry. Fura-2 pentapotassium salt was added to the sample to a final concentration of 0.5 µM. An initial fura-2 excitation scan was then acquired from the wavelengths of 320 to 400 nm at the emission wavelength of 505 nm. MeHg (50 µM final concentration) was then added to the cuvette and another fura-2 excitation scan was acquired. These two scans were compared for shifts in fura-2 fluorescence consistent with elevations in free Zn^{2+} concentration. Consecutive fractions which released Zn^{2+} upon MeHg addition were pooled, and frozen for subsequent analysis. Aliquots were withdrawn for protein determination and SDS-PAGE analysis. In some cases the peaks from the High Q column were further purified by gel filtration chromatography. The individual peaks were concentrated to approximately three ml by ultrafiltration as before, and applied to a Bio-Gel P-100 column (40 cm long x 2.5 cm dia) equilibrated with 50 mM Hepes (pH 8.0). A constant flow rate of 0.2 ml/min was maintained and fractions were collected every 10 min. Fractions which released Zn^{2+} upon addition of MeHg were pooled and saved for further analysis.

Protein Assays: Protein content was determined by the method of Lowry *et al.* (1951) using bovine serum albumin as a standard.

SDS-PAGE Analysis of Protein Fractions: Protein purity was evaluated by SDS-PAGE (Laemmli, 1970) using a Bio-Rad Protean II minigel electrophoresis system (Piscataway, NJ) according to manufacturer's instructions. Protein samples were boiled for two min in sample buffer containing ß-mercaptoethanol. Electrophoresis was performed at 200 V using 0.75 mm thick minigels containing 12% polyacrylamide.

Silver Staining of SDS-PAGE Minigels: Gels were stained using the ammoniacal silver method of Oakley *et al.* (1980).

RESULTS

Because these studies relied heavily on monitoring MeHg-induced changes in fura-2 fluorescence, the possibility that MeHg may interact directly with fura-2 was tested. MeHg concentrations up to 1 mM did not alter the fluorescence properties of fura-2 when added to a cuvette containing 0.5 μM fura-2 pentapotassium salt (not shown).

The effects of Ca^{2+} on the fluorescence properties of fura-2 have been well defined (Grynkiewicz *et al.*, 1985). The excitation maximum of fura-2 uncomplexed to Ca^{2+} is approximately 370 nm while that of Ca^{2+}-complexed fura-2 is near 340 nm (Fig. 4.1A). Thus, increases in the fluorescence intensity at the excitation wavelength of 340 nm concurrent with decreases in intensity at 380 nm are consistent with an increase in Ca^{2+} concentration. An important consequence of this shift in the fluorescence properties of fura-2 caused by Ca^{2+} is the presence of an excitation wavelength at 360 nm which is insensitive to changes in Ca^{2+} concentration, and is known as the isosbestic point. The fluorescence intensity at the excitation wavelength of 360 nm remains constant at any Ca^{2+} concentration. Thus, any change in the fluorescence intensity at 360 nm cannot be attributed to a change in Ca^{2+} concentration. By monitoring the fluorescence intensity at the excitation wavelength of 360 nm it is possible to study the interaction of fura-2 with cations other than Ca^{2+}.

Zn^{2+} interacts with fura-2 with a higher affinity than Ca^{2+} (Grynkiewicz *et al.*, 1985), but its effects on the fluorescence properties have not been studied systematically (Hechtenberg and Beyersmann, 1993). The effects of Zn^{2+} on fura-2 fluorescence were studied in EDDA-buffered Zn^{2+} solutions containing 0.5 μM fura-2 pentapotassium salt (Fig. 4.1B). Increasing the proportion of the Zn^{2+}-containing buffer caused a gradual

FIG. 4.1. Fura-2 excitation profiles of Ca^{2+} or Zn^{2+}. Fura-2 (0.5 μM) fluorescence intensity was monitored at the emission wavelength of 505 nm. Points were acquired for one sec at integer excitation wavelength values. The Ca^{2+} or Zn^{2+} concentration was varied by altering the proportions of buffers which contained a metal chelator only and one with equimolar concentrations of chelator and Ca^{2+} or Zn^{2+}. ***A:*** Fura-2 excitation profile in Ca^{2+}-containing buffers. Buffers contained 10 mM EGTA and 10 mM EGTA with 10 mM Ca^{2+}. ***B:*** Fura-2 excitation profile of Zn^{2+}. Buffers contained 10 mM EDDA and 10 mM EDDA with 10 mM Zn^{2+}.

Fig. 4.1.

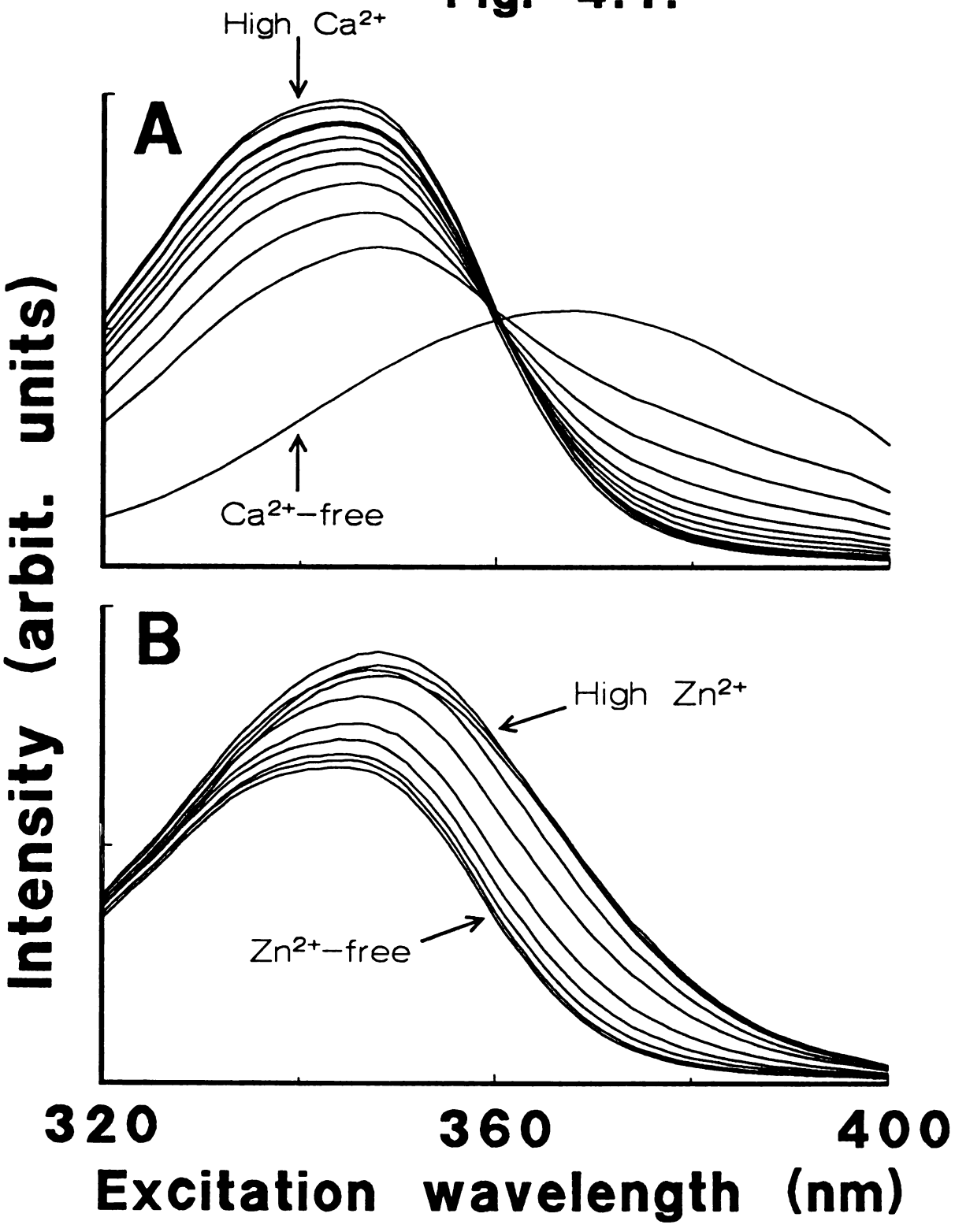
High Ca2+
A
Ca2+–free
B
High Zn2+
Zn2+–free
Intensity (arbit. units)
320
360
400
Excitation wavelength (nm)

increase in the fura-2 excitation spectrum. Unlike Ca^{2+} which shifted the excitation maximum of fura-2, Zn^{2+} increased the fluorescence intensity at all excitation wavelengths. The fluorescence intensity at the excitation wavelengths between 340 and 380 nm was particularly responsive to elevations in Zn^{2+} concentration. There was no isosbestic point for Zn^{2+} and fura-2. Based upon the profound difference in fura-2 spectra with Zn^{2+} or Ca^{2+}, the effects of MeHg on Zn^{2+} concentration could be discerned from those on Ca^{2+}.

MeHg increases $[Zn^{2+}]_i$ by acting on some endogenous pool of Zn^{2+} present in the nerve terminal. Zn^{2+} is associated with the synaptic vesicles of certain glutamatergic nerve terminals. The possibility that vesicular Zn^{2+} contributed to the MeHg-induced elevations in $[Zn^{2+}]_i$ was tested using fura-2 loaded synaptosomes pretreated with agents which mobilize synaptic vesicles. If a component of the MeHg-induced increases in $[Zn^{2+}]_i$ was vesicular in origin, then elevations $[Zn^{2+}]_i$ would be reduced by mobilization of synaptic vesicles prior to MeHg exposure. As such, the MeHg-induced elevations in $[Zn^{2+}]_i$ were assessed following mobilization of synaptic vesicles by three different treatments. Elevating K^+ concentration depolarizes the synaptosomal membrane, resulting in activation of voltage-dependent Ca^{2+} channels, Ca^{2+} influx, vesicle fusion and release of vesicular contents. Veratridine is a plant alkaloid which also mobilizes synaptic vesicles by a mechanism involving depolarization of the synaptosomal membrane and subsequent activation of Ca^{2+} channels. Veratridine prolongs the open time of voltage-dependent Na^+ channels, ultimately leading to membrane depolarization due to increased Na^+ influx. α-LTX is the primary active toxin of Black Widow spider venom. Although the precise mechanism of action of α-LTX is not clear, it is known to be dependent upon

binding to a synaptosomal membrane receptor. Following binding, α-LTX induces a massive release of vesicular stores which occurs in the presence or absence of Ca^{2+}_e (Meldolesi *et al.*, 1984).

Changes in the excitation spectrum of fura-2 loaded synaptosomes were monitored following each of the different treatments (Fig. 4.2). A similar experimental paradigm was used for each of agents. After acquiring an initial excitation spectrum of fura-2 loaded synaptosomes, the synaptosomal suspensions were exposed to buffer, 45 mM K^+, 6 nM α-LTX or 0.1 mM veratridine for five min. These concentrations have been shown to be sufficient to cause neurotransmitter release from synaptosomes (McMahon and Nicholls, 1993; Meldolesi *et al.*, 1984; Richards *et al.*, 1984). Following the five min interval for vesicle release, a second excitation spectrum was acquired. EGTA (20 μM) was added to the suspensions to reduce $[Ca^{2+}]_e$ to approximately 0.1 μM, and a third excitation scan was acquired after a four min incubation period (Denny *et al.*, 1993). A fourth excitation scan was acquired following addition of 25 μM MeHg to the synaptosomal suspension. The fifth scan was the acquired after addition of TPEN (5 μM) to verify the changes in fura-2 fluorescence were due to an increase in the intracellular concentration of an endogenous heavy metal.

By analyzing the changes in fura-2 excitation spectra caused by addition of the various agents, it is possible to differentiate between changes in $[Ca^{2+}]_i$ and $[Zn^{2+}]_i$. Elevating Ca^{2+} concentration increases fura-2 fluorescence intensity at 340 nm and decreases intensity at 380 nm, but does not alter the intensity at 360 nm. Zn^{2+} increases fura-2 intensity at all excitation wavelengths, particularly in the region between 340 and 380 nm. K^+, α-LTX and veratridine all caused changes in the fura-2 excitation spectrum

FIG. 4.2. Effects of MeHg on the excitation profiles of fura-2 loaded synaptosomes following treatment with agents which mobilize synaptic vesicles. An initial fura-2 excitation spectra of fura-2 loaded synaptosomes was obtained at the emission wavelength of 505 nm. Individual synaptosomal suspensions were then exposed to one of the following test agents for five min: HBS (***top left***), 45 mM K^+ (***top right***), 6 nM α-LTX (***bottom left***) or 0.1 mM veratridine (***bottom right***). EGTA (20 μM) was added to the suspensions to reduced $[Ca^{2+}]_e$. MeHg (25 μM) caused changes in the fura-2 excitation profile which resembled Zn^{2+}. TPEN (5 μM) reversed the changes in fluorescence intensity. The hatched area indicates the MeHg-induced changes in fura-2 fluorescence intensity which could be attributed to an elevation in $[Zn^{2+}]_i$. Each line is the average of four experiments performed in duplicate.

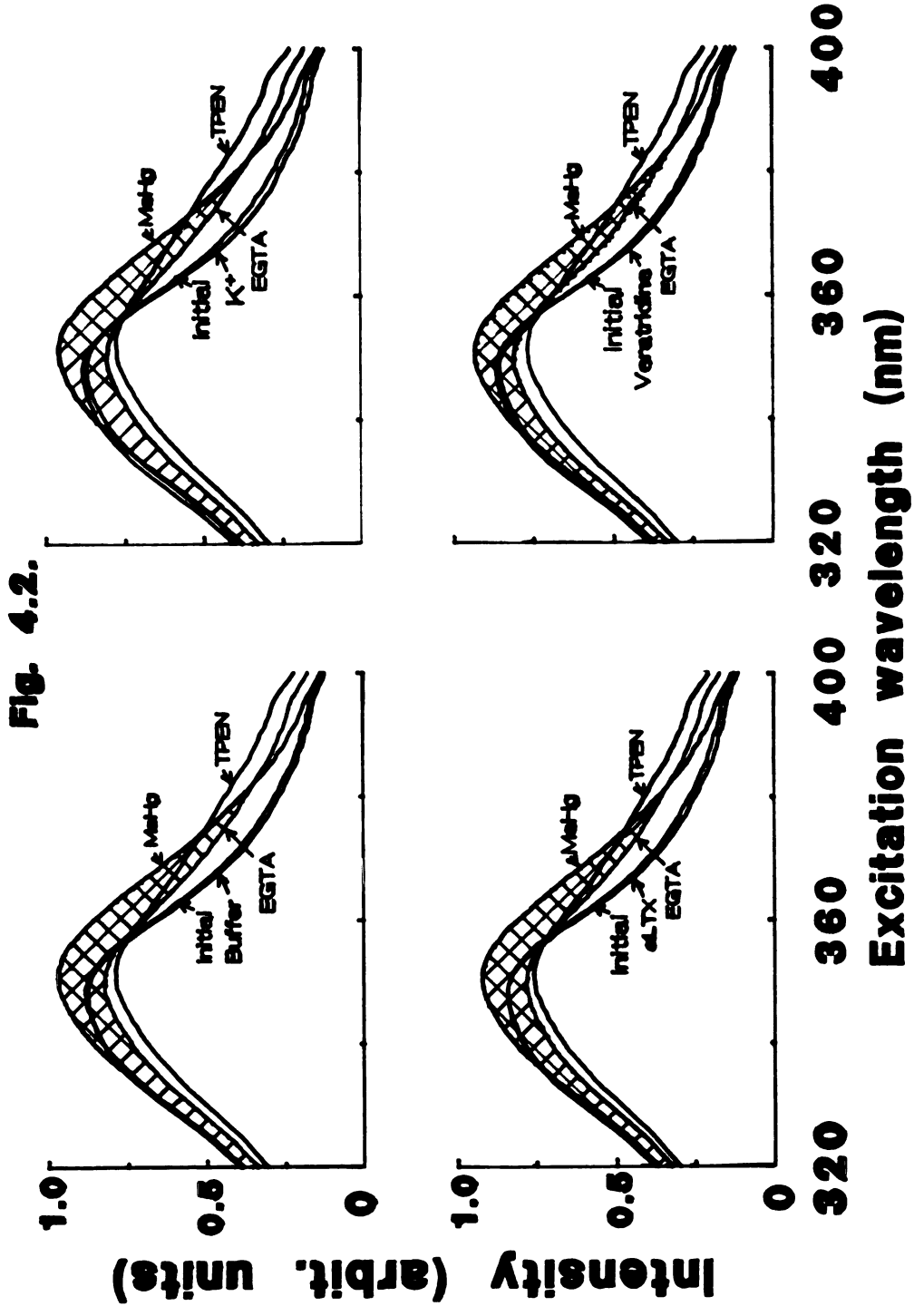
Intensity (arbit. units)
1.0
0.5
0
320
360
400
320
360
400
Excitation wavelength (nm)
Mn-Hb
TPEN
Initial
Buffer
EGTA
Mn-Hb
TPEN
Initial
K+
EGTA
Mn-Hb
TPEN
Initial
α-LTX
EGTA
Mn-Hb
TPEN
Initial
Verapamil
EGTA

Fig. 4.2.

consistent with an increase in $[Ca^{2+}]_i$ (Fig. 4.2). Similarly, the effect of EGTA was consistent with a decrease in $[Ca^{2+}]_i$. MeHg increased the fluorescence intensity in the region between 340 and 380 nm relative to the EGTA spectra. The MeHg-induced alterations in fura-2 fluorescence which are consistent with an increase in $[Zn^{2+}]_i$ are indicated by the cross hatched areas. It is important to note, however, that these were not totally identical to an increase in $[Zn^{2+}]_i$ alone. The increases observed in buffer-treated synaptosomal suspensions were of similar magnitude to those observed in synaptosomes treated with K^+, α-LTX or veratridine. Thus, mobilization of synaptic vesicles did not reduce the MeHg-induced elevation in $[Zn^{2+}]_i$. The effects of MeHg were reversed by the cell-permeant chelator TPEN.

The soluble fraction of brain extracts contains several Zn^{2+} binding proteins (Itoh *et al.*, 1983). It is possible the source of the MeHg-induced elevations in $[Zn^{2+}]_i$ is one or more of these proteins. If this is the case, it may be possible to purify these proteins using protein chromatography.

Fura-2 was used to monitor release of endogenous Zn^{2+} from different protein fractions following MeHg exposure. Unfortunately, as a consequence, it is not possible to include other chelators such as ethylenediaminetetraacetic acid or EGTA in the buffers since they would effectively out-compete fura-2 for any released Zn^{2+}. Similarly, the use of Tris as a buffer was avoided because it also chelates Zn^{2+}.

Synaptosomes were homogenized in 50 mM Hepes (pH 8.0), and centrifuged to separate the particulate and soluble fractions. The particulate fraction was resuspended in an equal volume of buffer. Fura-2 pentapotassium salt (0.5 μM) was added to 1.5 ml aliquots of each fraction, and an excitation spectrum was acquired. MeHg (50 μM) was

then added to the aliquots and another spectrum acquired. The two spectra were compared for changes consistent with a MeHg-induced elevation in Zn^{2+} concentration. An increase was observed in the soluble fraction (Fig. 4.3), but no activity was found in the particulate fraction (not shown). The soluble fraction was concentrated, applied to a High Q anion exchange column and proteins were eluted using a pH gradient. Three distinct peaks which release Zn^{2+} upon exposure to 50 μM MeHg were resolved by this procedure (Fig. 4.4). The first peak eluted in the second half of the flow through, the second peak eluted between pH 8.6 to 9.4, and the third peak eluted at pH 12.0 as indicated by the cross-hatched areas in the chromatograph.

The protein components of these three peaks were analyzed by SDS-PAGE under reducing conditions using 12% polyacrylamide minigels. The gels did not stain adequately using the Coomassie blue method; therefore the gel were silver stained (Fig. 4.5). The protein content of Peak 1 was very complex indicating that little purification of this peak was achieved. Peak 2 and Peak 3 each contained a few major protein bands and several minor bands, consistent with significant purification of proteins from the crude soluble fraction.

Because Peak 2 was more pure than Peak 1 and possessed greater total activity than Peak 3, it has been subjected to additional purifications steps. Peak 2 was concentrated to approximately five ml, and subjected to cation exchange chromatography using an Econo-prep High CM cartridge. A single active peak eluted in the flow through, no additional activity was observed following washing of the column with 0.1 or 1.0 M NaCl or 1M (not shown). Thus, the protein(s) did not appear to have any affinity for the cation exchange support. The active peak obtained from the cation exchange column was

FIG. 4.3. Effect of MeHg on the excitation profile of fura-2 in solution with soluble synaptosomal proteins. Fura-2 pentapotassium salt (0.5 μM) was added to a 1.4 ml sample of soluble synaptosomal proteins diluted eight-fold with 50 mM Hepes (pH 8.0), and an excitation spectrum was acquired between 320 and 400 nm (**solid line**). MeHg (50 μM) was added, and another excitation scan was acquired (**dashed line**). The MeHg-induced shift in fura-2 fluorescence is consistent with an elevation in Zn^{2+} concentration.

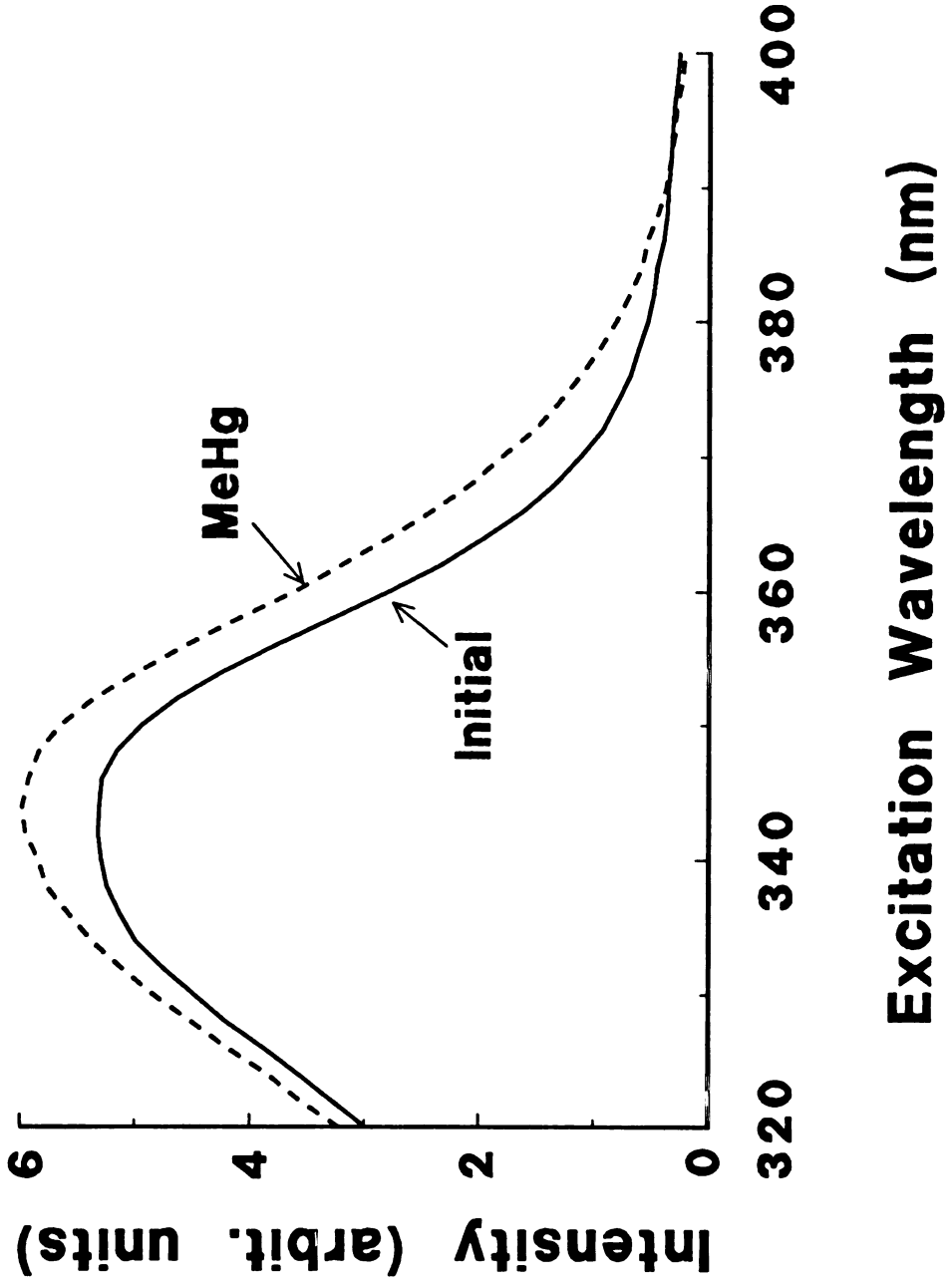
MeHg
Initial
Intensity (arbit. units)
0
2
4
6
320
340
360
380
400
Excitation Wavelength (nm)

Fig. 4.3.

FIG. 4.4. Anion exchange chromatography of soluble synaptosomal proteins. A sample (15-20 ml) of soluble synaptosomal proteins was loaded onto a Macro-Prep High-Q anion exchange column. Fractions were collected in six ml volumes every three min using a flow rate of two ml/min. The absorbance at 280 nm (A_{280})was measured continuously as an index of protein content (**solid line, left axis**). After A_{280} returned to baseline, a pH gradient was used to elute proteins from the column (**dashed line, right axis**). The initial buffer contained 250 ml of 50 mM Hepes (pH 8.0), and the final buffer consisted of 250 ml of initial buffer with an additional 1 M NaOH. Anion exchange chromatography separated the soluble fraction into three peaks which released Zn^{2+} upon addition of MeHg (**hatched area**). Alterations in fura-2 fluorescence were used to qualitatively measure Zn^{2+} release. Individual peaks which released Zn^{2+} were combined and saved for further analysis.

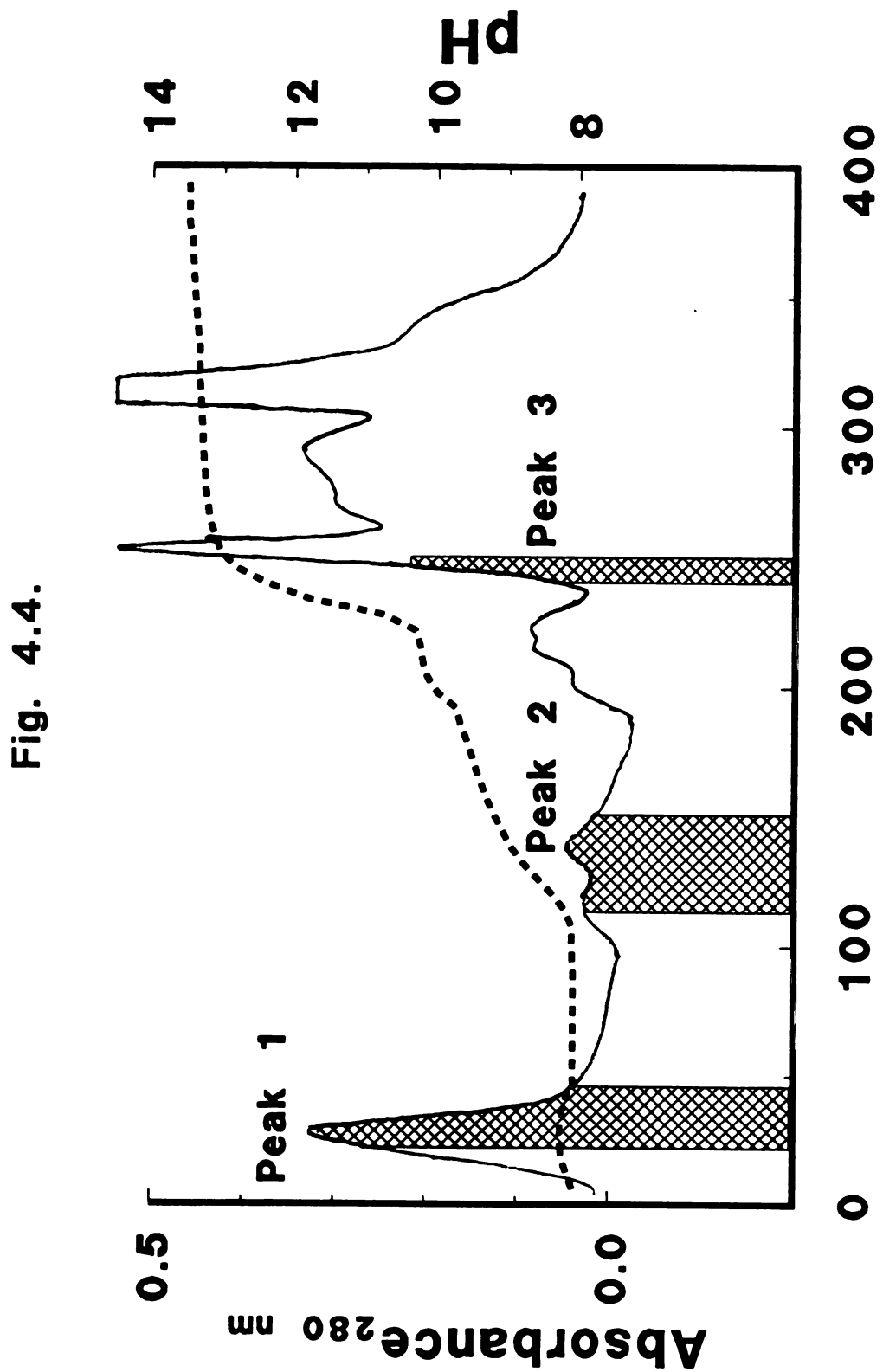
pH
14
12
10
8
Peak 1
Peak 2
Peak 3
0.5
0.0
Absorbance280 nm
0
100
200
300
400
Volume (ml)

Fig. 4.4.

FIG. 4.5. SDS-PAGE analysis of anion exchange chromatography peaks. Aliquots of the various fractions were analyzed by SDS-PAGE using 12% acrylamide minigels under reducing conditions. Lanes contained molecular weight standards (**Marker**), initial soluble fraction (**1**), Peak 1 (**2**), Peak 2 (**3**) or Peak 3 (**4**) obtained by anion exchange chromatography. Molecular weights (kDa) of the standards are indicated on the left.

Fig. 4.5.

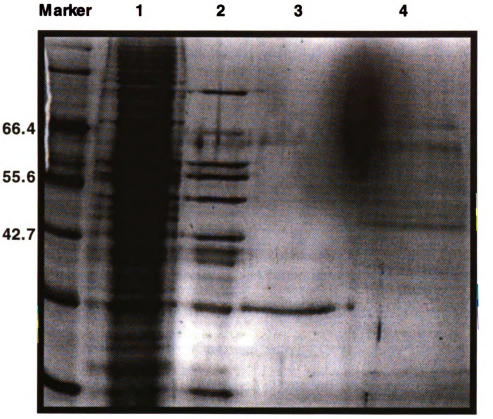

then applied to a Bio-Gel P-100 column for further purification by gel filtration. MeHg-induced Zn^{2+} release was observed in a single region consistent with a minor protein species in the molecular weight range of 50 to 55 kDa, as indicated by the chromatograph (Fig. 4.6). SDS-PAGE analysis of the active fraction revealed it contained several minor protein components of a similar molecular weight (Fig. 4.7). Thus, the source of the MeHg-induced elevations in Zn^{2+} in Peak 2 has not yet been purified to homogeneity. The complete purification of this fraction should allow for identification by N-terminal sequence analysis and/or Western blotting.

Future efforts will be directed toward purifying Peak 2 to homogeneity, and obtaining amino acid sequence information. Peak 1 consists of too many protein components to be purified effectively by gel filtration. It may be possible to use cation exchange chromatography to resolve this fraction into several protein components. Peak 3 is much less complex, however the total activity is very low. The protein may be denatured by the extremely high pH required for elution. Isolation of Peak 3 may require pooling the samples obtained from several isolations.

FIG. 4.6. Gel filtration chromatography of Peak 2 from anion exchange chromatography. Peak 2 was concentrated to approximately three ml and analyzed by gel filtration chromatography using Bio-Gel P-100. Fractions were collected in 2.5 ml volumes every ten min using a flow rate of 0.25 ml/min. A_{280} was monitored continuously (**solid line, right axis**). MeHg-induced Zn^{2+} release was analyzed using changes in fura-2 fluorescence. A single region of activity was observed (**hatched area**). This peak was pooled and saved for further analysis.

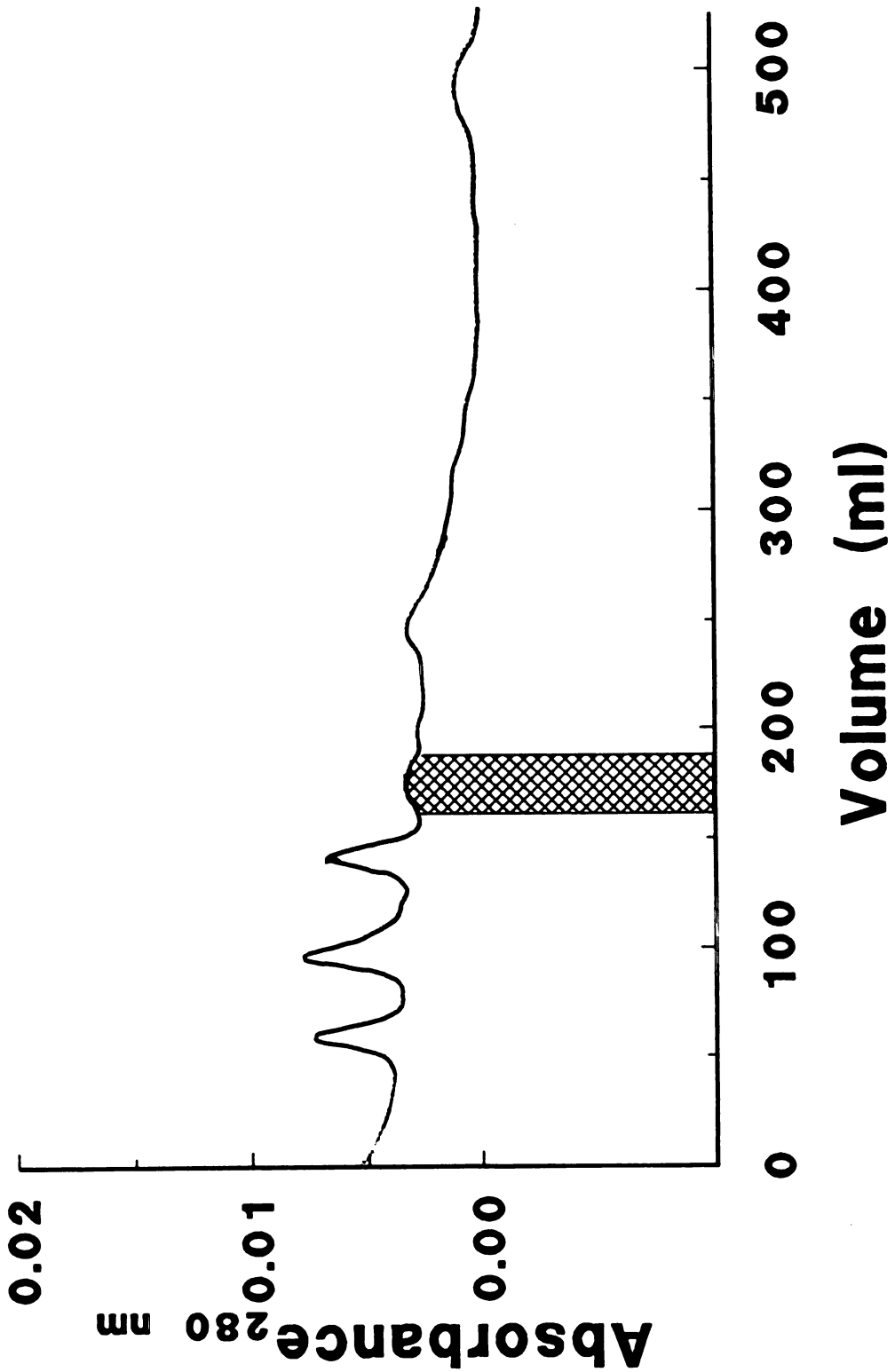

Fig. 4.6.

FIG. 4.7. SDS-PAGE analysis of active peak obtained by gel filtration chromatography of anion exchange Peak 2. Fractions were analyzed using 12% acrylamide minigels under reducing conditions. Lanes contained molecular weight standards (**Marker**), the initial soluble synaptosomal protein fraction (**1**), Peak 2 from anion exchange chromatography (**2**), active peak from subsequent cation exchange (**3**) and gel filtration chromatography (**4**). Two bands are present in Lane 3 between 50 and 55 kDa.

Fig. 4.7.

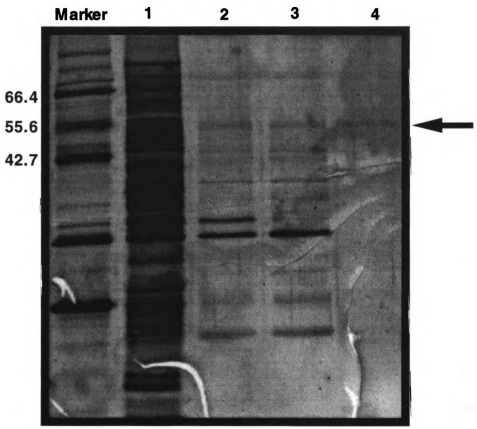

DISCUSSION

MeHg elevates $[Zn^{2+}]_i$ by an action at an endogenous source. The goal of this study was to determine if stores known to contain Zn^{2+} contributed to the MeHg-induced elevations in $[Zn^{2+}]_i$. The possible role of Zn^{2+} associated with the synaptic vesicles as well as synaptosomal proteins was investigated. Release of Zn^{2+} from synaptic vesicles and particulate synaptosomal proteins does not contribute to the MeHg-induced elevations in $[Zn^{2+}]_i$; the source of the Zn^{2+} appears to be several soluble synaptosomal proteins.

The possibility that the synaptic vesicles contributed to MeHg-induced elevations in $[Zn^{2+}]_i$ was investigated pharmacologically using fura-2 loaded synaptosomes treated with agents known to mobilize synaptic vesicles. If the Zn^{2+} was mobilized along with the vesicles, then pretreatment with the various pharmacological agents would reduce the MeHg-induced $[Zn^{2+}]_i$. Exposure of synaptosomal suspensions to 45 mM K^+, 6 nM α-LTX or 0.1 mM veratridine for five min had no effect on the MeHg-induced elevations in $[Zn^{2+}]_i$.

The results of the study involving mobilization of synaptic vesicles are consistent with vesicular Zn^{2+} not contributing to MeHg-induced elevations in $[Zn^{2+}]_i$. An alternative explanation is that vesicular Zn^{2+} contributes to the elevations, but the Zn^{2+} is not mobilized along with vesicular contents. Although this contingency was not tested directly, it is inconsistent with the work of others. Direct stimulation of Zn^{2+}-containing hippocampal pathways in slice preparations increased the Zn^{2+} concentration in the bathing solution (Assaf and Chung, 1984; Howell *et al.*, 1984). Furthermore, prolonged kainic acid-induced seizures reduce the amount of histochemically-stainable Zn^{2+} associated with hippocampal mossy fiber boutons (Frederickson *et al.*, 1988). These

studies provide evidence that vesicular Zn^{2+} is mobilized with transmitter following stimulation. The possibility that vesicular Zn^{2+} is released then resequestered rapidly is not consistent with the observation that cutting the fibers of a Zn^{2+}-containing system causes a loss of histochemically stainable Zn^{2+} in the terminals within 12-24 hr (Haug *et al.*, 1971), suggesting Zn^{2+} is taken in the soma and then transported to the terminal along the fibers.

Another possibility is that Zn^{2+} is mobilized with vesicular contents, but the different agents did not mobilize sufficient quantities of synaptic vesicles to affect the MeHg-induced elevations in $[Zn^{2+}]_i$. While transmitter release was not measured, all of these agents are capable of eliciting transmitter release (McMahon and Nicholls, 1993; Meldolesi *et al.*, 1984; Richards *et al.*, 1984). Significant mobilization of synaptic vesicles would be expected for the α-LTX treated synaptosomes since this toxin is active in the presence or absence of Ca^{2+}_e (Meldolesi *et al.*, 1984), and approximately ten min elapsed between the addition of α-LTX and MeHg. During this interval, α-LTX mobilized almost 50% of the radiolabeled norepinephrine loaded into guinea pig synaptosomes, with similar results for dopamine release from PC12 cells (Meldolesi *et al.*, 1984). Based on this information, the elevations would be attenuated in α-LTX treated synaptosomes if the Zn^{2+} associated with synaptic vesicles contributed to the increase in $[Zn^{2+}]_i$. The most plausible conclusion is that the Zn^{2+} associated with the synaptic vesicles does not contribute appreciably to the MeHg-induced elevations in $[Zn^{2+}]_i$.

Because vesicular Zn^{2+} did not appear to contribute to the MeHg-induced in $[Zn^{2+}]_i$, the next potential source investigated was the synaptosomal proteins.

Fractionation of homogenized synaptosomes into particulate and soluble components revealed that only the soluble fraction contained measurable MeHg-induced Zn^{2+} release. The protein components of the soluble fraction were resolved into three well defined peaks of MeHg-induced Zn^{2+} release by anion exchange chromatography after elution by increasing pH. Peak 1 eluted in the flow-through and, therefore, is likely to be a basic protein. Peak 2 eluted between pH 8.6 and 9.4, and Peak 3 eluted near pH 12.0. Thus, it appears more than one protein is responsible for the MeHg-induced elevations in $[Zn^{2+}]_i$.

Peak 2 was selected for further analysis by gel filtration chromatography because of its total activity and relative purity following anion exchange chromatography. Gel filtration chromatography of Peak 2 resolved the MeHg-induced Zn^{2+} release activity to a single region between 50 to 55 kD, which contained at least two proteins based on SDS-PAGE. Therefore, Peak 2 is likely to be composed of one or more proteins between the 50 and 55 kD. An additional purification step may resolve these two protein components. Once Peak 2 has been purified to homogeneity, it can be subjected to N-terminal sequence analysis. The sequence obtained can be used to search protein sequence data banks of N-terminal regions of known proteins. In addition to providing a means of identification of the protein present in Peak 2, this procedure may also assist in the identification of the other peaks as well. Because MeHg releases endogenous Zn^{2+} from proteins in all three peaks, it is possible the Zn^{2+}-binding motifs of these proteins are similar. As such, it may be possible to use sequence information obtained from Peak 2 to search for similar Zn^{2+}-binding structures in other proteins found in the nerve

terminal. This information would guide the purification of the remaining peaks, although this is entirely dependent upon the identification of the protein present in Peak 2.

In the event that Peak 2 cannot be identified by sequence analysis, it may still be possible to isolate the remaining peaks using protein chromatography. Peak 1 does not bind to the anion exchange column, and thus is likely to be a basic protein. Cation exchange or hydroxyapatite chromatography may be suitable to purify Peak 1 further. Peak 3 may be more difficult to isolate due to the low total activity and high pH of the sample. It may be necessary to combine the samples from several isolations before proceeding to the next step.

An area in need of refinement is the method of detection of MeHg-induced Zn^{2+} release. Currently, qualitative changes in fura-2 excitation spectra are used to measure activity. This is both a sensitive and rapid procedure to determine activity, but it lacks the potential for quantification due to the subtle changes in spectra observed in some samples. The use of 5F-BAPTA and ^{19}F-NMR spectroscopy (Denny *et al.*, 1994), instead of fura-2 spectrofluorometry, would provide more quantitative information. At this time, attempts to quantify Zn^{2+} release using ^{19}F-NMR spectroscopy have been unsuccessful due to the low sensitivity of the procedure, but this can be overcome by increasing the protein concentration of the samples.

Determination of the endogenous Zn^{2+} sources would be useful in the study of MeHg-induced neurotoxicity for several reasons. The loss of Zn^{2+} from these protein may disrupt normal protein function, leading to toxic responses. This could be tested directly by measuring protein activity before and after MeHg exposure. Because synaptosomes are a heterogenous population, it is not known if these proteins, and the associated MeHg-

induced elevations in $[Zn^{2+}]_i$, are found in all synaptosomes, or only a sensitive subpopulation. This question could be addressed by immunocytochemistry of brain slices using antibodies directed against the different target proteins. Because Zn^{2+} is toxic to neurons, it is also possible a component of MeHg neurotoxicity is due to the elevation in $[Zn^{2+}]_i$. The nature and consequences of the elevation in $[Zn^{2+}]_i$ are the topics of future research efforts.

This study addresses the endogenous sources of the MeHg-induced elevations in $[Zn^{2+}]_i$. The experiments focused on the two most logical potential sources of the Zn^{2+}: synaptic vesicle and soluble proteins. The Zn^{2+} associated with synaptic vesicles did not contribute to the elevations in $[Zn^{2+}]_i$. Prominent changes in fura-2 fluorescence consistent with an increase in Zn^{2+} concentration were observed following exposure of soluble synaptosomal proteins to MeHg. Anion exchange chromatography of soluble synaptosomal proteins separated this fraction into three distinct peaks. Subsequent analysis of Peak 2 by gel filtration chromatography revealed the protein(s) was between 50 and 55 kDa. Purification of this fraction to homogeneity will require additional chromatographic techniques. Hopefully, the identification of this protein will assist in the purification of the remaining peaks. Once these proteins are identified, the information could be used to study possible role of elevations in $[Zn^{2+}]_i$ in the mechanisms and specificity of MeHg neurotoxicity.

CHAPTER FIVE

CONCLUSIONS

A. Summary of research.

Previous investigations using fura-2 loaded synaptosomes lacked sufficient temporal resolution to distinguish clearly the onset of the intracellular and extracellular components of MeHg-induced elevations in $[Ca^{2+}]_i$ (Komulainen and Bondy, 1987b; Kauppinen *et al.*, 1989). Additional studies using fura-2 loaded synaptosomes were designed to resolve the contributions of mitochondrial and Ca^{2+}_e to the MeHg-induced elevations in $[Ca^{2+}]_i$ at the nerve terminal (Denny *et al.*, 1993). MeHg caused a biphasic elevation in ratio of fluorescence intensity at the Ca^{2+}-sensitive excitation wavelengths 340 and 380 nm (340/380 nm ratio). The initial phase occurred immediately, was independent of Ca^{2+}_e and maximal at a MeHg concentration of 25 μM. The second phase was strictly dependent upon Ca^{2+}_e, was concentration-dependent with respect to both MeHg and Ca^{2+}_e, and continued gradually over time. Using Mn^{2+} as a surrogate for Ca^{2+}, it was determined that the second phase elevations in 340/380 nm ratio were due to increased synaptosomal plasma membrane permeability leading to influx of Ca^{2+}_e.

Disruption of mitochondrial Ca^{2+} regulation was examined as a possible cause of the immediate elevations in 340/380 nm ratio. In the absence of Ca^{2+}_e, depolarization of synaptosomal mitochondria using NaN_3 and oligomycin did not affect 340/380 nm ratio. Thus, either the mitochondria did not store measurable amounts of Ca^{2+} under resting conditions, or mitochondrial depolarization alone was insufficient to cause mitochondrial Ca^{2+} release. Predepolarization of the mitochondria did not alter the response of synaptosomes to subsequent addition of MeHg, suggesting that the immediate elevation in 340/380 nm ratio was not mediated by depolarization of the mitochondrial membrane. Ruthenium red was also ineffective at blocking the immediate elevations in 340/380 nm

ratio caused by MeHg. This suggested that these elevations were not due to MeHg-induced disruption of mitochondrial Ca^{2+} regulation.

The ER was also explored as a possible source of the immediate elevations in 340/380 nm ratio. Neither thapsigargin, which inhibits the Ca^{2+}-ATPase of the ER, nor caffeine, which facilitates CICR, increased the 340/380 nm ratio, and both were similarly ineffective at altering the response to subsequent addition of MeHg. Therefore, the initial elevation in 340/380 nm ratio could not be ascribed to release of Ca^{2+} from established intracellular stores.

Experiments conducted at the Ca^{2+}-insensitive excitation wavelength of 360 nm, designed originally to monitor the timecourse of the MeHg-induced increase in Mn^{2+} permeability, revealed a pronounced increase in fluorescence intensity immediately upon addition of MeHg. This elevation in intensity was not due to an increase in $[Ca^{2+}]_i$, but rather an elevation in the intracellular concentration of some other cation which interacts with fura-2. The identification of this endogenous polyvalent cation as well as its intracellular source has been the topic of additional investigations (see below).

Based on investigations using fura-2 loaded synaptosomes it was apparent that MeHg increased the plasma membrane permeability to divalent cations. These experiments also suggested that MeHg does not release Ca^{2+} which was previously sequestered into the mitochondria or ER. However, it is possible that the Ca^{2+} sequestering capacity of these organelles may have been compromised by the preparation of the synaptosomes. As such, potential contributions of Ca^{2+} from these sources were also been evaluated in individual intact cells. Changes in fluorescence were monitored in single fura-2 loaded neuroblastoma × glioma hybrid cells (NG108-15) using digital

imaging microscopy (Hare *et al.*, 1993). Digital imaging microscopy also generates useful spatial information regarding the source of the elevations in $[Ca^{2+}]_i$. In the presence of Ca^{2+}_e, acute exposure to MeHg caused multiphasic alterations in fura-2 fluorescence. MeHg increased initially the ratio of fluorescence intensity at the excitation wavelengths of 340 and 380 nm. This was followed closely by a plateau phase, during which the ratio remained essentially constant, or declined slightly. A final phase consisting of a precipitous increase in 340/380 nm ratio occurred shortly thereafter. Increasing the concentration of MeHg from 2 to 5 μM did not alter the magnitude of these phases, but did hasten their onset.

Closer inspection of the fluorescence intensity profiles revealed effects of MeHg on fura-2 fluorescence which were inconsistent with an elevation in $[Ca^{2+}]_i$ alone. The initial elevation in ratio consisted of an increase in fluorescence intensity at the excitation wavelength of 340 nm and a simultaneous decrease at 380 nm, consistent with an elevation in $[Ca^{2+}]_i$. Following this initial elevation in $[Ca^{2+}]_i$ ("first Ca^{2+} phase"), the fluorescence intensity at both 340 and 380 nm rose steadily in tandem, inconsistent with an increase in $[Ca^{2+}]_i$ alone. The ionic basis for this effect of MeHg on fura-2 fluorescence cannot be attributed to an elevation in $[Ca^{2+}]_i$ ("non-Ca^{2+} phase"). This phase was followed by a drastic divergence of the fluorescence intensity at the excitation wavelengths of 340 and 380 nm, again consistent with an increase in $[Ca^{2+}]_i$ ("second Ca^{2+} phase"). Reducing $[Ca^{2+}]_i$ to 0.1 μM using EGTA did not affect the first Ca^{2+} phase or the non-Ca^{2+} phase, but ablated the second Ca^{2+} phase. Thus, the first Ca^{2+} phase and the non-Ca^{2+} phase were independent of Ca^{2+}_e, while the second Ca^{2+} phase was strictly dependent upon Ca^{2+}_e. MeHg causes a similar multiphasic response in fura-2 loaded

cerebellar granule cells in culture, however these cells are approximately ten times more sensitive to MeHg than NG108-15 cells (Marty *et al.*, 1995). This may account for the heightened sensitivity of this particular cell type following MeHg exposure (Takeuchi *et al.*, 1962).

The origin of the Ca^{2+} responsible for the first Ca^{2+} phase in NG108-15 cells has been examined in greater detail. The plasma membrane permeability to exogenously-administered Mn^{2+} was not increased during this phase, consistent with mobilization of Ca^{2+} from an intracellular source (Hare and Atchison, 1995). Predepolarization of the mitochondrial membrane did not elevate $[Ca^{2+}]_i$ or alter the response to subsequent addition of MeHg either in the presence or absence of Ca^{2+}_e (Hare *et al.*, 1993). Apparently, depolarization of the mitochondria *per se* is not sufficient to elevate $[Ca^{2+}]_i$ in these cells, and the elevations in $[Ca^{2+}]_i$ observed in the absence of Ca^{2+}_e can not be attributed to release of mitochondrial Ca^{2+} stores resultant from depolarization of the mitochondrial membrane. Because the mitochondria did not appear to contribute substantially to the first Ca^{2+} phase, other intracellular Ca^{2+} stores were investigated.

A prominent intracellular Ca^{2+} pool found in NG108-15 cells is located in the ER. The contents of this pool can be released by agents such as the nonapeptide bradykinin, which activates PLC to generate IP_3 (Ogura *et al.*, 1990). Mobilization of IP_3-sensitive ER Ca^{2+} stores with bradykinin causes a rapid elevation in $[Ca^{2+}]_i$. Upon depletion of Ca^{2+} stores, the ER is promptly refilled by a thapsigargin-sensitive Ca^{2+}-ATPase located on the ER membrane (Lo *et al.*, 1993). Pre-depletion of IP_3-sensitive Ca^{2+} stores with bradykinin and thapsigargin in NG108-15 cells greatly attenuated the magnitude of the first Ca^{2+} phase upon subsequent exposure to MeHg, both in the presence and absence of

Ca^{2+}_e (Hare and Atchison, 1995). Bradykinin did not elevate $[Ca^{2+}]_i$ in cells treated previously with MeHg, suggesting the first Ca^{2+} phase is mediated, at least in part, by mobilization of Ca^{2+} from an IP_3-sensitive intracellular store. Possible mechanisms for this effect include elevating cellular IP_3 content, or disruption of Ca^{2+} sequestration at the ER. MeHg did not increase cellular IP_3 levels during the time course of the first Ca^{2+} phase, thus the MeHg-induced disruption of ER Ca^{2+} regulation was not mediated by elevations in IP_3 content. However, similar concentrations of MeHg elevated IP_3 levels in cultured cerebellar granule cells following a 30 min exposure (Sarafian, 1993), possibly due to a secondary activation of Ca^{2+}-regulated PLC isoforms mediated by MeHg-induced elevations in $[Ca^{2+}]_i$ (Eberhard and Holz, 1988). Caffeine, which facilitates CICR, also decreased the magnitude of the first Ca^{2+} phase, suggesting a contribution of CICR to first Ca^{2+} phase. Pretreatment of cells with the L-type voltage-dependent Ca^{2+} channel blocker nifedipine alone or in combination with the N-type Ca^{2+} channel blocker ω-conotoxin GVIA did not affect the first Ca^{2+} phase (Hare and Atchison, 1995). Thus, the first Ca^{2+} phase was due to mobilization of IP_3-sensitive Ca^{2+} stores from the ER.

The second Ca^{2+} phase has also been studied using digital imaging microscopy of fura-2 loaded NG108-15 cells (Hare *et al.*, 1996). This phase was strictly dependent upon Ca^{2+}_e. The time to onset of the second Ca^{2+} phase was delayed by the L-type Ca^{2+} channel antagonist nifedipine (0.1-10 μM) in a concentration-dependent manner. At these concentrations nifedipine is unlikely to be specific for L-type Ca^{2+} channels, suggesting the second Ca^{2+} phase is mediated by a nifedipine-sensitive pathway other than L-type Ca^{2+} channels. Indeed, these channels have been reported to be blocked by MeHg (Shafer and Atchison, 1987). The nonspecific Ca^{2+} channel blocker Ni^{2+} did not delay the second

Ca^{2+} phase, providing further evidence that this phase is not mediated by Ca^{2+} influx through voltage-dependent Ca^{2+} channels. The second Ca^{2+} phase was also inhibited by TTX or reduction of extracellular Na^+ concentration, suggesting a role for voltage-dependent Na^+ channels. Both nifedipine and TTX also delayed the onset of the first Ca^{2+} phase and the non-Ca^{2+} phase. Because these phases are mediated by intracellular actions of MeHg, it has been proposed that nifedipine and TTX act by impeding MeHg uptake, thereby prolonging the time required to reach some critical toxic concentration within the cell.

MeHg inhibits the regulatory systems for other cations. MeHg blocks mitochondrial ATP synthesis and reduces cellular ATP content (Verity *et al.*, 1975; Kauppinen *et al.*, 1989). Both of these effects could ultimately elevate $[Ca^{2+}]_i$. Decreases in cellular ATP content could reduce the activity of the plasma membrane Ca^{2+}-ATPase, causing an elevation in $[Ca^{2+}]_i$. The Na^+/K^+-ATPase has a sensitivity to MeHg which is two-fold. First, the loss of cellular ATP reduces the activity of the Na^+/K^+-ATPase. Second, the activity of brain microsomal Na^+/K^+-ATPase is inhibited directly by MeHg, possibly due to modification of a sulfhydryl group within the protein (Rajanna *et al.*, 1990; Anner and Moosmayer, 1992). It is possible that a component of the elevations in $[Ca^{2+}]_i$ is mediated by effects of mercurials on these cation regulatory proteins.

The first study to suggest that MeHg altered Zn^{2+} homeostasis in the brain was conducted by Muto and coworkers (1991). Rats were administered a lethal dose of MeHg, and the metal content of tissue samples from brain, liver and kidney was analyzed by inductively coupled plasma atomic emission spectrometry. The primary effect of *in vivo* administration of MeHg was a disruption of brain Zn^{2+} and Ca^{2+} homeostasis.

Synaptosomal suspensions have been subjected to standard protein purification techniques to identify the protein(s) responsible for these elevations in $[Zn^{2+}]_i$. Synaptosomal homogenates were separated into particulate and soluble fractions by centrifugation. The particulate fraction was resuspended in an equal volume of buffer, and fura-2 pentapotassium salt was added to the both fractions. Fura-2 excitation scans were acquired before and after addition of MeHg, then compared for MeHg-induced alterations in the fura-2 excitation profile consistent with an elevation in free Zn^{2+} concentration (Hechtenberg and Beyersmann, 1993). MeHg altered the fura-2 spectrum of the soluble fraction in a manner consistent with Zn^{2+} release, but had no effect on the particulate fraction (Denny and Atchison, 1995). Thus, the source of the Zn^{2+} appears to be some soluble factor(s). Anion exchange chromatography of the soluble fraction resolved three distinct peaks of MeHg-induced Zn^{2+} release. Thus, more than one protein mediates the MeHg-induced elevations in $[Zn^{2+}]_i$.

Although it is not known what role the elevations in $[Zn^{2+}]_i$ play in MeHg-induced neurotoxicity, it is still possible to make some general speculations. Many proteins require Zn^{2+} for enzymatic activity or to stabilize their three-dimensional structure. Thus, the loss of essential Zn^{2+} could result in an inactivation of the enzyme or improper protein folding. The Zn^{2+}-binding region of these proteins may actually have a higher affinity for MeHg than Zn^{2+}. Since several metalloproteins generally utilize a common metal-binding motif which depends on both the metal and the function of the protein, such as the EF hand in Ca^{2+}-activated proteins or the Zn^{2+} fingers in DNA binding proteins, the loss of endogenous Zn^{2+} caused by MeHg may occur in an entire class of metalloproteins which contain a particular Zn^{2+}-binding motif. Another possible consequence in that the

elevation in $[Zn^{2+}]_i$ itself could be toxic. While it would appear that the elevations in $[Zn^{2+}]_i$ which occur in synaptosomes are quite modest, it nonetheless represents a three-fold elevation. Furthermore, because synaptosomes are a heterogenous population of nerve terminals, it is also possible that the elevations in $[Zn^{2+}]_i$ occur in only a subpopulation of synaptosomes. If this is the case, the actual $[Zn^{2+}]_i$ in this subpopulation would be considerably greater than the population average which would be reported by ^{19}F-NMR spectroscopy.

B. Relationship to previous work.

Previous research suggested that a component of the MeHg-induced elevations in $[Ca^{2+}]_i$ was due to disruption of mitochondrial Ca^{2+} regulation. Thus, the original goal of this work was to monitor changes in $[Ca^{2+}]_i$ following acute exposure of synaptosomes loaded with a fluorescent indicator to MeHg, and to evaluate the contributions of intra- and extracellular sources of Ca^{2+}. Substantial indirect evidence suggested that a component of the elevations in $[Ca^{2+}]_i$ would be due to disruption of mitochondrial Ca^{2+} regulation. However, exposure of synaptosomes to MeHg caused elevations in $[Ca^{2+}]_i$ which were strictly dependent upon Ca^{2+}_e. Depolarization of the mitochondrial membrane with NaN_3 and oligomycin was also ineffective at elevating $[Ca^{2+}]_i$ and did not alter the effects of MeHg. Moreover, the mitochondrial Ca^{2+} uniporter inhibitor ruthenium red did not block the effects of MeHg, suggesting that the effects of MeHg may be mediated by actions at other sites. While it is possible that the Ca^{2+} regulatory capacity of the mitochondria was compromised during synaptosomal preparation, it is unlikely, since similar findings were observed in NG108-15 cells in culture (Hare *et al.*, 1993).

Subsequent investigations in this cell type, as well as isolated cerebellar granule cells, have shown that a component of the elevations in $[Ca^{2+}]_i$ is mediated by release of Ca^{2+} previously sequestered in the ER. The ER pool is mobilized completely by IP_3, and to a limited extent by caffeine. Therefore, the mitochondria did not appear to contribute significantly to the MeHg-induced elevations in $[Ca^{2+}]_i$.

The results of this study are inconsistent with disruption of mitochondrial Ca^{2+} regulation contributing to the elevations in $[Ca^{2+}]_i$ following MeHg treatment. Also, the effects of MeHg on ER Ca^{2+} regulation and $[Zn^{2+}]_i$ must now be considered. As such, it is possible the MeHg-induced increases in MEPP frequency observed in Ca^{2+}-free solutions were actually mediated by release of Ca^{2+} from the ER, or possibly by elevations in $[Zn^{2+}]_i$., but perhaps not by disruption of mitochondrial Ca^{2+} regulation.

The inhibitors of mitochondrial function (dinitrophenol, dicoumarol and valinomycin) increased MEPP frequency after a twenty min delay. Pretreatment of hemidiaphragm preparations with these agents did not affect the subsequent elevations in MEPP frequency caused by MeHg. It is possible the 20 min delay preceding the elevations in MEPP frequency represented the time required for the mitochondrial inhibitors to reduce ATP levels in the nerve terminal. The reduction in cellular ATP content led to a secondary elevation in $[Ca^{2+}]_i$ and stimulation of spontaneous transmitter release, measured as an increase in MEPP frequency. Proper levels of ATP were then reinstated by increasing the rate of glycolysis, causing $[Ca^{2+}]_i$ and MEPP frequency to fall back to control levels. Subsequent addition of MeHg to these preparation caused elevations in $[Ca^{2+}]_i$ which could not be regulated, and MEPP frequency once again increased.

Support for this mechanism of action of the mitochondrial inhibitors comes from their similarity to the Na^+/K^+-ATPase inhibitor ouabain. Depletion of cellular ATP causes a reduction in the activity of the Na^+/K^+-ATPase; this is functionally equivalent to the action of ouabain. Loss of Na^+/K^+-ATPase activity causes a gradual depolarization of the nerve terminal which leads to activation of Ca^{2+} channels and an elevation in $[Ca^{2+}]_i$. Ouabain increased MEPP frequency following a 50 min delay, with a maximum frequency similar to that of the mitochondrial inhibitors. Like the mitochondrial inhibitors, the effects of MeHg were not prevented by ouabain, suggesting an additional site of action is not affected by ouabain.

The characteristics of the increases in MEPP frequency caused by ruthenium red were distinct, both qualitatively and quantitatively, from those of the mitochondrial inhibitors or ouabain. Unlike the mitochondrial inhibitors and ouabain, the increases in MEPP frequency elicited by ruthenium red were immediate. Also, the maximum MEPP frequency attained in ruthenium red-treated preparations was approximately one fifth that of those exposed to mitochondrial inhibitors or ouabain. However, neither MeHg nor dinitrophenol elevated MEPP frequency in preparations treated with ruthenium red. This effect could not attributed to depletion of vesicular contents from the nerve terminal since La^{3+} was capable of increasing MEPP frequency in ruthenium red-treated preparations.

The effects of disruption of ER Ca^{2+} regulation on MEPP frequency have been studied using hemidiaphragm preparations treated with caffeine. Caffeine elevates $[Ca^{2+}]_i$ by facilitating CICR. Caffeine caused changes in MEPP frequency which resembled those of ruthenium red. MEPP frequency increased immediately to a maximum similar

to that of ruthenium red, but half that of the mitochondrial inhibitors. Unlike ruthenium red, caffeine did not block the effects of MeHg.

The characteristics of the increases in MEPP frequency caused by caffeine and ruthenium red suggest they elevate $[Ca^{2+}]_i$ by similar mechanisms. These mechanisms are not identical, though, since caffeine-treated preparations are sensitive to MeHg, but ruthenium red-treated preparations are not. A possible explanation for the differential sensitivity of these preparations to MeHg may be related to the extent of depletion of ER Ca^{2+} stores caused by caffeine and ruthenium red. It is possible that caffeine does not deplete the ER of Ca^{2+}, but rather redistributes Ca^{2+} between the ER and cytosol; ruthenium red may completely mobilize the ER Ca^{2+} store. MeHg then mobilizes the remaining Ca^{2+} from the ER in caffeine-treated preparations, but has no effect following ruthenium red treatment. Depletion of ER Ca^{2+} stores with bradykinin and thapsigargin prior to MeHg or ruthenium red exposure may assist in determining the relative importance of the IP_3-sensitive Ca^{2+} pool as a source of Ca^{2+}.

It is difficult to rationalize the ability of ruthenium red to inhibit the effects of dinitrophenol based solely on actions at the ER. The dinitrophenol-induced elevations in $[Ca^{2+}]_i$ are presumably secondary to a reduction in cellular ATP levels. If ruthenium red blocks the actions of both MeHg and dinitrophenol by the same mechanism, it is unlikely to be due to effects exclusively at the ER. It is possible that ruthenium red acts as a permeability barrier to Ca^{2+} regulation at the ER and plasma membranes. Because the mechanisms which decrease $[Ca^{2+}]_i$ tend to exceed those which increase $[Ca^{2+}]_i$, this effect would cause $[Ca^{2+}]_i$ to rise slightly, leading to an increase in MEPP frequency. The elevations in $[Ca^{2+}]_i$ caused by MeHg or dinitrophenol may be blocked by ruthenium red.

Another explanation is that ruthenium red inhibits Ca^{2+}-mediated fusion of synaptic vesicles with the presynaptic membrane. If this is the case the vesicles would be rendered insensitive to changes in $[Ca^{2+}]_i$ and therefore, no increases in MEPP frequency would occur following MEPP treatment. This also would require La^{3+} to work through a mechanism independent of elevations in $[Ca^{2+}]_i$, possibly by causing vesicular fusion in a manner which is Ca^{2+}-independent.

The results concerning the effects of MeHg on $[Ca^{2+}]_i$ in synaptosomes are largely consistent with the work of others (Komulainen and Bondy, 1987b; and Kauppinen *et al.*, 1989). MeHg caused elevations in $[Ca^{2+}]_i$ which were time-dependent as well as concentration-dependent with respect to MeHg and Ca^{2+}_e (Komulainen and Bondy, 1987b). The accuracy of the values derived for $[Ca^{2+}]_i$ may be questionable, though since 20 µM Mn^{2+} was added to quench extrasynaptosomal fura-2 throughout the experiments. For subsequent calibration of R_{min} and R_{max}, only 10 µM DTPA was added to chelate this exogenous Mn^{2+}, thus at least 10 µM Mn^{2+} was not chelated. This may actually represent the best-case scenario since the buffer itself contained 1.2 mM Ca^{2+}; thus, some if not most, of the DTPA would be bound to Ca^{2+} rather than Mn^{2+}. In fact, in preliminary experiments using cell-free systems, I observed that 150 µM DTPA was necessary to reverse the quenching of 1 µM fura-2 caused by 40 µM Mn^{2+} in a buffer containing 200 µM Ca^{2+}. Furthermore, some of the changes in fura-2 fluorescence could have arisen from release of endogenous Zn^{2+}. Unlike the present study, depolarization of the mitochondria was shown to decrease the elevations in $[Ca^{2+}]_i$, suggesting a component of the elevations in $[Ca^{2+}]_i$ was from the mitochondrial Ca^{2+}. A possible explanation for the differences obtained is that rotenone was used in the previous work and NaN_3 was used

here. Rotenone acts at Site 1 in the electron transport chain while NaN_3 acts at Site 3. In mitochondria poisoned with rotenone, electron transport can still commence from Sites 2 and 3. Because NaN_3 acts at Site 3, like NaCN, the transfer of electrons to molecular oxygen in inhibited; thus respiration ceases completely. Perhaps these subtle differences in the mechanism of block of electron transport may account for the differences reported in these studies concerning the role of mitochondria in MeHg-induced elevations in $[Ca^{2+}]_i$.

C. Effects of MeHg on Ca^{2+} regulation.

The information gathered in these studies, as well as others, clearly indicates that MeHg causes an elevation in $[Ca^{2+}]_i$. In synaptosomes, the increases are mediated by influx of Ca^{2+}_e, while in NG108-15 cells the elevations are mediated by release of Ca^{2+} from IP_3-sensitive stores and influx of Ca^{2+}_e. This implies that MeHg disrupts plasma membrane integrity and interferes with Ca^{2+} regulation by the ER. Although the role of elevations in $[Ca^{2+}]_i$ in the neurotoxicity of MeHg is not known, based on the importance of Ca^{2+} as a second messenger it is reasonable to conclude that the disruption in Ca^{2+} homeostasis caused by MeHg has deleterious effects on cell function.

Many neurotoxic insults have been suggested to be mediated, at least in part, by elevations in $[Ca^{2+}]_i$ (Choi, 1988). The exact mechanism underlying toxicity is not known, but may be due to aberrant regulation of Ca^{2+}-sensitive proteins, and disruption of of Ca^{2+}-regulated signalling pathways. Many proteins either require Ca^{2+} for activity, or are regulated allosterically by the binding of Ca^{2+} or Ca^{2+}-activated regulatory proteins, such as calmodulin (Habermann and Richardt, 1986). Unregulated elevations in $[Ca^{2+}]_i$

have been associated with changes in phosphorylation of proteins and with the degradation of proteins, lipid membranes and nucleic acids (Nicotera *et al.*, 1992). It is believed that the increases in $[Ca^{2+}]_i$ activate various Ca^{2+}-regulated proteases, lipases and nucleases which lead to a cytotoxicity.

Many cells, including neurons, contain a family Ca^{2+}-activated neutral proteases called calpains (Melloni and Pontremoli, 1989). In their inactive form, calpains are normally found in the cytosol, but upon activation by Ca^{2+}, they associate with the plasma membrane and degrade cytoskeletal proteins. Calpain-mediated proteolysis can be inhibited by leupeptin, or by chelation of intra- or extracellular Ca^{2+} (Lee *et al.*, 1991). It is conceivable the unregulated elevations in $[Ca^{2+}]_i$ caused by MeHg could lead to an activation of calpain, and the destruction of cytoskeletal proteins, although this possibility has not been tested experimentally.

Cells also contain several Ca^{2+}-activated lipases. The two most prominent and widely studied classes of lipases are PLC and PLA_2. PLC hydrolyzes phosphotidylinositol into IP_3 and diacylglycerol, which together activate PKC by releasing an IP_3-sensitive Ca^{2+} store located in the ER, and by allosteric interactions with PKC, respectively. PLA_2 cleaves arachidonic acid from plasma membrane phospholipids for the biosynthesis of eicosinoids, and protects the cell against free radical-induced damage by removing peroxy-fatty acids from the plasma membrane. Because Ca^{2+} increases the activity of both of these lipases, unregulated elevations in $[Ca^{2+}]_i$ could cause extensive damage to the plasma membrane. The increase in PLC activity could also cause a secondary activation in PKC activity, further disrupting intracellular second messenger systems.

MeHg increases the activity of PLC and PLA_2 in neurons in culture (Sarafian, 1993; Verity *et al.*, 1994). A component of the MeHg-induced elevations in PLA_2 activity is dependent upon $[Ca^{2+}]_e$, suggesting that both intra- and extracellular sources of Ca^{2+} contribute to the increase in PLA_2 activity. It is unlikely the increased PLA_2 activity following MeHg treatment represented a physiological response to lipid peroxidation since α-tocopherol blocked lipid peroxidation (Sarafian and Verity, 1991), but did not prevent activation of PLA_2. The PLA_2 inhibitor mepacrine reduced free arachidonic acid generation by one-half, suggesting that either a mepacrine-insensitive PLA_2 existed, or MeHg also released arachidonic acid by some mechanism independent of PLA_2. The toxicological significance of the increases in PLA_2 activity is uncertain since mepacrine did not reduce MeHg-induced toxicity, as determined by uptake of trypan blue, and release of lactate dehydrogenase (Verity *et al.*, 1994).

Activation of a Mg^{2+}/Ca^{2+}-dependent endonuclease is the hallmark of induction of programmed cell death. This endonuclease is activated by pathologically high concentrations of Ca^{2+}, and is responsible for fragmentation of nuclear DNA (McCabe *et al.*, 1992). MeHg induces programmed cell death in cerebellar neurons in culture based on changes in nuclear morphology and the fragmentation of nuclear DNA (Kunimoto, 1994). Transfection of the neuronal cell line GT1-7 with the proto-oncogene *bcl-2* reduced the formation of reactive oxygen species in these cells and decreased the sensitivity of the cells to MeHg (Sarafian *et al.*, 1994). It was suggested that *bcl-2* attenuates MeHg toxicity by inhibiting formation of reactive oxygen species, thus preventing initiation of programmed cell death.

D. Effects of MeHg on Zn^{2+} regulation.

Acute exposure of synaptosomes (Denny *et al.*, 1993), NG108-15 cells (Hare *et al.*, 1993; Hare and Atchison, 1995), or cerebellar granule cells (Marty *et al.*, 1995) elevated the fluorescence intensity of fura-2 at the Ca^{2+}-insensitive wavelength of 360 nm. The increase was independent of Ca^{2+}_e, and occurred prior to loss of plasma membrane integrity. In synaptosomes, the elevation was immediate and complete within a few sec; in NG108-15 and cerebellar granule cells the increase occurred gradually following Ca^{2+} release from the ER pool ("first Ca^{2+} phase") and before the massive influx of Ca^{2+}_e ("second Ca^{2+} phase").

Because fura-2 has an affinity for cations other than Ca^{2+}, especially heavy metals (Grynkiewicz *et al.*, 1985), it was proposed that the elevations in fluorescence intensity were due to an increase in heavy metal concentration. It was unlikely that this effect was due to a direct interaction of MeHg with fura-2 since these compounds do not interact *in vitro*. Furthermore, the increase in fluorescence intensity at 360 nm could not be attributed to demethylation of MeHg because Hg^{2+} decreases, rather than increases, fura-2 fluorescence.

The cell-permeant heavy metal chelator TPEN reversed or inhibited these elevations, whereas the cell-impermeant chelator DTPA was ineffective. Thus, MeHg increased the intracellular concentration of a heavy metal whose source was likely to be endogenous. In synaptosomes, TPEN also prevented the immediate elevations in 340/380 nm ratio caused by MeHg, suggesting that this phase was due solely to an increase in the concentration of some other endogenous polyvalent cation. Due to the limitations of fluorometric analysis the cation could not be identified unequivocally, but was postulated

to be Zn^{2+} due to its characteristic effects on the fura-2 excitation spectrum (Grynkiewicz *et al.*, 1985; Hectenberg and Beyersmann, 1993).

To identify the endogenous heavy metal, changes in the ^{19}F-nuclear magnetic resonance spectrum of synaptosomes loaded with the fluorinated chelator 5F-BAPTA were evaluated following exposure to MeHg (Denny and Atchison, 1994). In the absence of Ca^{2+}_e, synaptosomes had a detectable $[Zn^{2+}]_i$. MeHg caused a concentration-dependent elevation in $[Zn^{2+}]_i$ which was reversed by TPEN, whereas $[Ca^{2+}]_i$ was not affected. While the MeHg-induced elevations in $[Zn^{2+}]_i$ were modest (1.37 nM prior to MeHg exposure versus 3.99 nM following addition of MeHg), they nonetheless represented a three-fold increase in $[Zn^{2+}]_i$. These results, along with previous results using fura-2, demonstrated that MeHg causes an immediate elevation in $[Zn^{2+}]_i$ in synaptosomes, and possibly NG108-15 cells. Higher concentrations of MeHg were required to observe the elevations in $[Zn^{2+}]_i$ in synaptosomes relative to those necessary in NG108-15 cells, possibly due to the higher protein content and associated nonspecific binding of MeHg in the synaptosomal suspensions. Alternatively, it is possible that the source of the MeHg-induced elevations in endogenous heavy metal content in NG108-15 cells is not identical to that which mediates the elevations in $[Zn^{2+}]_i$ in synaptosomes, and that this pool in NG108-15 cells is more sensitive to MeHg.

The observation that MeHg caused an elevation in $[Zn^{2+}]_i$ was a novel and unexpected finding of this research. Zn^{2+} is an essential heavy metal required by numerous proteins. The implications of this newly-discovered effect are that a component of the neurotoxicity of MeHg could be due to disruption of Zn^{2+} regulation. Zn^{2+} is associated with the synaptic vesicles of certain glutamatergic neurons in the CNS

(Frederickson *et al.*, 1987) and is released during neuronal activity (Assaf and Chung, 1984), suggesting that Zn^{2+} may be a modulator of postsynaptic glutamate receptors. In neuronal cells in culture, Zn^{2+} inhibited responses mediated by glutamate receptors sensitive to NMDA (Westbrook and Mayer, 1987), but increased responses mediated by AMPA-sensitive glutamate receptors (Xie *et al.*, 1993). Zn^{2+} also decreases responses mediated by γ-aminobutyric $acid_A$ receptors (Legendre and Westbrook, 1990), but potentiates ATP receptor-mediated responses (Li *et al.*, 1993). While Zn^{2+} may act as a neuromodulator, high concentrations are neurotoxic (Yokoyama *et al.*, 1986; Koh and Choi, 1994). Furthermore, Zn^{2+} toxicity may be potentiated by excessive AMPA receptor activation (Choi *et al.*, 1989; Weiss *et al.*, 1993).

Identification of the proteins responsible for the elevations in $[Zn^{2+}]_i$ was given priority over examination of the toxic effects of Zn^{2+} for several reasons, some of which related to the use of synaptosomes as a model system. Synaptosomes derived from brain represent a heterogenous population of nerve terminal with respect to vesicular contents. It is possible that the proteins responsible for the MeHg-induced elevations in $[Zn^{2+}]_i$ are present in only a subpopulation of nerve terminals. The methods used to detect and quantify the elevations in $[Zn^{2+}]_i$ are not capable of discriminating between identical increases in all synaptosomes, or greater increases in a subpopulation. In the latter case, the values of $[Zn^{2+}]_i$ obtained using ^{19}F-NMR spectroscopy of 5F-BAPTA loaded synaptosomes would underestimate the true $[Zn^{2+}]_i$ in this subpopulation.

There are several ways to address the issue of synaptosomal heterogeneity as it relate to the issue of MeHg-induced elevations in $[Zn^{2+}]_i$. One possible approach would be to test the effects of MeHg on synaptosomes derived from particular brain regions

which are enriched in nerve terminals containing a particular neurotransmitter. The advantage of this approach is that known targets of MeHg neurotoxicity could be tested directly, and correlations between target sites and elevations in $[Zn^{2+}]_i$ may be possible. There are many disadvantages to this procedure, though. Synaptosomes would have to be prepared from several brain regions to ensure adequate sampling of nerve terminals containing different neurotransmitters, as well as target sites of MeHg. Analysis of brain regions would only be useful if the terminals containing these MeHg-sensitive Zn^{2+}-binding proteins were localized in certain brain regions. Thus, if the proteins are expressed in a subpopulation of nerve terminals which is distributed evenly throughout the brain, these experiments would cause us to conclude incorrectly that a sensitive subpopulation of synaptosomes does not exist. Another problem is that even in brain regions which are enriched in nerve terminals containing a particular neurotransmitter, other nerve terminals are also present. If the proteins are expressed in the associated nerve terminal type rather than the enriched nerve terminals, we would conclude the elevations in $[Zn^{2+}]_i$ occur in the enriched population of nerve terminals when the changes are actually in the associated nerve terminals. Another contingency not addressed adequately by this method is that the elevations $[Zn^{2+}]_i$ do occur in a subpopulation of synaptosome, but expression of the target proteins is not related to neurotransmitter content or regional localization. At best, the results from analysis of synaptosomes prepared from different brain regions might provide some information regarding the localization of these proteins in the brain, and possibly some assistance identifying the protein. However, it would still be necessary to purify and identify the proteins to verify that MeHg is capable of releasing the associated Zn^{2+}.

A common approach to addressing the population dynamics of a suspension of particles is the use of fluorescence-activated cell sorting. In general, this technique uses differences in fluorescence intensity of a particular marker, or markers, to discriminate between subpopulations of particles on a individual basis. For instance, it is possible to determine what percentage of cells in a suspension contain a particular receptor by staining the cells with a fluorescently-tagged antibody to the receptor. When the cells pass through the sorter, the cells expressing the receptor fluoresce more intensely than those lacking the receptor. It would be possible to evaluate the population characteristics of the MeHg-induced elevations in $[Zn^{2+}]_i$ by loading synaptosomes with a Zn^{2+}-sensitive indicator, and monitoring changes in the fluorescence intensity histogram before and after MeHg exposure. If MeHg elevated $[Zn^{2+}]_i$ in the entire synaptosomal population, then the entire fluorescence intensity histogram would shift to slightly higher values. If, on the other hand, the elevations in $[Zn^{2+}]_i$ were restricted to a subpopulation of synaptosomes, the histogram would show a two distinct peaks, one at the initial value corresponding to cells not affected by MeHg, and another at much higher intensity than the initial value representing the sensitive subpopulation. Another feature of this technique is that the subpopulations can be separated based on these differences in fluorescence intensity.

A problem inherent with fluorescence-activated cell sorting is that because individual particles, or cells, are being analyzed they must be sufficiently labelled to allow for detection. In case of measuring changes in intracellular cation concentrations, the initial cell population also needs to be labelled uniformly. Otherwise, the peaks on the intensity histogram become so broad that it is not possible to evaluate changes in histogram characteristics. These problems limited the use of this technique in monitoring

the changes in $[Zn^{2+}]_i$ following MeHg exposure. Due to their small size, the synaptosomes were difficult to detect and could not loaded uniformly with the indicator. Because the system utilizes an argon laser as the source of excitation light, it was not possible to use fura-2. Synaptosomes had to be loaded with fluo-3 to monitor changes in $[Zn^{2+}]_i$. While fluo-3 exhibits large changes in fluorescence intensity upon Ca^{2+} binding, Zn^{2+} is only 70% as effective as Ca^{2+}. Thus, these experiments were hampered by the small size of the synaptosomes, and the lack of an ideal indicator. Nonetheless, synaptosomes could be loaded with the indicator and detected, but it was not realistic to draw conclusions about the population distribution of the elevations in $[Zn^{2+}]_i$ based on the fluo-3 fluorescence intensity histograms. Perhaps when a more suitable Zn^{2+} indicator becomes available, it may be possible to use this technique to analyze and sort the synaptosomes.

Purification of the proteins responsible for the elevation in $[Zn^{2+}]_i$ would assist in addressing the questions which arise due to the heterogeneous nature of synaptosomes. The purified proteins could possibly be identified based on sequence information. The distribution patterns of several proteins within the neuron are already known, making extrapolation of protein expression to the synaptosomal population relatively simple. In the event that a protein cannot be identified based on sequence information, or its cellular distribution is not known, it would still be possible to determine its localization within the synaptosomal population by immunocytochemistry. This would require generating antibodies to the protein and probing brain slices for immunoreactivity. If a particular brain region, or areas within the brain, are stained to a greater extent than others, it is likely the protein is found only in a particular subpopulation of synaptosomes.

Conversely, if the entire brain is stained to a similar extent, this suggests the particular protein is relatively evenly distributed, and the elevations in $[Zn^{2+}]_i$ likely to occur in the entire synaptosomal population. Another advantage of purification of the soluble proteins from the total synaptosomal homogenate is that all of the proteins which release Zn^{2+} can be isolated at once. This means that should multiple subpopulations exist, they can be evaluated using the immunocytochemical procedure outlined above.

Purification and identification of these Zn^{2+}-releasing proteins also provides valuable structural information. Because Zn^{2+} is bound to proteins using certain motifs, and MeHg releases Zn^{2+} from more than one protein, it is reasonable to conclude that a common Zn^{2+}-binding configuration is sensitive to MeHg. Thus, this may represent an effect of MeHg on an entire class of proteins. If the Zn^{2+}-binding motif of these proteins can be identified, it should be possible to evaluate the effects of MeHg on other proteins which possess this particular configuration.

The relevance of this effect of MeHg on Zn^{2+} regulation to MeHg-induced neurotoxicity is not clear. Because release of Zn^{2+} from soluble synaptosomal proteins mediates the elevations in $[Zn^{2+}]_i$, it is possible that the loss of Zn^{2+} from these proteins, or the increases in $[Zn^{2+}]_i$, is toxic. Thus far, no attempt has been made to correlate the elevations in $[Zn^{2+}]_i$ with the toxicity of MeHg either *in vitro* or *in vivo*. It is clear that the MeHg-induced elevations in $[Zn^{2+}]_i$ are not an artifact due to synaptosomal preparation. Similar elevations have been observed in NG108-15 cells and isolated cerebellar granule cells in culture, but the effects of MeHg on $[Zn^{2+}]_i$ in non-neuronal cells have not been evaluated.

Changes in $[Zn^{2+}]_i$ have been reported for a number of physiological and toxic agents in a variety of systems. Exposure of NG108-15 cells to Pb^{2+} increases the intracellular concentrations of Ca^{2+}, Pb^{2+} and Zn^{2+} as determined by ^{19}F-NMR spectroscopy (Schanne *et al.*, 1989). Prolonged exposure of cerebrocortical slices to excitatory amino acids has also been demonstrated to cause in elevation in $[Ca^{2+}]_i$ and $[Zn^{2+}]_i$ using this technique (Badar-Goffer *et al.*, 1994). Hypochlorous acid mobilizes intracellular Zn^{2+} in rat heart myocytes loaded with a Zn^{2+}-sensitive fluorescent indicator TSQ (Tatsumi and Fliss, 1994). External application of Zn^{2+} causes increases in $[Zn^{2+}]_i$ mediated by voltage-dependent Ca^{2+} channel in fura-2 loaded GH3 pituitary tumor cells and primary bovine chromaffin cells (Vega *et al.*, 1994; Atar *et al.*, 1995). Glucose causes a reduction in $[Zn^{2+}]_i$ in isolated pancreatic islet cells loaded with the fluorescent indicator zinquin (Zalewski *et al.*, 1994).

The toxic consequences of disruption of Zn^{2+} regulation as well as the toxicity of Zn^{2+} itself have been studied to some extent, although most information remains phenomenological rather than mechanistic at this time (Vallee and Falchuk, 1993). Maternal Zn^{2+} deficiency causes pronounced developmental deficits in the offspring. Characteristics of developmental toxicity mediated by Zn^{2+} deficiency include a disruption of brain and bone formation. While the mechanisms responsible for these malformations are not known, they are believed to be due to lack of essential Zn^{2+} required by the DNA-binding proteins which regulate development. A bacterial DNA-binding protein which regulates expression of mercurial resistance genes contains a putative Zn^{2+}-binding region also capable of binding Hg^{2+}. The binding of mercury is necessary for activation of

transcription of the mercury resistance genes. Thus, gene expression can be altered by changes in the Zn^{2+} status of a regulatory protein.

Zn^{2+} affects several voltage- and ligand-gated channels which are essential for neuronal function (Harrison and Gibbons, 1994). Like many other divalent cations, external application of Zn^{2+} blocks voltage-dependent Ca^{2+} channels, but Zn^{2+} can permeate the channel (Büsselberg *et al.*, 1994). Zn^{2+} reduces voltage-dependent Na^{+} channel conductance, possibly by an action at the voltage sensor. In hippocampal neurons, the response of voltage-dependent K^{+} channel A current to Zn^{2+} is dependent upon channel subtype and experimental parameters such as holding potential and voltage step. This has been interpreted as discrete actions of Zn^{2+} on both the activation and inactivation gates. Zn^{2+} also affects the biophysical properties of many ligand-gated channels. The first class of neurotransmitter receptors demonstrated to be regulated by Zn^{2+} were the opioid receptors. The distribution patterns of enkephalins and Zn^{2+} within the brain are identical in some species. In these brain regions the binding of a opioid receptor ligand was inhibited by 10-100 μM Zn^{2+}, a concentration that is likely to be encountered physiologically. Zn^{2+} also modulates the receptors for the amino acids GABA and glutamate. Zn^{2+} depresses Cl^{-} conductance mediated by GABA, and blocks glutamate channels which are sensitive to NMDA by a mechanism that is distinct from the voltage-dependent block caused by Mg^{2+}. Zn^{2+} enhances the conductances of AMPA-sensitive glutamate channels as well as ATP receptors. It bears noting that in all instances listed above, the putative Zn^{2+} binding site is located on the *extracellular* surface of the channel protein. Thus, these effects are most likely due to conformational changes in the protein structures rather than intracellularly-mediated events.

Because MeHg causes elevations in $[Zn^{2+}]_i$, it is likely the effects would be limited to disruption of *intracellular* processes. Exposure of mouse hemidiaphragm preparations to 50 or 100 μM Zn^{2+} increased MEPP frequency in a concentration-dependent manner (Nishimura, 1988). Bathing solutions containing 2 mM Ca^{2+} and 10 mM K^+ were less effective at increasing MEPP frequency in these Zn^{2+}-treated preparations. Thus, either Zn^{2+} inhibited the transmitter release process, possibly by blocking voltage-dependent Ca^{2+} channels, or it caused depletion of vesicular stores. Disruption of ER Ca^{2+} regulation attenuated the increases in MEPP frequency induced by Zn^{2+}. Dantrolene sodium, which blocks release of Ca^{2+} sequestered in the ER (Statham and Duncan, 1976), or neomycin, which inhibits IP_3 production (Schacht, 1976), both reduced the elevations in MEPP frequency caused by Zn^{2+}. This suggested that a component of the increases in MEPP frequency was mediated by mobilization of intracellular Ca^{2+} stores. However, the effect of neomycin may have been due to block of Zn^{2+} influx through voltage-dependent Ca^{2+} channels (Atchison *et al.*, 1988). More detailed analysis of the effects of Zn^{2+} on transmitter release suggested that Zn^{2+} enters the nerve terminal through voltage-dependent Ca^{2+} channels and acts as a partial agonist at Ca^{2+}-sensitive release apparatus (Wang and Quastel, 1990). Zn^{2+} blocked Ca^{2+}-stimulated transmitter release by inhibiting Ca^{2+} influx and causing irreversible alterations in the release mechanisms, rendering them insensitive to Ca^{2+}. The main difficulty in relating these studies of the effects of Zn^{2+} on spontaneous transmitter release to those observed following MeHg treatment is that the $[Zn^{2+}]_i$ necessary to elicit these changes is not known. Performing similar experiments except in the presence of Zn^{2+} and the Zn^{2+} ionophore pyrithione may assist in determining whether MeHg causes elevations in $[Zn^{2+}]_i$ sufficient to disrupt the transmitter release

process directly. Similarly, the contribution of elevated $[Zn^{2+}]_i$ to the MeHg-induced alterations in MEPP frequency could be evaluated using the cell-permeant chelator TPEN.

Zn^{2+} has been shown to regulate the activity of many enzymes, and alter intracellular signalling pathways. The regulatory domain of PKC contains four Zn^{2+}-binding sites which are necessary for binding of phorbol esters as revealed by mutational analysis (Hubbard *et al.*, 1991). This suggests that the conserved Zn^{2+}-binding sites in PKC are responsible for the binding of diacylglycerol, the physiological activator of PKC. The key Ca^{2+}-binding regulatory protein calmodulin also binds Zn^{2+}, which is a partial agonist of calmodulin activity as measured by increases in calmodulin-dependent phosphodiesterase activity (Chao *et al.*, 1984). Zn^{2+} is a potent inhibitor of Ca^{2+}-dependent PLA_2 isolated from snake venoms (Mezna *et al.*, 1994). It is believe that Zn^{2+} occupies at least one Ca^{2+}-binding site which is necessary for the activity of this enzyme. Zn^{2+} inhibits the endonuclease responsible for the nuclear dissolution observed during apoptosis in bovine liver (Lohmann and Beyersmann, 1994), and inhibits apoptosis induced by treatment of human lymphoma cells in culture with drugs which disrupt microtubules (Takano *et al.*, 1993). However, initiation of apoptosis of peripheral blood lymphocytes caused by mitogen deprivation has been reported to be dependent upon Zn^{2+}, but not Ca^{2+} (Treves *et al.*, 1994).

The proteins responsible for the elevations in $[Zn^{2+}]_i$ are not yet known, but a few candidates have been identified based on zinc-binding characteristics and molecular weight. Microtubules are composed of dimers of the 50 kDa acidic proteins α- and β-tubulin (Lemischka *et al.*, 1981; Ginzburg *et al.*, 1985). The presence of Zn^{2+} influences the polymer characteristics and crystal structure of tubulin (Wolf *et al.*, 1993). Neuron-

specific proteins possessing a similar molecular weight include an 53.5 kDa intermediate filament called peripherin (Thompson and Ziff, 1989), the 45 kDa microtubule-associated protein tau (Kosik *et al.*, 1989), and the 53.1 kDa granule cell specific Ca^{2+}/calmodulin-dependent protein kinase IV (Ono and Means, 1989). The Zn^{2+}-binding properties of these proteins have not been reported.

The stromelysins are a family of metalloendoproteases which cleave collagen in the extracellular matrix upon activation, and are synthesized as inactive zymogens of approximately 54.2 kDa (Matrisian *et al.*, 1986; Breathnach *et al.*, 1987). These proteins contain an autoinhibitory region in which a cysteine residue sterically hinders the active site by interacting with a Zn^{2+} atom essential for catalysis (Kleiner and Stetler-Stevenson, 1993). Activation occurs when this steric hinderance is removed and the binding site is revealed. Normally the autoinhibitory region is cleaved from the protein, however organomercurials can also activate the stromelysins by interacting with the cysteine in the autoinhibitory region, causing it to move out of the active site. Because the Zn^{2+} in the binding site is essential for protease activity, the possible displacement of Zn^{2+} by MeHg would be expected to inactivate the enzyme.

The possible ramifications of the elevation in $[Zn^{2+}]_i$ are difficult to deduce, because in many cases Zn^{2+} acts as a regulator of Ca^{2+}-sensitive processes. Because elevations in $[Ca^{2+}]_i$ occur along with the elevations in $[Zn^{2+}]_i$, it will be difficult to establish clearly what role each cation plays in MeHg-induced neurotoxicity. While it is clear that MeHg disrupts divalent cation homeostasis, the toxicological significance of this effect is less certain. Very few studies have been designed specifically to evaluate the role of elevations in $[Ca^{2+}]_i$ in MeHg-induced toxicity. As a rule, MeHg causes a myriad

of effects on the cellular and biochemical level including depolarization of the plasma and mitochondrial membranes (Hare and Atchison, 1992), depletion of cellular ATP (Kauppinen *et al.*, 1989), block of protein (Cheung and Verity, 1981) and DNA synthesis (Gruenwedel and Cruikshank, 1979), changes in lipid metabolism (Sarafian, 1993; Verity *et al.*, 1994), alterations in protein phosphorylation (Sarafian and Verity, 1990a; 1990b) and disruptions in microtubule structure (Imura *et al.*, 1980). Due to the importance of Ca^{2+} as an intracellular second messenger, it is conceivable that some of these effects could be mediated, at least in part, by unregulated elevations in $[Ca^{2+}]_i$. In summary, disruption of divalent cation homeostasis should be considered an a intermediate step in MeHg-induced toxicity rather than as a toxic consequence in and of itself. To this end, additional studies are needed to assess the impact this loss of divalent cation regulation has on neuronal structure and function on the both biochemical and cellular level. This may ultimately broaden our knowledge of both the mechanisms of MeHg-induced neurotoxicity, as well as the physiological regulators of neuronal development and function.

BIBLIOGRAPHY

BIBLIOGRAPHY

Åkerman, K.E.O. and Nicholls, D.G. (1983) Physiological and bioenergetic aspects of mitochondrial calcium transport. *Rev. Physiol. Biochem. Pharmacol.* **95**, 149-201.

Alnaes, E. and Rahamimoff, R. (1975) On the role of mitochondria in transmitter release from motor nerve terminals. *J. Physiol. (Lond.)* **248**, 255-278.

Anderson, D.C., King S.C., and Parsons, S.M. (1983) Pharmacological characterization of the acetylcholine transport system in purified *Torpedo* electric organ synaptic vesicles. *Mol. Pharmacol.* **24**, 48-54.

Anner, B.M. and Moosmayer, M. (1992) Mercury inhibits Na-K-ATPase primarily at the cytoplasmic side. *Am. J. Physiol.* **262**, F843-F848.

Arakawa, O., Nakahiro, M., and Narahashi, T. (1991) Mercury modulation of GABA-activated chloride channels and non-specific cation channels in rat dorsal root ganglion neurons. *Brain Res.* **551**, 58-63.

Arslan, P., Di Virgilio, F., Beltrame, M., Tsien, R.Y., and Pozzan, T. (1985) Cytosolic Ca^{2+} homeostasis in Ehrlich and Yoshida carcinomas. *J. Biol. Chem.* **260**, 2719-2727.

Assaf, S.Y. and Chung, S.H. (1984) Release of endogenous Zn^{2+} from brain tissue during activity. *Nature (Lond.)* **308**, 734-736.

Atar, D., Backx, P.H., Appel, M.M., Gao, W.D., and Marban, E. (1995) Excitation-transcription coupling mediated by zinc influx through voltage-dependent calcium channels. *J. Biol. Chem.* **270**, 2473-2477.

Atchison, W.D. (1986) Extracellular calcium-dependent and -independent effects of methylmercury on spontaneous and potassium-evoked release of acetylcholine at the neuromuscular junction. *J. Pharmacol. Exp. Ther.* **237**, 672-680.

Atchison, W.D. (1987) Effects of activation of sodium and calcium entry on spontaneous release of acetylcholine induced by methylmercury. *J. Pharmacol. Exp. Ther.* **241**, 131-139.

Atchison, W.D., Joshi, U., and Thornburg, J.E. (1986) Irreversible suppression of calcium entry in nerve terminals by methylmercury. *J. Pharmacol. Exp. Ther.* **238**, 618-648.

Atchison, W.D., Adgate, L., and Beaman, C.M. (1988) Effects of antibiotics on uptake of calcium into isolated nerve terminals. *J. Pharmacol. Exp. Ther.* **245**, 394-401.

Atchison, W.D. and Hare, M.F. (1994) Mechanisms of methylmercury-induced neurotoxicity. *FASEB J.* **8**, 622-629.

Atchison, W.D. and Narahashi, T. (1982) Methylmercury-induced depression of neuromuscular transmission in the rat. *NeuroToxicology* **3**, 37-50.

Atchison, W.D. and Spitsbergen, J.M. (1994) The neuromuscular junction as a target for toxicity. In: *Principles of Neurotoxicology*, Chang LW, ed, New York, Marcel Dekker, Inc., 265-307.

Bachelard, H. and Badar-Goffer, R. (1993) NMR spectroscopy in neurochemistry. *J. Neurochem.* **61**, 412-429.

Badar-Goffer, R.S., Ben-Yoseph, O., Dolin, S.J., Morris, P.G., Smith, G.A., and Bachelard, H.S. (1990) Use of 1,2-bis(2-amino-5-fluorophenoxy)ethane-*N,N,N',N'*-tetraacetic acid (5FBAPTA) in the measurement of free intracellular calcium in brain by ^{19}F-nuclear magnetic resonance spectroscopy. *J. Neurochem.* **55**, 878-884.

Badar-Goffer, R.S., Morris, P., Thatcher, N., and Bachelard, H. (1994) Excitotoxic amino acids cause appearance of magnetic resonance spectroscopy-observable zinc in superfused cortical slices. *J. Neurochem.* **62**, 2488-2491.

Baimbridge, K.G., Celio, M.R., and Rogers, J.H. (1992) Calcium-binding proteins in the nervous system. *Trends Neurosci.* **15**, 303-308.

Bakir, F., Damluji, S.F., Amin-Zaki, L., Murtadha, M., Khalidi, A., Al-Rawi, N.Y., Tikriti, S., Dhahir, H.I., Clarkson, T.W., Smith, J.C., and Doherty, R.A. (1973) Methylmercury poisoning in Iraq. *Science* **181**, 230-241.

Bartfai, T. (1979) Preparation of metal-chelate complexes and the design of steady-state kinetic experiments involving metal nucleotide complexes. *Adv. Cyc. Nucl. Res.* **10**, 219-242.

Bertolino, M. and Llinàs, R. (1992) The central role of voltage-dependent and receptor-operated calcium channels in neuronal cells. *Ann. Rev. Pharmacol. Toxicol.* **32**, 399-421.

Blaustein, M.P. (1988) Calcium transport and buffering in neurons. *Trends Neurosci.* **10**, 438-443.

Blaustein, M.P., Ratzlaff, R.W., and Schweitzer, E.S. (1978) Calcium buffering in presynaptic nerve terminals: II. Kinetic properties of the nonmitochondrial Ca sequestration mechanism. *J. Gen. Physiol.* **72**, 43-66.

Blaustein, M.P., Ratzlaff, R.W., and Schweitzer, E.S. (1980) Control of intracellular calcium in presynaptic nerve terminals. *Fed. Proc.* **39**, 2790-2795.

Binah, O., Meiri, U., and Rahamimoff, H. (1978) The effects of $HgCl_2$ and mersalyl on the mechanisms regulating intracellular calcium and transmitter release. *Eur. J. Pharmacol.* **51**, 453-457.

Breathnach, R., Matrisian, L.M., Gesnel, M.-C., Staub, A., and Leroy, P. (1987) Sequences coding for part of oncogene-induced transin are highly conserved in a related rat gene. *Nucleic Acids Res.* **15**, 1139-1151.

Büsselberg, D., Evans, M.L., Rahmann, H., and Carpenter, D.O. (1991) Effects of inorganic and triethyl lead and inorganic mercury on the voltage activated calcium channel of *Aplysia* neurons. *NeuroToxicology* **12**, 733-744.

Büsselberg, D., Platt, B., Michael, D., Carpenter, D.O., and Haas, H.L. (1994) Mammalian voltage-dependent calcium channel currents are blocked by Pb^{2+}, Zn^{2+}, and Al^{3+}. *J. Neurophysiol.* **71**, 1491-1497.

Chang, L.W. (1977) Neurotoxic effects of mercury- A review. *Environ. Res.* **14**, 329-373.

Chang, L.W. (1980) Mercury. In *Experimental and Clinical Neurotoxicology* (Spencer P.S. and Schaumburg H.H., eds.), The Williams and Wilkins Co.

Chao, S.-H., Suzuki, Y., Zysk, J.R., and Cheung, W.Y. (1984) Activation of calmodulin by various metal cations as a function of ionic radius. *Molec. Pharmacol.* **26**, 75-82.

Cheung, M. and Verity, M.A. (1981) Methyl mercury inhibition of synaptosome protein synthesis: role of mitochondrial dysfunction. *Environ. Res.* **24**, 286-298.

Choi, D.W. (1987) Ionic dependence of glutamate neurotoxicity in cortical cell culture. *J. Neurosci.* **7**, 369-379.

Choi, D.W. (1988) Calcium-mediated neurotoxicity: relationship to specific channel types and role in ischemic damage. *Trends Neurosci.* **11**, 465-469.

Choi, D.W., Weiss, J.H., Koh, J., Christine, C.W., and Kurth, M.C. (1989) Glutamate neurotoxicity, calcium and zinc. *Ann. New York Acad. Sci.* **568**, 219-224.

Clarkson, T.W. (1986) Effects and general principles underlying the toxic action of metals. In *Handbook of Toxicity of Metals, Second edition* (Friberg L., Nordburg G.F., and Vouk V., eds.), Elsevier Science Publ.

Clementi, E., Scheer, H, Zacchetti, D., Fasolato, C., Pozzan, T., and Meldolesi, J. (1992) Receptor-activated Ca^{2+} influx. *J. Biol. Chem.* **267**, 2164-2172.

Coleman, J.E. (1992) Zinc proteins: enzymes, storage proteins, transcription factors, and replication proteins. *Annu. Rev. Biochem.* **61**, 897-946.

Cooper, G.P., Suszkiw, J.B., and Manalis, R.S. (1984) Presynaptic effects of heavy metals. In: *Cellular and Molecular Neurotoxicology*, Narahashi T, ed, New York, Raven Press, pp 1-21.

Corcoran, G.B., Fix, L., Jones, D.P., Moslen, M.T., Nicotera, P., Oberhammer, F.A., and Buttyan, R. (1994) Apoptosis: molecular control point in toxicity. *Toxicol. Appl. Pharmacol.* **128**, 169-181.

Deana, R., Panato, L., Cancellotti, F.M., Quadro, G., and Calzigna, L. (1984) Properties of a new calcium ion antagonist on cellular uptake and mitochondrial efflux of calcium ions. *Biochem. J.* **218**, 899-905.

Denny, M.F. and Atchison, W.D. (1994) Methylmercury-induced elevations in intrasynaptosomal zinc concentrations: an ^{19}F-NMR study. *J. Neurochem.* **63**, 383-386.

Denny, M.F. and Atchison, W.D. (1995) Methylmercury causes release of zinc from soluble synaptosomal proteins. *The Toxicologist* (abstr) **15**, 14.

Denny, M.F., Hare, M.F., and Atchison, W.D. (1993) Methylmercury alters intrasynaptosomal concentrations of endogenous polyvalent cations. *Toxicol. Appl. Pharmacol.* **122**, 222-232.

DiVirgilio, F., Fasolato, C., and Steinberg, T.H. (1988) Inhibitors of membrane transport system for organic anions block fura-2 excretion from PC12 and N2A cells. *Biochem. J.* **256**, 959-963.

Drapeau, P. and Nachshen, D.A. (1984) Manganese fluxes and manganese-dependent neurotransmitter release in presynaptic nerve endings isolated from rat brain. *J. Physiol. (Lond.)* **348**, 493-510.

Dowd, T.L. and Gupta, R.K. (1991) ^{19}F study of the effect of lead on intracellular free calcium in human platelets. *Biochim. Biophys. Acta* **1092**, 341-346.

Dowd, T.L. and Gupta, R.K. (1993) NMR studies of the effect of hyperglycemia on intracellular cations in rat kidney. *J. Biol. Chem.* **268**, 991-996.

Eberhard, D.A. and Holz, R.W. (1988) Intracellular Ca^{2+} activates phospholipase C. *Trends Neurosci.* **11**, 517-520.

Frederickson, C.J., Kasarskis, E.J., Ringo, D., and Frederickson, R.E. (1987) A quinoline fluorescence method for visualizing and assaying the histochemically reactive zinc (bouton zinc) in the brain. *J. Neurosci. Meth.* **20**, 91-103.

Frederickson, C.J., Hernandez, M.D., Goik, S.A., Morton, J.D., and McGinty, J.F. (1988) Loss of zinc staining from hippocampal mossy fibers during kainic acid-induced seizures: a histofluorescence study. *Brain Res.* **446**, 383-386.

Ginzburg, I., Teichman, A., Dodemont, H.J., Behar, L., and Littauer, U.Z. (1985) Regulation of three beta-tubulin mRNAs during rat brain development. *EMBO J.* **4**, 3667-3673.

Goddard, G.A. and Robinson, J.D. (1976) Uptake and release of calcium by rat brain synaptosomes. *Brain Res.* **110**, 331-350.

Goldman, W.F. and Blaustein, M.P. (1990) Non-homogeneous Mn^{2+} quench of fura-2 signals in cultured arterial myocytes visualized with digital imaging. *Biophys. J.* **57**, 162a.

Gray, E.G. and Whittaker, V.P. (1962) The isolation of nerve endings from brain: An electron-microscopic study of cell fragments derived by homogenization and centrifugation. *J. Anat.* **96**, 79-87.

Greene, L.A. and Tischler, A.S. (1976) Establishment of a noradrenergic clonal line of rat adrenal pheochromocytoma cells which respond to nerve growth factor. *Proc. Natl. Acad. Sci. (USA)* **73**, 2424-2428.

Gruenwedel, D.W. and Cruikshank, M.K. (1979) Effect of methylmercury(II) on the synthesis of deoxyribonucleic acid, ribonucleic acid and protein in HeLa S3 cells. *Biochem. Pharmacol.* **28**, 651-655.

Grynkiewicz, G., Poenie, M., and Tsien, R.Y. (1985) A new generation of Ca^{2+} indicators with greatly improved fluorescence properties. *J. Biol. Chem.* **260**, 3440-3450.

Habermann, E. and Richardt, G. (1986) Intracellular calcium binding proteins as targets for heavy metal ions. *Trends Pharmacol. Sci.* **7**, 298-300.

Hamer, D.H. (1986) Metallothionein. *Ann. Rev. Biochem.* **55**, 913-951.

Hare, M.F. and Atchison, W.D. (1992) Comparative action of methylmercury and divalent inorganic mercury on nerve terminal and intraterminal mitochondrial membrane potentials. *J. Pharmacol. Exp. Ther.* **261**, 166-172.

Hare, M.F. and Atchison, W.D. (1995) Methylmercury mobilizes Ca^{++} from intracellular stores sensitive to inositol 1,4,5-trisphosphate in NG108-15 cells. *J. Pharmacol. Exp. Ther.* **272**, 1016-1023.

Hare, M.F., McGinnis, K.M., and Atchison, W.D. (1993) Methylmercury increases intracellular concentrations of Ca^{++} and heavy metals in NG108-15 cells. *J. Pharmacol. Exp. Ther.* **266**, 1626-1635.

Hare, M.F. and Atchison, W.D. (1995) Nifedipine and tetrodotoxin (TTX) delay the onset of the methylmercury (MeHg)-induced Ca^{2+}_e-dependent increase in $[Ca^{2+}]_i$ in NG108-15 cells. *Toxicol. Appl. Pharmacol.* in press.

Harrison, N.L. and Gibbons, S.J. (1994) Zn^{2+}: an endogenous modulator of ligand- and voltage-gated ion channels. *Neuropharmacology* **33**, 935-952.

Haug, F.M.S., Blackstad, T.W., Simonsen, A.H., and Zimmer, J. (1971) Timm's sulphide silver reaction for zinc during experimental anterograde degeneration of hippocampal mossy fibers. *J. Comp. Neurol.* **142**, 23-32.

Hechtenberg, S. and Beyersmann, D. (1993) Differential control of free calcium and free zinc levels in isolated bovine liver nuclei. *Biochem. J.* **289**, 757-760.

Heinonen, E., Åkerman, K.E.O., and Kaila, K. (1984) Depolarization of the mitochondrial membrane potential increases free cytosolic calcium in synaptosomes. *Neurosci. Lett.* **49**, 33-37.

Henzi, V. and MacDermott, A.B. (1992) Characteristics and function of Ca^{2+}- and inositol 1,4,5-trisphosphate-releasable stores of Ca^{2+} in neurons. *Neuroscience* **46**, 251-273.

Hewett, S.J. and Atchison, W.D. (1992) Effects of charge and lipophilicity on mercurial-induced reduction of $^{45}Ca^{2+}$ uptake in isolated nerve terminals of the rat. *Toxicol. Appl. Pharmacol.* **113**, 267-273.

Hinkle, P.M., Shanshala, E.D., and Nelson, E.J. (1992) Measurement of intracellular cadmium with fluorescent dyes. Further evidence for the role of calcium channels in cadmium uptake. *J. Biol. Chem.* **267**, 25553-25559.

Hokin, L.E. (1985) Receptors and phosphoinositide-generated second messengers. *Annu. Rev. Biochem.* **54**, 205-235.

Holliday, J., Adams, R.H., Sejnowski, T.J., and Spitzer, N.C. (1991) Calcium-induced release of calcium regulates differentiation of cultured spinal neurons. *Neuron* **7**, 787-796.

Howell, G.A., Welch, M.G., and Frederickson, C.J. (1984) Stimulation-induced uptake and release of zinc in hippocampal slices. *Nature (Lond.)* **8**, 736-738.

Hubbard, S.R., Bishop, W.R., Kirschmeier, P., George, S.J., Cramer, S.P., and Hendrickson, W.A. (1991) Identification and characterization of zinc binding sites in protein kinase C. *Science* **254**, 1776-1779.

Hunt, J.B., Neece, S.H., Schachman, H.K., and Ginsburg, A. (1984) Mercurial-promoted Zn^{2+} release from *Escherichia coli* aspartate transcarbamoylase. *J. Biol. Chem.* **259**, 14793-14803.

Hunter, D. and Russell, D.S. (1954) Focal cerebral and cerebellar atrophy in a human subject due to organic mercury compounds. *Neurol. Neurosurg. Psychiat.* **17**, 235-241.

Imura, N., Miura, K., Inokawa, M., and Nakada, S. (1980) Mechanism of methylmercury cytotoxicity: by biochemical and morphological experiments using cultured cells. *Toxicology* **17**, 241-254.

Itoh, M., Ebadi, M., and Swanson, S. (1983) The presence of zinc-binding proteins in brain. *J. Neurochem.* **41**, 823-829.

Johnson, M.E., Gores, G.J., Uhl, C.B., and Sill, J.C. (1994) Cytosolic free calcium and cell death during metabolic inhibition in a neuronal cell line. *J. Neurosci.* **14**, 4040-4049.

Juang, M.S. (1976a) Depression of frog muscle contraction by methylmercuric chloride and mercuric chloride. *Toxicol. Appl. Pharmacol.* **35**, 183-185.

Juang, M.S. (1976b) An electrophysiological study of the action of methylmercuric chloride and mercuric chloride on the sciatic nerve-sartorius muscle preparation of the frog. *Toxicol. Appl. Pharmacol.* **37**, 339-348.

Juang, M.S. and Yonemura, K. (1975) Increased spontaneous transmitter release from presynaptic nerve terminal by methylmercuric chloride. *Nature (Lond.)* **256**, 211-213.

Kass, G.E., Wright, J.M., Nicotera, P., and Orrenius S. (1988) The mechanism of 1-methyl-4-phenyl-1, 2, 3, 6-tetrahydropyridine toxicity: Role of intracellular calcium. *Arch. Biochem. Biophys* **260**, 789-797.

Kass, G.E.N., Llopis, J., Chow, S.C., Duddy, S.K., and Orrenius, S. (1990) Receptor-operated calcium influx in rat hepatocytes. *J. Biol. Chem.* **265**, 17486-17492.

Kauppinen, R.A., Komulainen, H., and Taipale, H. (1989) Cellular mechanisms underlying the increase in cytosolic free calcium concentration induced by methylmercury in cerebrocortical synaptosomes from guinea pig. *Toxicol. Appl. Pharmacol.* **248**, 1248-1254.

Kinter, W.B. and Pritchard, J.B. (1977) Altered permeability of cell membranes. In: *Handbook of Physiology*, Lee DKA, Falk HL, Murphy SD, eds, Washington, D.C., American Physiological Society, pp 563-576.

Kleiner, D.E., Jr. and Stetler-Stevenson, W.G. (1993) Structural biochemistry and activation of matrix metalloproteases. *Curr. Opin. Cell Biol.* **5**, 891-897.

Komulainen, H. and Bondy, S.C. (1987a) The estimation of free calcium within synaptosomes and mitochondria with fura-2; comparison to quin-2. *Neurochem. Int.* **10**, 55-64.

Komulainen, H. and Bondy, S.C. (1987b) Increased free intrasynaptosomal Ca^{2+} by neurotoxic organometals: distinctive mechanisms. *Toxicol. Appl. Pharmacol.* **88**, 77-86.

Koh, J. and Choi, D.W. (1994) Zinc toxicity on cultured cortical neurons: involvement of *N*-methyl-D-aspartate receptors. *Neuroscience* **60**, 1049-1057.

Kunimoto, M. (1994) Methylmercury induces apoptosis of rat cerebellar neurons in primary culture. *Biochem. Biophys. Res. Comm.* **204**, 310-317.

Laemmli, U.K. (1970) Cleavage of structural proteins during the assembly of the head of bacteriophage T4. *Nature (Lond.)* **227**, 680-685.

Lee, K.S., Frank, S., Vanderklish, P., Arai, A., and Lynch, G. (1991) Inhibition of proteolysis protects hippocampal neurons from ischemia. *Proc. Natl. Acad. Sci. USA* **88**, 7233-7237.

Legendre, P. and Westbrook, G.L. (1990) The inhibition of single *N*-methyl-D-aspartate-activated channels by zinc ion on cultured rat neurones. *J. Physiol. (Lond.)* **429**, 429-449.

Lehninger, A.L., Reynafarje, B., Vereesi, A., and Tew, W.P. (1978) Transport and accumulation of calcium in mitochondria. *Ann. N.Y. Acad. Sci.* **307**, 160-176.

Lemischka, I.R., Farmer, S., Racaniello, V.R., and Sharp, P.A. (1981) Nucleotide sequence and evolution of mammalian alpha-tubulin messenger RNA. *J. Mol. Biol.* **151**, 101-120.

Levesque, P.C. and Atchison, W.D. (1987) Interactions of mitochondrial inhibitors with methylmercury on spontaneous quantal release of acetylcholine. *Toxicol. Appl. Pharmacol.* **87**, 315-324.

Levesque, P.C. and Atchison, W.D. (1988) Effect of alteration of nerve terminal Ca^{2+} regulation on increased spontaneous quantal release of acetylcholine by methylmercury. *Toxicol. Appl. Pharmacol.* **94**, 55-65.

Levesque, P.C. and Atchison, W.D. (1991) Disruption of brain mitochondrial calcium sequestration by methylmercury. *J. Pharmacol. Exp. Ther.* **256**, 236-242.

Levesque, P.C., Hare, M.F., and Atchison, W.D. (1992) Inhibition of mitochondrial Ca^{2+} release diminishes the effectiveness of methyl mercury to release acetylcholine from synaptosomes. *Toxicol. Appl. Pharmacol.* **115**, 11-20.

Levy, L.A., Murphy, E., and London, R.E. (1987) Synthesis and characterization of ^{19}F NMR chelators for measurement of cytosolic free Ca. *Am. J. Physiol.* **252**, C441-C449.

Li, C., Peoples, R.W., Li, Z., and Weight, F.F. (1993) Zn^{2+} potentiates excitatory action of ATP on mammalian neurons. *Proc. Natl. Acad. Sci. USA* **90**, 8264-8267.

Llinás, R.R., Sugimori, M., and Silver, R.B. (1992) Microdomains of high calcium concentration in a presynaptic terminal. *Science* **256**, 677-679.

Lo., T-M. and Thayer, S.A. (1993) Refilling the inositol 1,4,5-trisphosphate-sensitive Ca^{2+} store in neuroblastoma × glioma hybrid NG108-15 cells. *Am. J. Physiol.* **264**, C641-C653.

Lohmann, R.D. and Beyersmann, D. (1994) Effects of zinc and cadmium on apoptotic DNA fragmentation in isolated bovine liver nuclei. *Environ. Health Persp.* **102**, 269-271.

Lowry, O.H., Rosenbrough, N.J., Farr, A.L., and Randall, R.J. (1951) Protein measurements with the folin phenol reagent. *J. Biol. Chem.* **193**, 265-275.

MacDermott, A.B., Mayer, M.L., Westbrook, G.L., Smith, S.J., and Barker, J.L. (1986) NMDA-receptor activation increases cytoplasmic calcium concentration in cultured spinal cord neurones. *Nature (Lond.)* **321**, 519-522.

Malinow, R., Otmakhov, N., Blum, K.I., and Lisman, J. (1994) Visualization of hippocampal synaptic function by optical detection of Ca^{2+} entry through the N-methyl-D-aspartate channel. *Proc. Natl. Acad. Sci. USA* **91**, 8170-8174.

Marty, M.S., Hare, M.F., and Atchison, W.D. (1995) Methylmercury alters intracellular calcium concentration ($[Ca^{2+}]_i$) in rat cerebellar granule cell cultures. *The Toxicologist* (abstr) **15**, 259.

Mason, M.J. and Grinstein, S. (1990) Effect of cytoplasmic acidification on the membrane potential of T-lymphocytes: role of trace metals. *J. Memb. Biol.* **116**, 139-148.

Matrisian, L.M., Leroy, P., Ruhlmann, C., Gesnel, M.-C., and Breathnach, R. (1986) Isolation of the oncogene and epidermal growth factor-induced transin gene: complex control in rat fibroblasts. *Mol. Cell. Biol.* **6**, 1679-1686.

McCabe, M.J., Nicotera, P., and Orrenius, S. (1992) Calcium-dependent cell death. Role of the endonuclease, protein kinase C, and chromatin conformation. *Ann. N.Y. Acad. Sci.* **663**, 269-278.

McGraw, C.F., Somlyo, A.V., and Blaustein, M.P. (1980) Probing for calcium at presynaptic nerve terminals. *Fed. Proc.* **39**, 2796-2801.

McMahon, H.T. and Nicholls, D.G. (1993) Barium-evoked glutamate release from guinea-pig cerebrocortical synaptosomes. *J. Neurochem.* **61**, 110-115.

McPherson, P.S. and Campbell, K.P. (1993) The ryanodine receptor/Ca^{2+} release channel. *J. Biol. Chem.* **268**, 13765-13768.

Meldolesi, J.C., Huttner, W.B., Tsien, R.Y., and Pozzan, T. (1984) Free cytoplasmic Ca^{2+} and neurotransmitter release: studies on PC12 cells and synaptosomes exposed to α-latrotoxin. *Proc. Natl. Acad. Sci. USA* **81**, 620-624.

Meldolesi, J., Villa, A., Podini, P., Clementi, E., Zacchetti, D., D'Andrea, P., Lorenzon, P., and Grohavaz, F. (1992) Intracellular Ca^{2+} stores in neurons. Identification and functional aspects. *J. Physiol. (Lond.)* **86**, 23-30.

Meldolesi, J., Volpe, P., and Pozzan, T. (1988) The intracellular distribution of calcium. *Trends Neurosci.* **11**, 449-452.

Meloni, E. and Pontremoli, S. (1989) The calpains. *Trends Neurosci.* **12**, 438-444.

Menza, M., Ahmad, T., Chettibi, S., Drainas, D, and Lawrence, A.J. (1994) Zinc and barium inhibit the phospholipase A_2 from *Naja naja atra* by different mechanisms. *Biochem. J.* **301**, 503-508.

Merritt, J.E., Jacob, R, and Hallam, T.J. (1989) Use of manganese to discriminate between calcium influx and mobilization from internal stores in stimulated human neutrophils. *J. Biol. Chem.* **264**, 1522-1527.

Michaelis, M.L., Kitos, T.E., Nunley, E.W., Lecluyse, E., and Michaelis, E.K. (1987) Characteristics of Mg^{2+}-dependent, ATP-activated Ca^{2+} transport in synaptic and microsomal membranes and in permeabilized synaptosomes. *J. Biol. Chem.* **262**, 4182-4189.

Miledi, R. (1973) Transmitter release induced by injection of calcium ions into nerve terminals. *Proc. R. Soc. Lond. Ser. B* **183**, 421-425.

Miller, R.J. (1988) Calcium signalling in neurons. *Trends Neurosci.* **11**, 415-419.

Minnema, D.J., Cooper, G.P., and Greenland, R.D. (1989) Effects of methylmercury on neurotransmitter release from rat brain synaptosomes. *Toxicol. Appl. Pharmacol.* **99**, 510-521.

Minta, A., Kao, J.P.Y., and Tsien, R.Y. (1989) Fluorescent indicators for cytosolic calcium based on rhodamine and fluorescein chromophores. *J. Biol. Chem.* **264**, 8171-8178.

Miyamoto, M.D. (1983) Hg^{2+} causes neurotoxicity at an intracellular site following entry through Na and Ca channels. *Brain Res.* **267**, 375-379.

Moore, C.L. (1971) Specific inhibition of mitochondrial Ca^{2+} transport by ruthenium red. *Biochem. Biophys. Res. Comm.* **42**, 298-305.

Moutin, M.J., Rapin, C., and Dupont, Y. (1992) Ruthenium red affects the intrinsic fluorescence of the calcium-ATPase of skeletal sarcoplasmic reticulum. *Biochim. Biophys. Acta* **1100**, 321-328.

Murphy, E., Levy, L., Berkowitz, L.R., Orringer, E.P., Gabel, S.A., and London, R.E. (1986) Nuclear magnetic resonance measurement of cytosolic free calcium levels in human red blood cells. *Am. J. Physiol.* **251**, C496-C504.

Muto, M., Shinada, M., Tokuta, K., and Takizawa, Y. (1991) Rapid changes in concentrations of essential elements in organs of rats exposed to methylmercury chloride and mercuric chloride as shown by simultaneous multielemental analysis. *Br. J. Ind. Med.* **48**, 382-388.

Nachshen, D.A. (1985) Regulation of cytosolic calcium concentration in presynaptic nerve endings isolated from rat brain. *J. Physiol. (Lond.)* **363**, 87-101.

Nahorski, S.R. (1988) Inositol polyphosphates and neuronal calcium homeostasis. *Trends Neurosci.* **11**, 444-448.

Nelson, M.T. (1986) Interactions of divalent cations with single calcium channels from rat brain synaptosomes. *J. Gen. Physiol.* **87**, 201-222.

Nicotera, P., Bellomo, G., and Orrenius, S. (1992) Calcium-mediated mechanisms in chemically induced cell death. *Ann. Rev. Pharmacol. Toxicol.* **32**, 449-470.

Nishimura, M. (1988) Zn^{2+} stimulates spontaneous transmitter release at mouse neuromuscular junctions. *Br. J. Pharmacol.* **93**, 430-436.

Oakley B., Kirsch D., and Morris N. (1980) A simplified ultrasensitive silver stain for detecting proteins in polyacrylamide gels. *Anal. Biochem.* **105**, 361.

Ogura, A., Myojo, Y., and Higashida, H. (1990) Bradykinin-evoked acetylcholine release via inositol trisphosphate-dependent elevation in free calcium in neuroblastoma × glioma hybrid NG108-15 cells. *J. Biol. Chem.* **265**, 3577-3584.

Ono, T. and Means, A.R. (1989) Calspermin is a testis specific calmodulin-binding protein closely related to Ca^{2+}/calmodulin-dependent protein kinases. *Adv. Exp. Med. Biol.* **255**, 263-268.

Persechini, A., Moncrief, N.D., and Kretsinger, R.H. (1989) The EF-hand of calcium-modulated proteins. *Trends Neurosci.* **12**, 462-467.

Preston, S.F., Sha'afi, R.I., and Berlin, R.D. (1991) Regulation of Ca^{2+} during mitosis: Ca^{2+} influx and depletion of intracellular Ca^{2+} stores are coupled in interphase but not mitosis. *Cell Reg.* **2**, 915-925.

Rahamimoff, R., Rahamimoff, H., Binah, O., and Meiri, U. (1975) Control of neurotransmitter release by calcium ions and the role of mitochondria. In: *Calcium Transport in Contraction and Secretion*, pp 253-269, ed. E. Carafoli, North-Holland Publishing Co.

Rajanna, B., Chetty, C.S., and Rajanna, S. (1990) Effect of mercuric chloride on the kinetics of cationic and substrate activation of the rat brain microsomal ATPase system. *Biochem. Pharmacol.* **39**, 1935-1940.

Rasgado-Flores, H. and Blaustein, M.P. (1987) ATP-dependent regulation of cytoplasmic free calcium in nerve terminals. *Am. J. Physiol.* **252**, C588-C594.

Rehder, V. and Kater, S.B. (1992) Regulation of neuronal growth cone filopodia by intracellular calcium. *J. Neurosci.* **12**, 3175-3186.

Reuhl, K.R. and Chang, L.W. (1979) Effects of methylmercury on the development of the nervous system: a review. *NeuroToxicology* **1**, 21-55.

Richards, C.D., Metcalfe, J.C., Smith, G.A., and Hesketh, T.R. (1984) Changes in free-calcium levels and pH in synaptosomes during transmitter release. *Biochim. Biophys. Acta* **803**, 215-220.

Rizzuto, R., Brini, M., Murgia, M., and Pozzan, T. (1993) Microdomains with high Ca^{2+} close to IP_3-sensitive channels that are sensed by neighboring mitochondria. *Science* **262**, 744-747.

Rizzuto, R., Simpson, A.W.M., Brini, M., and Pozzan, T. (1992) Rapid changes of mitochondrial Ca^{2+} revealed by specifically targeted recombinant aequorin. *Nature (Lond.)* **358**, 325-327.

Rossi, A., Manzo, L., Orrenius, S., Vahter, M., and Nicotera, P. (1991) Modifications of cell signalling in the cytotoxicity of metals. *Pharmacol. Toxicol.* **68**, 424-429.

Sacchi, O. and Perri, V. (1973) Quantal mechanisms of transmitter release during progressive depletion of the presynaptic stores at ganglionic synapse. The action of hemicholinium-3 and thiamine depletion. *J. Gen. Physiol.* **61**, 342-360.

Sanchez-Armass, S. and Blaustein, M.P. (1987) Role of sodium-calcium exchange in regulation of intracellular calcium in nerve terminals. *Am. J. Physiol.* **252**, C595-C603.

Sarafian, T.A. (1993) Methyl mercury increases intracellular Ca^{2+} and inositol phosphate levels in cultured cerebellar granule neurons. *J. Neurochem.* **61**, 648-657.

Sarafian, T.A., Vartavarian, L., Kane, D.J., Bredesen, D.E., and Verity, M.A. (1994) *bcl-2* expression decreases methyl mercury-induced free-radical generation and cell killing in a neural cell line. *Toxicol. Lett.* **74**, 149-155.

Sarafian, T. and Verity, M.A. (1986) Mechanism of apparent transcription inhibition by methyl mercury in cerebellar neurons. *J. Neurochem.* **47**, 625-631.

Sarafian, T. and Verity, M.A. (1990a) Altered patterns of protein phosphorylation and synthesis caused by methyl mercury in cerebellar granule cell culture. *J. Neurochem.* **55**, 922-929.

Sarafian, T. and Verity, M.A. (1990b) Methyl mercury stimulates protein ^{32}P phospholabeling in cerebellar granule cell culture. *J. Neurochem.* **55**, 913-921.

Sarafian, T.A. and Verity, M.A. (1991) Oxidative mechanisms underlying methyl mercury neurotoxicity. *Int. J. Devl. Neurosci.* **9**, 147-153.

Schacht, J. (1976) Inhibition by neomycin of polyphosphoinositide turnover in subcellular fractions of guinea-pig cerebral cortex *in vitro*. *J. Neurochem.* **27**, 1119-1124.

Schanne, F.A.X., Dowd, T.L., Gupta, R.K., and Rosen, J.F. (1989a) Lead increases free Ca^{2+} concentration in cultured osteoblastic bone cells: Simultaneous detection of intracellular free Pb^{2+} by ^{19}F NMR. *Proc. Natl. Acad. Sci.* **86**, 5133-5135.

Schanne, F.A.X., Moskal, J.R., and Gupta, R.K. (1989b) Effect of lead on intracellular free calcium ion concentration in a presynaptic neuronal model: ^{19}F-NMR study of NG108-15 cells. *Brain Res.* **503**, 308-311.

Schanne, F.A.X., Dowd, T.L., Gupta, R.K., and Rosen, J.F. (1990) Development of ^{19}F NMR for measurement of $[Ca^{2+}]_i$ and $[Pb^{2+}]_i$ in cultured osteoblastic bone cells. *Environ. Health Perspect.* **84**, 99-106.

Schanne, F.A.X., Moskal, J.R., and Gupta, R.K. (1989) Effect of lead on intracellular free calcium ion concentration in a presynaptic neuronal model: ^{19}F-NMR study of NG108-15 cells. *Brain Res.* **503**, 308-311.

Scott, I.D., Åkerman, K.E.O., and Nicholls, D.G. (1980) Calcium-ion transport by intact synaptosomes. *Biochem. J.* **192**, 873-880.

Shafer, T.J. and Atchison, W.D. (1989) Block of ^{45}Ca uptake into synaptosomes by methylmercury: Ca^{++}- and Na^{+}-dependence. *J. Pharmacol. Exp. Ther.* **248**, 696-702.

Shafer, T.J. and Atchison, W.D. (1991a) Transmitter, ion channel and receptor properties of pheochromocytoma (PC12) cells: a model for neurotoxicological studies. *NeuroToxicology* **12**, 473-492.

Shafer, T.J. and Atchison, W.D. (1991b) Methylmercury blocks N- and L-type Ca^{++} channels in nerve growth factor-differentiated pheochromocytoma (PC12) cells. *J. Pharmacol. Exp. Ther.* **258**, 149-157.

Shafer, T.J., Contreras, M.L., and Atchison, W.D. (1990) Characterization of interactions of methylmercury with Ca^{2+} channels in synaptosomes and pheochromocytoma cells: radiotracer flux and binding studies. *Mol. Pharmacol.* **38**, 102-113.

Shalton, P.M. and Wareham, A.C. (1979) Calcium ionophore A-23187 and spontaneous miniature end-plate potentials of mammalian skeletal muscle. *Exp. Neurol.* **63**, 379-387.

Smith, G.A., Hesketh, R.T., Metcalfe, J.C., Feeney, J., and Morris, P.G. (1983) Intracellular calcium measurements by ^{19}F NMR of fluorine-labeled chelators. *Proc. Natl. Acad. Sci.* **80**, 7178-7182.

Smith, J.B., Dwyer, S.D., and Smith, L. (1989) Cadmium evokes inositol polyphosphate formation and calcium mobilization. *J. Biol. Chem.* **264**, 7115-7118.

Springman, E.B., Angleton, E.L., Birkedal-Hansen, H., and Van Wart, H.E. (1990) Multiple modes of activation of latent human fibroblast collagenase: evidence for the role of a Cys-73 active-site zinc complex in latency and a "cysteine switch" mechanism for activation. *Proc. Natl. Acad. Sci. USA* **87**, 364-368.

Steel, R.G.D. and Torrie, J.H. (1980) *Principles and Procedures of Statistics*, McGraw-Hill, New York.

Statham, J.H. and Duncan, C.J. (1976) Dantrolene and the neuromuscular junction: evidence for intracellular Ca stores. *Eur. J. Pharmacol.* **39**, 143-152.

Takano, Y., Okudaira, M., and Harmon, B.V. (1993) Apoptosis induced by microtubule disrupting drugs in cultured human lymphoma cells. Inhibitor effects of phorbol ester and zinc sulphate. *Pathol. Res. Pract.* **189**, 197-203.

Takeuchi, T., Kambara, T., Morikawa, N., Matsumoto, H., Shiraishi, Y., and Ito, H. (1959) Pathological observations of the Minamata disease. *Acta Pathologica Japonica* **9**, 769-783.

Takeuchi, T., Morikawa, N., Matsumoto, H., and Shiraishi, Y. (1962) A pathological study of Minamata Disease in Japan. *Acta Neuropathol.* **2**, 40-57.

Tapia, R., Sitges, M., and Morales, E. (1985) Mechanism of the calcium-dependent stimulation of transmitter release by 4-aminopyridine in synaptosomes. *Brain Res.* **361**, 373-382.

Tatsumi, T. and Fliss, H. (1995) Hypochlorous acid mobilizes intracellular zinc in isolated rat heart myocytes. *J. Mol. Cell. Cardiol.* **26**, 471-479.

Thompson, M.A. and Ziff, E.B. (1989) Structure of the gene encoding peripherin, an NGF-regulated neuronal-specific type III intermediate filament protein. *Neuron* **2**, 1043-1053.

Tomsig, J.L. and Suszkiw, J.B. (1990) Pb^{2+}-induced secretion from bovine chromaffin cells: fura-2 as a probe for Pb^{2+}. *Am. J. Physiol.* **259**, C762-C768.

Traxinger, D.L. and Atchison, W.D. (1987) Reversal of methylmercury-induced block of nerve-evoked release of acetylcholine at the neuromuscular junction. *Toxicol. Appl. Pharmacol.* **90**, 23-33.

Treves, S., Trentini, P.L., Ascanelli, M., Bucci, G., and DiVirgilio, F. (1994) Apoptosis is dependent on intracellular zinc and independent of intracellular calcium in lymphocytes. *Exp. Cell Res.* **211**, 339-343.

Tsien, R.Y., Pozzan, T., and Rink, T.J. (1982) Calcium homeostasis in intact lymphocytes: cytoplasmic free calcium monitored with a new intracellularly trapped fluorescent indicator. *J. Cell. Biol.* **94**, 325-334.

Tsokos-Kuhn, J.O. (1989) Evidence *in vivo* for elevation of intracellular free Ca^{2+} in the liver after diquat, acetaminophen and CCl_4. *Biochem. Pharmacol.* **38**, 3061-3065.

Tsokos-Kuhn, J.O., Smith, C.V., Mitchell, J.R., Tate, C.A., and Entman, M.L. (1986) Evidence for increased membrane permeability of plasmalemmal vesicles from livers of phenobarbital-induced CCl_4-intoxicated rats. *Mol. Pharmacol.* **30**, 444-451.

Tymianski, M., Charlton, M.P., Carlen, P.L., and Tator, C.H. (1993) Source specificity of early calcium neurotoxicity in cultured embryonic spinal neurons. *J. Neurosci.* **13**, 2085-2104.

Vallee, B.L. and Auld, D.S. (1990) Zinc coordination, function, and structure of zinc enzymes and other proteins. *Biochemistry* **29**, 5647-5659.

Vallee, B.L. and Falchuk, K.H. (1993) The biochemical basis of zinc physiology. *Physiol. Rev.* **73**, 79-118.

Vega, M.T., Villalobos, C., Garrido, B., Gandía, L., Bulbena, O., García-Sancho, J., García, A.G., and Artalejo, A.R. (1994) Permeation by zinc of bovine chromaffin cell calcium channels: relevance to secretion. *Pflügers Arch.* **429**, 231-239.

Verity, M.A., Brown, W.J., and Cheung M. (1975) Organic mercurial encephalopathy: *in vivo* and *in vitro* effects of methyl mercury on synaptosomal respiration. *J. Neurochem.* **25**, 759-766.

Verity, M.A., Sarafian, T., Pacifici, E.H.K., and Sevanian, A. (1994) Phospholipase A_2 stimulation by methyl mercury in neuron culture. *J. Neurochem.* **62**, 705-714.

Vernino, S., Amador, M., Luetje, C.W., Patrick, J., and Dani, J.A. (1992) Calcium modulation and high calcium permeability of neuronal nicotinic acetylcholine receptors. *Neuron* **8**, 1-20.

Vignes, M., Guiramand, J., Sassetti, I., and Récasens, M. (1993) Effect of thiol reagents on phosphoinositide hydrolysis in rat brain synaptoneurosomes. *Eur. J. Neurosci.* **5**, 327-33.

Wang, Y.-X. and Quastel, D.M.J. (1990) Multiple actions of zinc on transmitter release at mouse end-plates. *Pflügers Arch.* **415**, 582-587.

Weiss, J.H., Hartley, D.M., Koh, J., and Choi, D.W. (1993) AMPA receptor activation potentiates zinc neurotoxicity. *Neuron* **10**, 43-49.

Westbrook, G.L. and Mayer, M.L. (1987) Micromolar concentrations of Zn^{2+} antagonize NMDA and GABA responses of hippocampal neurons. *Nature (Lond.)* **328**, 640-643.

Wolf, S.G., Mosser, G., and Downing, K.H. (1993) Tubulin conformation in zinc-induced sheets and macrotubes. *J. Struct. Biol.* **111**, 190-199.

Xiang, J.Z., Morton, J., Brammer, M.J., and Campbell, I.C. (1990) Regulation of calcium concentrations in synaptosomes: α_2-adrenoceptors reduce free Ca^{2+} by closure of N-type Ca^{2+} channels. *J. Neurochem.* **55**, 303-310.

Xie X., Gerber U., Gahwiler B.H., and Smart T.G. (1993) Interaction of zinc with ionotropic and metabotropic glutamate receptors in rat hippocampal slices. *Neurosci. Lett.* **159**, 46-50.

Yokoyama, M., Koh, J., and Choi, D.W. (1986) Brief exposure to zinc is toxic to cortical neurons. *Neurosci. Lett.* **71**, 351-355.

Zalewski, P.D., Millard, S.H., Forbes, I.J., Kapaniris, O., Slavotinek, A., Betts, W.H., Ward, A.D., Lincoln, S.F., and Mahadevan, I. (1994) Video image analysis of labile zinc in viable pancreatic islet cells using a specific fluorescent probe for zinc. *J. Histochem. Cytochem.* **42**, 877-884.